UCRL 9002

UNIVERSITY OF CALIFORNIA

Ernest O. Lawrence Radiation Laboratory

CONTROLLED THERMONUCLEAR RESEARCH QUARTERLY REPORT

September, October, November 1959

TWO-WEEK LOAN COPY

This is a Library Circulating Copy which may be borrowed for two weeks. For a personal retention copy, call Tech. Info. Division, Ext. 5545

DISCLAIMER

This document was prepared as an account of work sponsored by the United States Government. While this document is believed to contain correct information, neither the United States Government nor any agency thereof, nor the Regents of the University of California, nor any of their employees, makes any warranty, express or implied, or assumes any legal responsibility for the accuracy, completeness, or usefulness of any information, apparatus, product, or process disclosed, or represents that its use would not infringe privately owned rights. Reference herein to any specific commercial product, process, or service by its trade name, trademark, manufacturer, or otherwise, does not necessarily constitute or imply its endorsement, recommendation, or favoring by the United States Government or any agency thereof, or the Regents of the University of California. The views and opinions of authors expressed herein do not necessarily state or reflect those of the United States Government or any agency thereof or the Regents of the University of California.

Research and Development

UCRL-9002
Controlled Thermo-
nuclear Process
TID-4500(15th Ed.)

UNIVERSITY OF CALIFORNIA

Lawrence Radiation Laboratory
Berkeley and Livermore, California

Contract No. W-7405-eng-48

CONTROLLED THERMONUCLEAR RESEARCH QUARTERLY REPORT

September, October, November 1959

December 10, 1959

Printed for the U. S. Atomic Energy Commission

Printed in USA. Price $3.00. Available from the
Office of Technical Services
U. S. Department of Commerce
Washington 25, D.C.

CONTROLLED THERMONUCLEAR RESEARCH QUARTERLY REPORT

September, October, November 1959

Contents

GENERAL INTRODUCTION 4

I. PYROTRON (MAGNETIC MIRROR) PROGRAM

Introduction and Summary 6
Magnetic High-Compression Experiments 7
Electron-Distribution Analysis 11
Plasma Potential Diagnostics 14
Adiabatic Low-Energy Injection and Capture Experiment (ALICE) 15
Grid Source Development 16
Beam Neutralization 17
Vacuum and Surface Studies 18
Containment of Positrons in the Mirror Machine 21
P-4 (Steady-State Plasma) System 25

II. HIGH-ENERGY INJECTION

A Parameter Study of the High-Energy Molecular-Ion Injection System 27
Dissociation of D_2^+ 32

III. ASTRON PROGRAM

Introduction 32
Interaction of Relativistic Electron Beams with a Quasi-Neutral Plasma 35
Astron E-Layer Calculations 38
Thin-Fiber Scintillation Counters for Exploring the Electron Distribution in the Astron Device 42
Description of Astron Experiments 45

IV. LIVERMORE PINCH PROGRAM

The Linear Hard-Core Pinch 53
Small Levitron Experiment 58
Electron-Beam Pinch 62
Plasma Acceleration 64
Liquid Sodium Experiment 64
The 12-Inch Levitron 66
High-Magnetic-Field Research 66
Theory 67

*Preceding Quarterly Reports: UCRL-8887, UCRL-8775, UCRL-8682

V. BERKELEY PINCH PROGRAM
Sheet Pinch Studies 68
Homopolar Program 73
VI. ION MAGNETRON 76
VII. THEORETICAL RESEARCH
The Heating Up of Electrons in a Plasma 80
Scattering Loss Rate in Mirror Geometry 82
Hydromagnetic Stability of a Tubular Pinch 85
VIII. BASIC EXPERIMENTAL RESEARCH
Plasma Physics and Microwave Diagnostics 90
Hydromagnetic Wave Propagation 100
Axial Transfer of Radio-Frequency Energy to the Center of a "Magnetic Mirror" 103
Atomic and Molecular Beam Research 113
Ion-Source Development 114
IX. ENGINEERING AND TECHNOLOGICAL DEVELOPMENT
Ultrahigh-Vacuum Development 115
Cryogenic Pumping 121
Mechanical Engineering Development 123
Electrical Engineering Development 136
TALKS AND PUBLICATIONS 148

CONTROLLED THERMONUCLEAR RESEARCH QUARTERLY REPORT

September, October, November 1959

Lawrence Radiation Laboratory
University of California
Berkeley and Livermore, California

December 10, 1959

GENERAL INTRODUCTION

C. M. Van Atta

A great deal of thought has gone into a thorough review of the Livermore and Berkeley components of the controlled thermonuclear research program in an effort to define the areas for emphasis and de-emphasis. Although a tightening of the budget required that the spending rate be reduced somewhat, the motivation for the review was principally to assess the various projects in terms of their probable contribution to a better understanding of the attainment and containment of high-temperature plasma.

The internal review dealt with all aspects of the program except the Astron, for which a special committee of scientists from outside the Lawrence Radiation Laboratory, under the chairmanship of Professor Kenneth M. Watson, was requested to provide an independent judgment with special emphasis upon the proposed high-current electron accelerator, injection scheme, and electron-layer stability. The written report of the special committee is not yet completed, but an oral report by a portion of the committee was in favor of proceeding with the Astron accelerator and injection system with the objective of testing the stability of the electron layer and the feasibility of reversing the field near the axis. No concrete evidence for instability of the electron layer by itself was discovered, and the phase space available for injecting electrons into the layer as proposed appears to be adequate to permit reversal of the field. If the layer proves to be stable by itself, then the layer plus plasma should be stable up to some value of the plasma β which can perhaps be determined only by experiments.

The most significant decision made as a result of the internal review of the program is concerned with the high-energy molecular-ion injection program. Results of analytical studies on the LRL scheme for multiple-pass injection and dissociation on a hydrogen arc are encouraging in terms of plasma build-up. However, we find that the ORNL group is now thinking in terms of a very similar scheme. In order to avoid expensive duplication of effort it was decided that we should transmit our conclusions in detail to the Oak Ridge group and then terminate all projects at Livermore directed toward high-energy molecular-ion injection. Several LRL staff members

directly concerned attended a meeting at Oak Ridge in which all aspects of high-energy molecular-ion injection were discussed in some detail. A final report is now being written giving the analytical results and conclusions of the LRL group. The termination of these projects will provide some flexibility in the budget for pursuing the remaining projects effectively.

The magnetic-mirror multiple-compression (Toy Top) project was singled out for greater emphasis because it was judged to be most likely to produce plasma temperatures and densities of interest in the shortest time (such as one year). A number of minor independent projects are being terminated and some elements of technological development will receive less effort. These adjustments in the program should be completed by December 31, 1959.

The manpower assigned to controlled thermonuclear research during the period August, September, and October (lagging technical reporting by one month) is given in the following table.

	Approximate direct heads		
	Livermore	Berkeley	Total
August 1959	265	70	335
September 1959	263	69	332
October 1959	253	64	317

I. PYROTRON (MAGNETIC MIRROR) PROGRAM

INTRODUCTION AND SUMMARY

Richard F. Post

In the past quarter the efforts of the Pyrotron group lay primarily in four areas:

(a) intensive study of plasma injection and trapping into static magnetic fields of various configurations (Frederic H. Coensgen et al., Magnetic High-Compression Studies),

(b) detailed analysis of the data obtained in the Table Top experiments, in order to document the existence of a stably confined plasma (Robert E. Ellis, Walton A. Perkins, and Richard F. Post),

(c) additional analysis of the plasma in the P-4 plasma generator, to the end of writing a comprehensive report on the generator and its operation (Andrew L. Gardner, William L. Barr, Raymond L. Kelly, et al.), and

(d) ion source, vacuum pumping, and theoretical build-up studies of the ALICE fast neutral atom injection studies (C. C. Damm et al.).

In connection with the plasma-injection studies (a), some very significant measurements were made relating to the possibility of "entropy trapping" or trapping by diamagnetic effects into a cusp-geometry magnetic field, an idea which has been recently revived by James L. Tuck of Los Alamos. It was shown that, under the conditions of these experiments, the expected trapping did not occur for any appreciable fraction of the plasma, contrary to the theoretical expectations set forth by Tuck.

In the analysis of the data from the Table Top confinement experiments, additional evidence was obtained which corroborates the general picture of a stably confined plasma of very high electron temperature. These data were critically compared with the predictions of stability theory to show that the observed confinement times ranged up to 10^5 times the instability times. At this point we have not isolated the reason why confinement is indeed achieved for times much longer than instability periods.

Considerable encouragement to the ALICE program came from the successful operation of a very simple molybdenum evaporator which produced ultravacuum conditions for extended periods in an unbaked system with a known leak, and which exhibited high pumping speeds for hydrogen gas.

MAGNETIC HIGH-COMPRESSION EXPERIMENTS

Frederic H. Coensgen

Injection Studies

A. Rotational Energy Distributions

The 12-channel ion-energy analyzer has been added to the end of the system in which the angular distributions of the plasma ions have been determined (see previous reports). It is now possible to determine angular distribution of ions in any energy interval and hence possible to deduce rotational energy distributions. Two methods of injection have been investigated in a 400-gauss magnetic field.

1. Longitudinal injection through a magnetic cusp

Previously a broad angular distribution was found. Although the total quantity of injected plasma was less, the method appeared attractive as it could be used at low fields. It has now been found that the wide angular distribution is associated with only the low-energy ions. Most of the high-energy particles from the generator are lost, and those which are injected are nearly aligned with the magnetic field.

2. Longitudinal injection into a uniform magnetic field

It is found that the higher-energy ions have wider angular distributions than the low-energy ions. Rotational energy distributions have been determined for a single generator aligned with a 400-gauss field for radial positions at 6, 4-1/2, 2, and 0 inches. The zero position is the axis of the generator. From these data it is possible to estimate the fraction of the deuterium ions that have radial energies in a given interval. It is found that 50% have rotational energies greater than 50 ev and 10% have rotational energies in the interval between 50 and 100 ev. This work is being reported at the Monterey meeting by Arthur E. Sherman.

B. Colliding Plasma Streams

It has been predicted that under certain conditions the collision of two streams of plasma should result in the transformation of their relative translational energy into electron and ion oscillations in a time of the order of the electron or ion plasma period, and in a distance of the order of the product of the translational velocity and the plasma period. One of the limiting sets of conditions that have been examined occurs when the random energy of the electrons in the plasma stream is large compared with their translational energy and the random energy of the ions is small compared with their translational energy. In this case, it has been predicted that there would be no interaction between the electrons, but an interaction would occur between the two ion streams. The effect of the electrons would be to reduce the ion-plasma frequency and lengthen the distance over which the interaction would occur. The experimental setup was chosen to closely duplicate the intitial conditions required for this interaction. We have observed only slight if any indication that such interaction is occurring.

Certainly there is no violent interaction. The chief difference between the theoretical calculations and the experiment lies in the presence of a longitudinal magnetic field. Since the predicted interaction involves longitudinal electrostatic oscillations, the effect of the field should be negligible. We have requested Marvin Mittleman to look at this more closely, theoretically. William F. Cummins and William E. Nexsen, Jr., have been principally responsible for this work, and Nexsen will report it at the Monterey meeting.

C. Injection from Zero or Weak Magnetic Fields Through a Magnetic Mirror Into a Magnetic Cusp

It has been predicted[1] that a directed plasma stream can penetrate only magnetic fields having less than a critical value B_c. $B_c^2 = 12\ \pi\rho v^2$, where ρ is the plasma density and v its translational velocity. It was proposed that plasma can be injected into a cusp region through a magnetic field less than B_c and stopped by a second field greater than B_c. If plasma flow is consistent with these predictions, injection from a zero magnetic field might be useful in the multistage experiment. However, the results of our previous experiments, in which the conditions were similar, did not agree with the above predictions. Therefore we have set up a cusp instrumented with several ion-extraction and magnetic probes, so that ρ and v can be determined.

1. Penetration of a single magnetic mirror

The amount of plasma that penetrates a mirror has been determined for plasmas generated in a zero field and directed along the axis of symmetry towards a magnetic mirror. A large part of the plasma passes through the mirror whether or not the above condition is satisfied. The transmitted ion flux was measured as a function of the magnitude of the magnetic field and found to increase very rapidly as the field increased from 0 to 200 gauss, then decrease slowly. About 40% of the ion flux penetrated a field of 3500 G. The maximum ion density at the field maximum was found to be $n_{max} = 2.6 \times 10^{11}$ ions/cm^3. The corresponding value of B_c is 172 G, which is about 5% as large as the field penetrated.

A weak signal can be detected by a magnetic probe located at the position of field maximum for zero field. The magnetic-probe signal rapidly increases as the field is increased to 12 gauss. Thereafter the signals decrease at first rapidly and then more slowly as the field is further increased. They disappear at approximately 1000 G, which is within 20% of the critical field value predicted from n and v. As the magnetic probe can detect only plasma ions that have appreciable rotational momentum about the magnetic field lines, the above results indicate that as the plasma encounters the magnetic field most of the vectors of most of the ions become aligned with the magnetic field. Some of the ions, however, have rotational momentum. As the magnitude of the magnetic mirror is increased, those ions with considerable rotational energy are reflected and do not penetrate to the magnetic probe, thus the magnetic probe signal decreases.

[1] J. L. Tuck, Phys. Rev. Letters 3, 313 (1959).

Most of the plasma ions have very little rotational energy and just continue along the magnetic flux lines through the mirror. As the magnitude of the mirror is increased to very large values, ions with even small rotational energies are reflected, so that the transmitted signal is slowly decreased.

2. Injection into a cusp

The ion flux entering, striking the walls, and leaving a cusp region has been determined for several conditions of field intensity and plasma injection. A typical accounting of the ions is: 100% enter, 97.5% strike the wall in the region of the zero field, and 24% leave the second mirror. This indicates that the number leaving exceeds the number entering. For a weaker field the ratio was observed to be 157%. We postulate that the excess charge is due to wall bombardment by the energetic ions. Indeed, the ion-flux signals at the wall in the vicinity of the zero plane persist 50 to 100 μsec longer than other signals, and at first might be interpreted as evidence of containment. As the magnitude of the slow component represents an ion flux which is nearly equal to that represented by the 21% excess ions, we are inclined to interpret the slow component as due to slow ions traversing the volume, rather than containment. Ion-energy measurements could provide a conclusive answer. This work will be reported at Monterey by Frederic H. Coensgen.

Plasma Generators

A. Toy Top Generators

There has been no experimental work done on these generators this quarter; experience and data have been obtained only as the generators have been used in the experiments described above.

It has been found that the velocity distributions in the center-of-mass coordinate systems are nearly Maxwellian. Thus the plasma can be characterized by a center-of-mass velocity and a mean random energy. We are now reducing all the data obtained in the parametric study of the generator to determine whether or not there is a dependence of the c. m. velocity or of the mean random energy upon the various parameters. It was shown that the angular distributions cannot be explained on the basis of an isotropic distribution with the observed c. m. velocity and mean random energy. This result indicates that the influence of the external magnetic field results in a directed radial acceleration, rather than a simple increase in the mean random energy. William F. Cummins will report this work at Monterey.

B. Gas-Fed Plasma Generators

1. The gas-fed generator in which the plasma is produced and heated by a rapidly rising magnetic field is being studied by Walton A. Perkins as a source for the Table Top experiment.

2. There is considerable interest in the gas-fed generator developed by John Marshall at LASL, and we are planning to build and study a similar device.

Instrumentation

A. Ion Coupling from Longitudinal Magnetic Fields to Analyzer

This problem does not appear to cause great trouble inasmuch as angular distributions of all ion energies have been obtained. It was found that the plasma density does not decrease as fast as the adiabatic laws would predict as the plasma flows from a uniform to zero magnetic field. There is continuing effort to improve the ion analyzers and calibrate them so that absolute ion densities within the longitudinal fields can be determined.

B. Data-Handling System

There has been considerable trouble with the printer, the scanner, and the digital voltmeter. These parts have been returned to the manufacturer twice. At this time, David R. Branum has decided to trouble-shoot these units here, and has progressed to the point where a single channel of the system is ready to be tested.

Multistage Magnetic Compression

A number of possible designs of multistage compression experiments have been examined. In particular, we are interested in a design based on the injection data discussed above. The principal problems arise in trapping the plasma ions in the first stage. Although 10% of the deuterium ions have rotational energies in a suitable range, the longitudinal velocity range of these ions is large. Trapping can be accomplished by the use of long sections or by the use of fast gating fields. If long sections are used, the plasma density will be low. Longitudinal compression cannot be used to increase the density, as the initial angular distribution extends to low angles. A reasonably satisfactory design has been evolved in which the plasma is allowed to self-compress from the 18-inch section to the 9-inch section, to be trapped by a fast pulsed (gate) field. Transfer to the 4-inch section will probably be carried out in one stage. The final compression will reach fields of the order of 10^5 G. Space should be allowed at the injection end of the system to accommodate changes in injection and to allow the addition of 18-inch and 12-inch transfer sections. All parts of the system appear to be well within the limits of present technology.

ELECTRON-DISTRIBUTION ANALYSIS

Robert E. Ellis and Walton A. Perkins

Plasma Diagnostics on the Table Top Machine

Scintillator Probe Measurements

For further examination of the spatial characteristics of a compressed plasma, the effects of inserting metal and plastic probes into the plasma region have been observed. For example, the 1-in.-diameter stainless steel fluor detector probe was inserted radially between the mirrors to various distances from the longitudinal axis of the plasma established by injecting from an axial source located near one mirror. Starting at 6 in. from the axis, the radial probe was moved in steps of 1 in. to a position 1 in. from the axis. The signal produced by electrons escaping from the plasma through the smaller mirror and entering the four-channel fluor detector probe located 4 in. outside the mirror was noted. The corresponding reduction in the observed signal indicated that the presence of the radial probe began to significantly interfere with the plasma when the probe was ~ 1-1/2 in. from the axis. At 1 in. from the axis a small signal was still observed in the four-channel detector. A small plastic probe, introduced at the same position as the radial probe, gave a similar result. This result ties in well with the previously reported measurements of the radial electron flux distribution made with the four-channel detector.[2] In these measurements the central pulsed field was about 7 kilogauss, with a mirror ratio of 2.

To obtain information on the axial extent of the plasma, a 4-in.-diameter lucite disc was inserted axially through the mirror opposite the one at which the four-channel detector was located, and its effect on the plasma (generated by injecting from two opposed radial sources) was observed. The signals at the four-channel fluor detector showed a significant interference with the plasma at a position of the disc between 4-1/2 and 5 in. from the mid-plane of the mirrors. This would imply a plasma length of from 25 to 30 cm.

Electron Energy Distribution

To facilitate the analysis of electron energy distribution measurements recently made, as well as those previously reported,[2, 3] an IBM 709 computer program has been written.

---

[2] Robert E. Ellis and Walton A. Perkins, in Controlled Thermonuclear Research Quarterly Report, UCRL-8887, Sept. 1959, p. 10.

[3] F. H. Coensgen, F. C. Ford, and R. E. Ellis, Proc. of Second International Conference on the Peaceful Uses of Atomic Energy, Geneva, 1958 (United Nations, 1959) Vol. 32, p. 266.

The program solves for $\phi(E)$, the electron flux, in the integral equation

$$Q(E_0) = K \int_{E_0}^{\infty} \phi(E)\, F(E, E_0)\, dE. \tag{1}$$

$Q(E_0)$ is the pulse height as a function of the absorber thickness R_0 and therefore a function of E_0, the minimum energy possessed by an electron that will just pass through the absorber. The quantity E_0 is related to R_0 by the formula

$$R_0 = a\, E_0^{(b - c\, \ell n\, E_0)} .$$

This formula and the numerical values for a, b, and c were obtained from an article by L. Katz and A. Penfold.[4]

$F(E, E_0)$ is proportional to the scintillation output for an electron of energy E and an absorber of thickness R_0,

$$F(E, E_0) = (E - E_a)\, \eta(E - E_a), \tag{2}$$

where E_a is the energy lost in the absorber and $\eta(E - E_a)$ is the efficiency of the scintillator, calculated by the formula

$$\eta(E - E_a) = \frac{E - E_a - E_c}{E - E_a} , \tag{3}$$

where E_c is the intercept on the energy axis in the plot of pulse height versus energy for monoenergetic electrons on anthracene. The formula for the efficiency was obtained experimentally by Johnston et al. with an anthracene scintillator.[5]

Using the range-energy relation by Katz and Penfold, one obtains

$$E - E_a = \exp\left(\frac{b}{2c}\right) \exp -\left\{\left(\frac{b}{2c}\right)^2 - \frac{1}{c} \ln \left[E^{b - c\ell nE} - E_0{}^{b - c\ell n\, E_0}\right]\right\}^{1/2} . \tag{4}$$

---

[4] L. Katz and A. Penfold, Revs. Modern Phys. 24, 28 (1952).

[5] Lloyd W. Johnston, R. D. Birkhoff, J. S. Cheka, H. H. Hubbell, and B. G. Saunders, Response of the Anthracene Scintillation Counter to Low-Energy Electrons, ORNL-2298, May 1957.

The infinite integral in Eq. (1) was approximated by a finite sum,

$$Q_j \approx K \sum_{k=j+1}^{k\,max} \phi_k F_{kj} \Delta E. \tag{5}$$

The program was tested with a Maxwellian distribution and was shown to have an accuracy greater than 99%.

Plasma Source

Work has begun on the development of a new plasma source for Table Top. The present source has the following shortcomings:

a. Fluctuations: it is not very reproducible from one shot to the next.

b. Incompatibility: its energy distribution is somewhat incompatible with the magnetic trapping field of Table Top, producing an ion of substantially higher average energy than can be trapped, under normal conditions.

c. Impurity content: it releases significant percentages of impurities.

d. Inflexible: one cannot readily change the gas to be ionized or the number of ions formed.

We hope to develop a source that will overcome most of these difficulties. We plan to use a fast-acting pulsed gas valve to emit a gas slug, and then ionize and accelerate the gas with a rapidly changing magnetic field.

50-kev Electron Accelerator (for Fluor Calibration)

An electron-beam apparatus with one of the single-channel scintillator probes in place for calibration has been set up. Although the 6-kv pulse circuit for the beam deflector is not yet satisfactorily operating, a 0.6-kv circuit is now available, and by suitable modifications of the deflector plates we will be able to make preliminary measurements at somewhat lower voltages than the full 50 kv. A beam spot ~ 1/16 in. in diameter at the probe position has been obtained with no collimation other than that in the electron gun itself. (Westinghouse type 35-424, oxide-coated cathode.)

PLASMA POTENTIAL DIAGNOSTICS

Measurements of Electric Fields in the Compressed Plasma Spindle Mirror Machine - Table Top

Thomas O. Passell*

Charged-particle beams directed parallel to the magnetic axis of axially symmetric devices (such as Table Top) are subject to a deflection by the $\vec{E} \times \vec{B}$ drift mechanism if electric fields perpendicular to $\vec{B}$ exist. Such fields will exist if the plasma spindle acquires an electric potential due to the imbalance of positive and negative charge. Since the deflections are directly proportional to $\vec{E}$ they can be used to measure $\vec{E}$.

The expected magnitudes of E and the known magnitude of B in Table Top lead to the choice of the heavier charged particles (of lower velocity at a given kinetic energy). One of the simplest pulsable sources of heavy charged particles is based upon the emission of Li^+ ions by glass of composition $Li_2O \cdot Al_2O_3 \cdot 2\,Si\,O_2$ at 1200°C. A hot anode coated with the above material and placed in a standard electron gun arrangement (with reversed potentials) has been reported to emit up to 1 ma per cm^2 of exposed anode surface.[6]

Design of a Li^+ ion gun of the above type is nearly complete. After being built and tested it will be used in the measurement of the Table Top plasma electric fields.

---

*Stanford Research Institute, Menlo Park, California.

[6] J. P. Blewett and G. J. Jones, Phys. Rev. 50, 465 (1936).

ADIABATIC LOW-ENERGY INJECTION AND CAPTURE EXPERIMENT (ALICE)

Charles C. Damm in charge

Preliminary Build-Up Experiment ("BABY ALICE")

James F. Steinhaus and Charles C. Damm

We have undertaken an experiment to study plasma build-up by the trapping of 17-kev hydrogen atoms in a magnetic mirror field, with the dominant trapping mechanism being the ionization by impact with the residual gas. The charge-exchange neutralization of the trapped protons is expected to be the major loss process. The approximate differential equation for the ion-density growth on the magnetic axis within the atom beam is

$$\frac{d\rho(0)}{dt} = J_0 \rho_0 \sigma_t^n - \rho_0 \rho(0) \sigma_c^n v.$$

The notation is that of our previous progress reports. The equilibrium density is therefore independent of the neutral gas density ρ_0,

$$\rho_f(0) = \frac{J_0 \quad \sigma_t^n}{v \quad \sigma_c^n} .$$

We expect to obtain information on the ion-density distribution in both the (r, θ) and (r, Z) planes, as well as plasma build-up and decay times, for detailed comparison with theory. (We will shortly have numerical computations available for the radial ion-density distribution.) In particular in this experiment we are searching for any deviations from the expected behavior which might indicate trouble spots in the initial build-up phase of the "ALICE" experiment itself.

The apparatus is now 95% complete. The mirror coils have been tested for a central field strength of up to 15 kilogauss, with a mirror ratio of 1.5:1. At this field strength, magnet on-times of the order of a minute are possible, which is more than ample for the attainment of equilibrium conditions.

The proton beam will be neutralized in a simple hydrogen gas cell. With the presently available external ion-beam intensity of 20 ma, we can expect trapped-ion densities of about $5 \times 10^6/cm^3$ with hydrogen as the residual gas, and up to $2 \times 10^7/cm^3$ with helium as the dominant residual component. These equilibrium densities can be expected to increase as improvements in the ion source are made. No attempt will be made in this apparatus to reduce the neutral density to the value required for exponential plasma growth. The minimum ρ_0 will probably be about 3×10^{10} molecules/cm^3 (10^{-6} mm Hg).

GRID SOURCE DEVELOPMENT

Frank J. Gordon and James F. Steinhaus

In the preceding report we mentioned that it appeared feasible to extract a beam from the magnetic field of the pair of 24-in. (i. d.) solenoidal coils used for source development. However, the arc had to be positioned 8 in. off coil center and tilted 30 deg with respect to a radius line. It was assumed that the field curvature in this position would not cause too much difficulty. However, ion output dropped to essentially zero in the actual experiment.

Field maps made by freezing iron filings in Epon indicated that the curvature was such that the arc ran approximately 0.080 in. below the exit slit. This was disastrous for a hydrogen ion source. Straightening the arc with a magnetic shim helped the output considerably, but introduced field aberrations which distorted beam trajectories.

Finally, we have shortened the exit slit from 3 in. to 1 in. in order to minimize field curvature effects, and have made other small corrections in arc-chamber geometry for the same purpose. At the same time we added a filter to the accelerating voltage supply to suppress a 4% rms ripple. These changes have brought our collected and collimated beam to about 20 ma some 6 feet from the source. This is the beam presently available for the "BABY ALICE" experiment.

New rectangular magnetic field coils have been designed which will remove our curved-field difficulties in the arc region and should therefore bring back the high output reported previously. Field-intensity maps have been plotted from a mockup of these new coils, and beam trajectories have been traced by using the mechanical-particle analog. Arrangements showing acceptable focusing properties in both dimensions have been found, and a major improvement in beam intensity should result with the new magnetic-field geometry.

BEAM NEUTRALIZATION

Archer H. Futch

Work on the hydrogen jet experiment has been discontinued for the present. Before work on the hydrogen jet was initiated, a condensable-vapor neutralizer had been considered. Condensable vapors have the obvious advantage of being readily pumped by a cold surface. In particular, water vapor looked interesting; however, there were also disadvantages associated with water vapor. The higher atomic number of oxygen increases the multiple Coulomb scattering of the beam traversing the neutralizer, and an application of Fermi's formula for the rms scattering angle indicated an excessive beam dispersion in this case. In addition, the charge-exchange cross sections for water vapor were unknown.

The scattering of a hydrogen beam by water vapor was recently measured in England by Sweetman[7] and found to be considerably smaller than predicted theoretically. Both because of considerations of the effort involved and as a result of the above data, water vapor is being reconsidered as a neutralizer for "ALICE." A neutralizer has been designed and is being built for experimental study.

[7] D. R. Sweetman (Atomic Weapons Research Establishment, Aldermaston, England), private communication.

VACUUM AND SURFACE STUDIES

Charles C. Damm, Angus L. Hunt, and Earl C. Popp

The studies reported here concern gettering and getter-pump development, high-vacuum mass spectrometric studies, and the interaction of surfaces with energetic ions and atoms. Some aspects of development of the demountable vacuum seal are also reported here.

Getters and Getter-Pump Development

It has been found possible to attain pressures at least as low as 2×10^{-9} mm Hg in an unbaked stainless steel vessel which has a volume of 85 liters. This vessel can be held for at least 3 hours in the 10^{-9} range by the fusion of a single molybdenum filament, although it is known to have an air leak with a rate of 10^{-7} micron-liter/sec. During the 25 minutes chosen for evaporation of a filament, a hydrogen influx of 3×10^{16} molecules per second has been continuously gettered. After all surfaces were saturated with hydrogen, the vessel was evacuated again by the fusion of another filament.

Previously, it had been reported that sufficient molybdenum could be evaporated from a simple hairpin filament to make a pump appear feasible. A vessel was constructed which would allow installation of 169 identical molybdenum filaments. Each filament is 0.050 in. in diameter and about 6 in. long. Five hundred watts per filament is required to produce an appreciable evaporation rate. The vessel is connected to a small oil diffusion pump through two liquid nitrogen traps in series. The trap nearest the vessel is of ultrahigh-vacuum design. The walls of the vessel are water-cooled by means of copper tubing hard-soldered to the exterior walls. Three ionization gauges of the inverted structure were included. Two of three gauges agreed throughout the course of the experiment. The third gauge was defective and its indications were disregarded.

Figure 1 shows the typical pressure changes in the vessel as a filament is evaporated. In this particular case, the interior wall surfaces and all molybdenum deposits had been saturated with hydrogen to a pressure of 2×10^{-6} mm Hg. After the hydrogen was valved off, the vessel was evacuated with the diffusion pump to the base pressure of 5×10^{-8} mm Hg, the initial point of Fig. 1. Before the 500-watt evaporation was started, the filament was outgassed with a power input of 200 watts. The filament evaporated molybdenum for about 25 minutes before it fused and separated. After fuse-out, the pressure dropped to 2.5×10^{-9} mm Hg in 10 min., followed by a slow decrease to 2×10^{-9} mm Hg.

Development of Demountable Vacuum Seal

Previously we reported failure of the copper gasket in the step or pinch type of demountable vacuum seal. The seals often failed when the system was baked to 400°C.

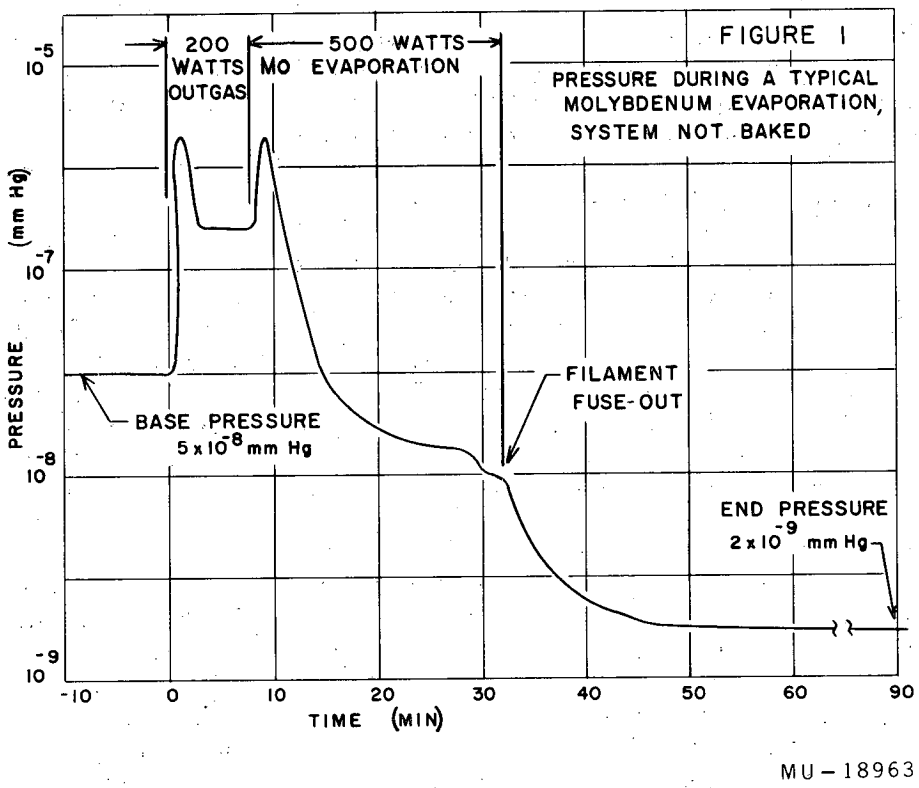

Fig. 1. Pressure during a typical molybdenum evaporation (system not baked).

Presumably, the metal gasket effects a vacuum seal for two reasons: its initial softness allows it to conform to the machining irregularities on the flange surfaces, and its hardness after deformation--a result of work hardening--provides sufficient stress in the flange assembly to maintain intimate contact between the flange and gasket surfaces. If the gasket creeps or is subject to grain growth at the operating temperature, the vacuum seal can be expected to fail.

At 400°C, the creep strength of copper is practically zero and, at that temperature, copper is 125°C above the temperature required for complete recrystallization or at which rapid grain growth can be expected.[8]

The copper gaskets were 0.040 in. thick, and the pinch overlap on the radius was 0.010 in. The final gasket thickness, with 304 stainless steel flanges shouldered, was 0.012 in., making the pinch depth 0.028 in. Failure occurred on cooling from 400°C to room temperature on all sizes from 2 in. to 16 in. in nominal diameter. Most of the gaskets were electrolytic tough-pitch copper which were annealed to a Rockwell hardness of about F 45. Similar failures occurred with annealed OFHC copper gaskets.

The Cupronickel alloys are now under investigation as a gasket material. These alloys have a creep strength at 400°C and thermal coefficients of expansion comparable to 304 stainless steel. The Cu-Ni alloys are softer than 304 stainless steel if they are annealed at 850°C for 12 to 14 hours in a hydrogen atmosphere. Grain growth is slow at the baking temperature of 400°C, and the recrystallization temperature lies between 500°C and 600°C, depending on exact composition.

Because of immediate availability, the 70% Cu–30% Ni alloy (No. 702) was examined. Five alloy gaskets were tested: three of 6 in. o.d. and two of 16 in. o.d.. They were tested on the same flanges as the copper gaskets. All alloy gaskets were annealed to at least R_B 28, as determined by test pieces accompanying the anneal. None of these gaskets leaked when baked, but they did deform the machined surfaces of the flanges.

The alloy No. 755 (10% Ni) appears to be a better choice for a gasket material with 304 stainless steel flanges. Cupronickel 755 anneals to R_B 15 while retaining a creep strength of 4500 psi for 0.01% elongation per 1000 hr at 400°C.[9] The only gasket tested to date was 6 in. in nominal diameter and remained leak-free through two thermal cycles to 400°C. The flange surfaces were not damaged. Evaluation of the reliability of the gasket of 90/10 Cu-Ni alloy No. 755 must await experience with a larger number of gaskets of various diameters.

---

[8] H. C. Mierzwinski (American Brass and Copper Company), private communication.

[9] R. C. Waltemade (Chase Brass and Copper Company), private communication.

CONTAINMENT OF POSITRONS IN THE MIRROR MACHINE

Gordon Gibson,* Willard C. Jordan,† and Eugene J. Lauer

For a description of this experiment see the earlier quarterly reports.[10, 11]

The relative counting rate due to positrons which are initially trapped (T) and which escape promptly (P) has been calculated by numerically adding the contributions from 16 equal-length axial segments, assuming all the trapped positrons escape from the weaker mirror (see Fig. 2). (Volume elements outside the mirrors contribute to P but not to T.) The ratio $F = T_s/(T_e + P)$ is measured on the fast-empty curves, where T_s is the zero-time intercept of the straight-line part of the decay curve (determined graphically), and $T_e + P$ is the equilibrium counting rate just before time zero. Assuming $T_s \cong T_e$, then $T_s/P = F/(1-F)$. The fast-empty points on Fig. 2 were obtained by multiplying the theoretical P values by $(1 + F/(1-F) \times 0.72)$, where the factor 0.72 is estimated to correct for the effect of the change in the distribution in energy of the trapped positrons due to energy loss in the gas. If T_s were less than T_e because a component of the trapped positrons enters the escape cone with a shorter time constant than τ, or if T_e/P were less than theoretically predicted because of a radial loss of trapped positrons, the measured bias curve (at positive bias) would fall below the theoretical. Experiment and theory agree for bias values greater than about 30%, showing that most of the initially trapped particles escape because of gas scattering into the end loss cones. For $-30\% < \text{bias} < +30\%$ a significant number of the trapped positrons suffer sufficiently large individual changes of direction to escape through the stronger mirror. The equilibrium bias curve ($T_e + P$) obtained when the N_e^{19} is not pumped out (normalized to the same amplitude as the fast-empty curve at -20% bias) is also shown. The agreement between the two measured curves confirms the conclusion $T_s = T_e$.

Equilibrium bias curves for larger orbit diameters have a smaller amplitude on positive bias, indicating a radial loss. At least part of this loss may be caused by radial diffusion due to gas scattering. The fact that the equilibrium positive-bias counting rate is independent of pressure (for argon pressures from 3.1×10^{-7} to 3.1×10^{-5} mm Hg) is consistent with the hypothesis that the effect is caused by diffusion due to gas scattering. However, this observation does not rule out other possibilities, e.g., a fast nonadiabatic loss.

---

*Visiting from Westinghouse Atomic Power Department, Pittsburgh, Pa.

†Visiting from Bendix Aviation Corp., Research Laboratories Division, Detroit, Michigan.

[10] Gibson, Jordan, and Lauer, in Controlled Thermonuclear Research Quarterly Report, UCRL-8775, May 1959, p. 20.

[11] Gibson, Jordan, and Lauer, in Controlled Thermonuclear Research Quarterly Report, UCRL-8887, Aug. 1959, p. 26.

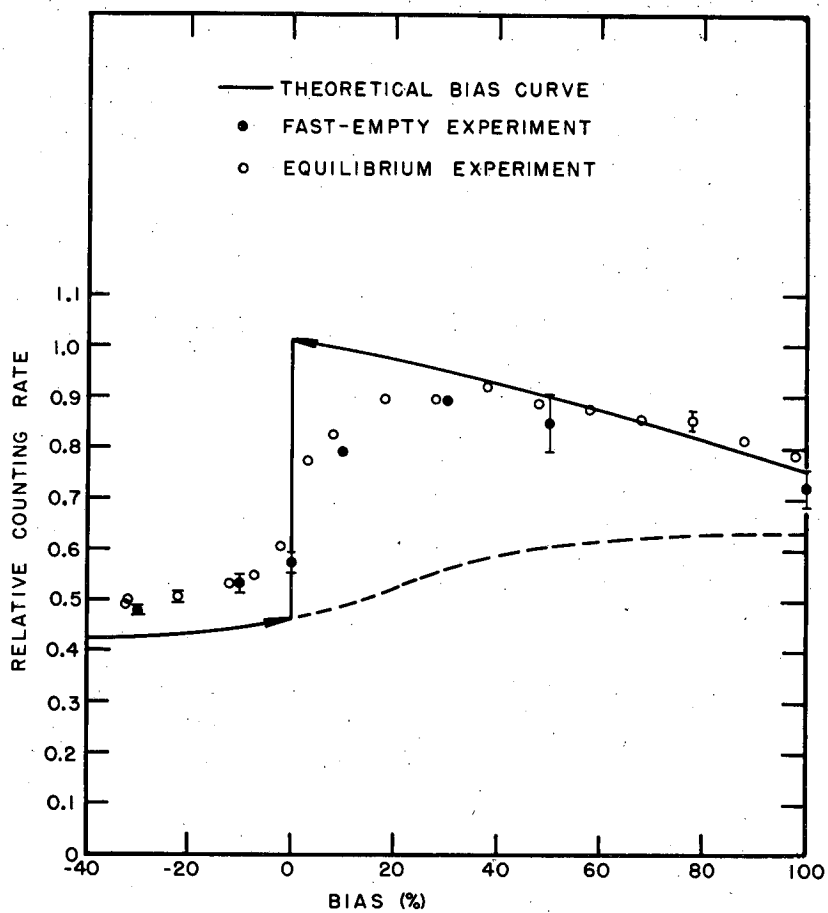

MU-18910

Fig. 2. Comparison of the theoretical bias curve with the fast-empty measurement (argon pressure = 3.1×10^{-7} mm Hg) and equilibrium measurement (argon pressure = 4.4×10^{-6} mm Hg). Single-channel analyzer = 0.5 Mev ± 10%. Central field = 1300 gauss. Counter on axis. Zero bias mirror ratio = 1.8.

These results are being checked in other gases. More accurate energy-loss correction factors are being calculated (taking account of the counter energy resolution). The effect of radial diffusion due to gas scattering is also being calculated. After data have been collected on different scattering gases, different orbit diameters, and different radial positions of the paddle (the position of the inner edge of the paddle is the effective position of the wall), it is planned to replace the present coils of 60-in. mean diameter with coils of 30-in. mean diameter; the 64-in. coil spacing will be changed to 32 in. If other parameters are held constant, this should increase the importance of nonadiabatic effects.

Large effects have been observed on the bias curves due to a small angular tilting (about 1 part in 50) of the coils. More theoretical work must be done (predicting the precessional surfaces by making use of the action integral theorem) in order to understand the significance of these effects.

Figure 3 presents some equilibrium counting-rate measurements with electric potentials up to ± 1500 volts applied to a 0.01-in.-diameter wire stretched parallel to the axis 0.8 in. from the grounded cyclindrical vacuum chamber. It is seen that these potentials caused no significant difference in the counting rate of particles escaping from the end of the machine. Fast-emptying runs were also made with wire potentials up to ± 1500 volts. Again the potentials had no significant effect upon the mean lifetimes or upon the zero-time intercepts of the decay curves. These results are of some basic interest, and also are important, since they show that it is unlikely that any of the observations are influenced by electrical fields arising from the ionization produced by the Ne^{19}.

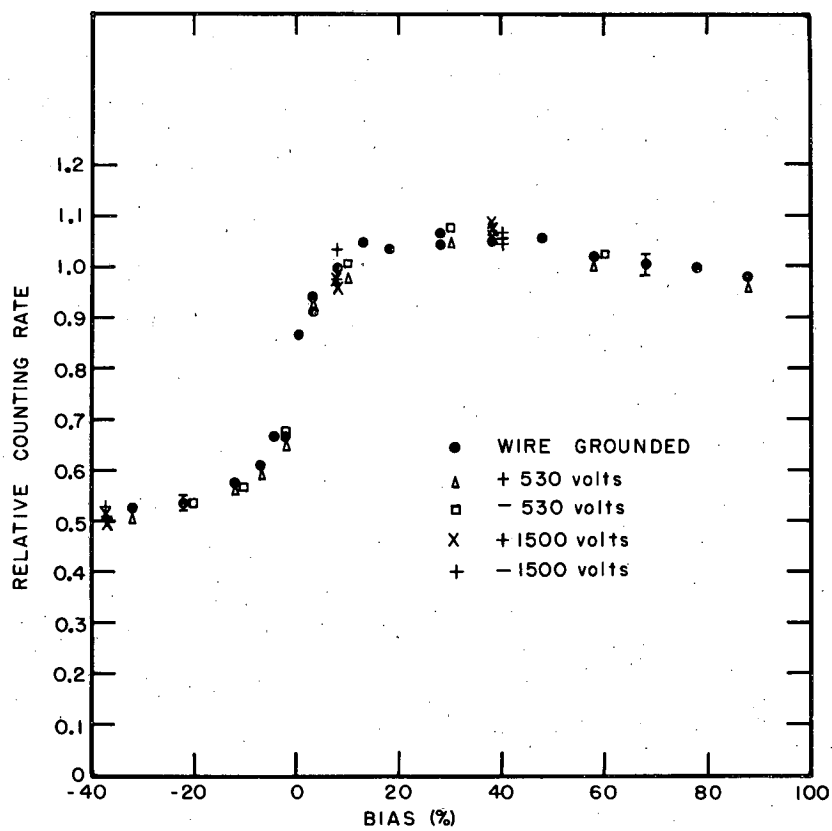

MU-18911

Fig. 3. Equilibrium bias curve--effect of electrical potential. Argon scattering gas pressure = 4.4×10^{-6} mm Hg. Single-channel analyzer = 0.5 Mev ± 10%. Central field = 1300 gauss.

P-4 (STEADY-STATE PLASMA) SYSTEM

William L. Barr, Daune M. Gall,* Andrew L. Gardner, Laurence S. Hall, Raymond L. Kelly,† and Norman L. Oleson*

The following features have been incorporated into the P-4 system to improve its performance and versatility:

(a) A corrugated bellows section has been substituted as part of the arc chamber to permit better alignment of the electrodes. This allows one to achieve greater symmetry of the plasma column.

(b) A system for directly metering the anode voltage of the discharge has been installed. Since the operating voltage is sensitively dependent on the magnetic-field configuration, this provides a worth-while monitor, particularly when potential measurements of the plasma column are being made.

(c) Provision has been made for shunting a portion or all of the input gas to a side port along the channel. This will be useful in the measurements of the pumping speed of the plasma in connection with a study of the diffusion that occurs across the magnetic field.

(d) A manual switch for quickly shorting the PIG discharge has been tested on the system. This will permit making some transient measurements on a decaying plasma.

Fabrication of the mounting units for the 50-kw tungsten lamp bank is complete, but installation will await the availability of rather limited manpower.

Installation of the remaining equipment for end injection of a pulsed beam of electrons from an Eimac 4K 50,000 LQ gun is likewise not expected immediately.

Spectroscopic Measurements

Additional measurements have been made of the Doppler broadening of the 4686-A He^+ line. At the downstream portion of the plasma column line widths corresponding to ion temperatures up to 8 ev were observed.

A study was made of the variation of the intensity of several spectral lines with distance along the plasma column. It was found that the intensity of the ion lines fell off more slowly with distance from the PIG than did the intensity of the neutral lines.

Some preliminary measurements have been made in which the intensity of a particular line was recorded as a monochromator scanned vertically through the horizontal plasma beam. Such data together with probe data will be useful in the study of radial diffusion of the plasma.

---

*U. S. Naval Postgraduate School, Monterey, California.

†Stanford Research Institute, Menlo Park, California.

Probe Measurements

Design and most of the fabrication of a rotating probe mechanism have been completed. Three probes will be mounted in spoke fashion on a continuously rotating axle, and it is hoped that meaningful measurements may be made all the way to the axis of the plasma column.

Additional data have been analyzed from the stationary probe measurements made in the outer portions of the plasma. The plasma potential was found to fall about 20 volts as the probe was moved radially inward from the outer boundary to the edge of the dense core of the plasma.

Immediate Program

Work in the immediate future will be oriented toward a study of plasma diffusion across a magnetic field and a survey of methods for measuring excitation and ionization cross sections of lithium-like impurity ions in the plasma.

Technical Report

A technical report describing the P-4 system is nearing completion.

Papers for Monterey Meeting

Abstracts have been submitted for three papers to be presented at the forthcoming Plasma Physics Division meeting of the APS in Monterey. These will describe:

1. The over-all system: Andrew L. Gardner, Laurence S. Hall, and D. E. Edwards, P-4 - A Steady-State Plasma System. (Presented by Gardner.)

2. Probe measurements: Norman L. Oleson and Daune M. Gall, Probe Measurements in P-4. (Presented by Oleson.)

3. Spectroscopic measurements: William L. Barr and Raymond L. Kelly, Spectroscopic Measurements in P-4. (Presented by Barr.)

II. HIGH-ENERGY INJECTION

A PARAMETER STUDY OF THE HIGH-ENERGY MOLECULAR-ION INJECTION SYSTEM

Francis C. Gilbert, Warren Heckrotte, and Ross E. Hester

The solutions of the energy-dependent equations indicated that the ion energy loss to the arc electrons may be the dominant process limiting build-up in machines using high-density arcs. It is therefore necessary to design the machine in such a manner that it is possible to transfer from the arc-on to the arc-off mode of operation and maintain a large trapping fraction for the injected beam at all times.

The results one obtains using the energy-dependent equations for build-up may be crudely predicted by

$$n_\tau = \frac{I \cdot \tau}{V_1}, \tag{1}$$

where

n_τ = density of trapped ions (of all energies) at which the arc energy loss locks the system,

I = input molecular-beam current,

V_1 = volume of the trapped plasma,

τ = time for ion energy to be reduced to 20 kev (τ may be further defined as $\tau = \frac{a}{n_A}$),

n_A = average arc electron density seen by the trapped ions.

a = a function of arc ion density, arc electron temperature, and a given ion injection energy.

In order to insure that most of the beam is trapped at all times, we require that Eq. (2) be satisfied:

$$\frac{n_A}{2} \sigma_t L + \frac{n_\tau}{3} \sigma_t L \geqslant 2, \tag{2}$$

where

σ_t = an average trapping cross section per arc electron,

L = path length of the molecular ion before it returns to the inflector.

The factors 1/2 and 1/3 which appear in Eq. (2) depend upon the fractions of time that the molecular ion spends in the arc and in the trapped plasma, respectively. Equation (2) may be satified by allowing n_A to reduce while n_τ increases. Coupling Eqs. (1) and (2), one finds that a minimum occurs for the left-hand side of Eq. (2) for a critical transfer current,

$$I_\tau = \frac{6V_1}{a\sigma_t{}^2 L^2} \quad . \tag{3}$$

This transfer current is different from the critical current that satisfies the burnout condition and may be a much larger current.

We now define $$L = \frac{\ell P}{\theta} \quad ,$$

where

ℓ = distance between the mirrors,

P = number of traversals of the machine length that the molecular beam makes before returning to the inflector, and

θ = pitch angle of beam orbits.

It is obviously desirable to minimize θ; the dimunition of θ is limited by the divergence of the beam and the physical size of the inflector. Perhaps one of the best ways to minimize θ is to inject the beam into a bump in the field near one mirror at a fairly large value of θ which will be tightened up as the beam enters the straight section of the machine. If $\Delta\theta$ is the total divergence of the beam and if the minimum pitch angle at the inflector for any beam component is θ_1, the maximum pitch angle is $\theta_1 + \Delta\theta$. The pitch angle of θ_1 must be large enough to allow the beam to miss the inflector on the first turn, i. e.,

$$\theta_1 = \frac{R}{2\pi\rho} \quad ,$$

where

R = the half width of the inflector,

ρ = radius of curvature of the molecular ions.

If the magnetic fields are adjusted to reduce the pitch angle of this inflector grazing ray to zero as the beam enters the straight section of the machine, it can be shown that we have

$$\theta \simeq 2\theta_1 \Delta\theta = R \frac{\Delta\theta}{\pi \rho} \quad .$$

We shall now assume that the size of the inflector varies as the square root of the magnetic field and of the injected current, as shown in Eq. (4),

$$R = r_0 \left(\frac{B\, I_\tau}{B_0 I_0}\right)^{1/2} \quad , \tag{4}$$

where

$$\rho = \frac{(2Em)^{1/2}}{Be},$$

$E =$ energy of H_2^+,

$E = 2Ve$, where Ve is the energy of the H^+ ions in electron volts,

$m =$ mass of H_2^+ ion.

For H_2^+ energies greater than 200 kilovolts the trapping cross section σ_t varies approximately as the reciprocal of the square root of the molecular ion energy, as given by Eq. (5),

$$\sigma_t = \sigma_0 \left(\frac{V_0}{V}\right)^{1/2}, \tag{5}$$

where V is once again the potential of the trapped H^+ ion.

Energies less than 200 kev are uninteresting because the burnout condition,[1]

$$k > \left(1 + \frac{\beta + i/I}{\alpha}\right) \frac{\sigma_{cx}}{\sigma_{cx} + \sigma_i} > 0.4, \tag{6}$$

is too difficult to achieve.

Equation (3) may now be written as

$$I_\tau = \frac{1.44 \times 10^2 \, r_0^2 \, m \, (\Delta\theta)^2}{B \, B_0 \, e \, \ell^2 V_0^2 \, \sigma_0^4 P^4 \, I_0} \cdot \frac{V^3}{a^2} \text{ ions/sec.} \tag{7}$$

As an example we shall now use the values listed in Table I to calculate the transfer current as a function of the electron temperature.

[1] Gilbert, Heckrotte, Hester, Killeen, and Shanack, Calculation of Plasma Buildup from High-Energy Injection, in Controlled Thermonuclear Research Quarterly Report, UCRL-8775, June 1959, p. 16.

Table I

Parameters for calculating transfer current

B	=	1 weber/meter^2
r_0	=	5×10^{-2} meters for B_0 = I weber/meter^2 and $I_0 = 2\times10^{18}$ ions/sec
m	=	3.3×10^{-27} kg
$\Delta\theta$	=	$\frac{1}{30}$ radian
e	=	1.6×10^{-19} coulombs
σ_0	=	3×10^{-20} meter^2 for H_2^+ energy ($2V_0$) of $2\times10^{+5}$ volts
P	=	8
ℓ	=	3 meters

Figure 4 shows a plot of the transfer current I_T versus the electron temperature T, for the parameters in Table I plotted for three initial H_2^+ energies. One must conclude from Fig. 1 that, if the transfer current should be the limiting factor in the build-up process, then for a given investment in mirror-machine parameters, there is little point in exceeding the injection energy that satisfies the burnout condition, Eq. (6).

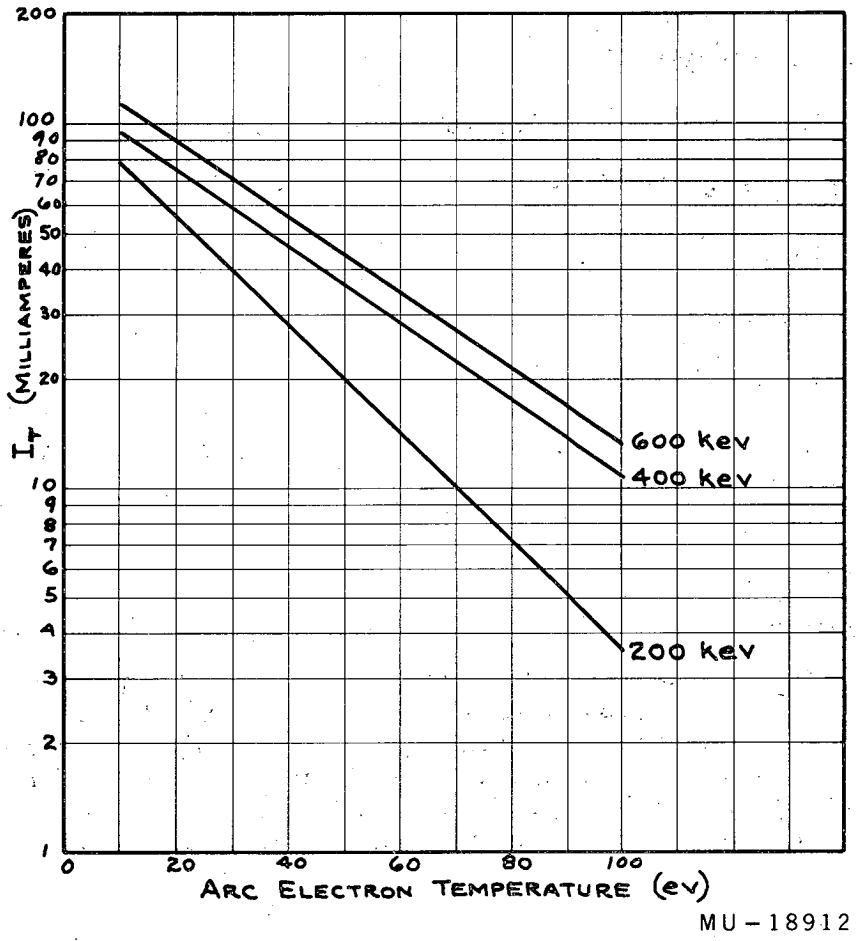

Fig. 4. Transfer current as a function of arc electron temperature for three different H_2^+ energies.

DISSOCIATION OF D_2^+

Gordon Gibson,* Willard C. Jordan,† Eugene J. Lauer,
Robert L. Leber, Cornelius H. Woods, and John R. Ullman

During the past quarter an administrative decision to discontinue the High-Energy Injection Program has led to a decision to discontinue this experiment. On the basis of the experience gained to date there is no technical reason to believe that the method being developed for measuring the rate of dissociation of a D_2^+ beam in a D^+ target arc[2] would not yield a significant result.

The status of the experiment at the time it was discontinued was as follows: The reflex target arc had been operated approximately 50 hours, with--at various times--argon, neon, nitrogen, deuterium, and air. Particular attention was paid to the performance when the latter two gases were used. Air was used to compare the performance with that of arcs previously made,[3] and deuterium was used in the same configuration to determine the corresponding performance of the D^+ arc.

With air, the pressure, with a given air leak into the arc chamber, could be made to drop by a factor of fifteen when the arc was turned on. With deuterium, this factor was about one-third as large. This ratio is significant because it is an indication of the ion density in the arc relative to the density of molecules surrounding the arc. In the dissociation measurement it is necessary to maximize this ratio. The pressure around the arc was 1×10^{-4} mm Hg for air and 5×10^{-4} mm Hg for deuterium.

For making the dissociation measurement it is desirable to have a space on each side of the arc where the beam can be deflected in and out of the arc and be magnetically analyzed, and where the pressure is less than 1×10^{-7} mm Hg.

---

*Consultant from Westinghouse Corporation, Atomic Power Division, Pittsburgh, Pennsylvania.

†Consultant from Bendix Aviation Corporation, Research Laboratories Division, Detroit, Michigan.

[2]Gordon Gibson and others, in Controlled Thermonuclear Research Quarterly Reports, UCRL-8775, June, 1959, p. 74; UCRL-8887, Sept. 1959, p. 115.

[3]John Stuart Foster, Some Measurements on a High-Vacuum High-Speed Ion Pump (Thesis), UCRL-2312, Aug. 1953.

The next step in making the dissociation measurement would be to make an arc chamber of twice the previous length, and attach it to an analyzing manifold (rectangular box) which would be evacuated at 2000 liters per second. The length of arc inside the collimators would then be several times the original length, and according to Foster[3] the center pressure could be expected to be reduced by a factor of eight or ten. Further, if the conductance between the arc chamber and the analyzing manifold were made as small as possible commensurate with passage of the D_2^+ beam through the arc (approximately 200 liters per second), the D_2^+ beam could be deflected and analyzed in a region where the pressure would be determined only partly by the pressure in the arc chamber. The parts already fabricated for this assembly in which the dissociation measurements were to be accomplished include

(a) the solenoid coils,

(b) the analyzing manifold,

(c) a 20-in. -diameter gate valve for connecting the analyzing manifold to the pump,

(d) a 20-in. diffusion pump.

The power sources and control apparatus used in operating the experimental target arc were purposely designed to function equally well for the longer arc, and these have been so arranged that they permit operation of the system in the experimental area of the Cockcroft-Walton accelerator.

III. ASTRON PROGRAM

INTRODUCTION

N. C. Christofilos

During the past quarter the emphasis of effort was more on experimental aspects and on the design of the 2-Mev step than on theoretical work. However, an initial formulation of the problem of interaction of electron beams of finite size with an infinite plasma has been attempted. The results are described briefly in the next part of this section, (p. 35) as well as the contemplated steps for the solution of this problem under the parameters and geometry of the E layer. The first results appear encouraging in that no unstable normal modes have been found in the first approximation. Furthermore it appears that the behavior of a finite-sized beam with a smoothly varying density is markedly different from the behavior of the infinite medium. Consequently no comparison of the E layer with results on infinite beams (two-stream instability, etc.) is justified.

Dr. Lewi Tonks extended his calculations on the self-consistent field of the E layer, including the slow-down process. For the parameters of interest it appears that a smooth transition from unreversed to reversed field is possible. His results appear below.

The experimental work was concentrated on measuring the lifetime of the electrons injected in the "dry-run" experiment. A special scintillation counter designed by Dr. Hans Mark and Dr. Robert Jopson is described, and W. A. S. Lamb and Dr. Jopson give the experimental results they obtained with the use of these special counters.

It appears that the trapping time is a function of the gas pressure and that the trapped electrons die naturally by scattering through the mirror. Trapping times longer than 1 second have been observed. Since the counters are saturated with relatively low electron density, more measurements are contemplated with magnetic probes, so that the field reduction caused by the E-layer current will be directly observed. Then it is possible to calculate the total number of the trapped electrons and their lifetime.

The design of the 2-Mev accelerator has been completed up to the point where some hardware, especially the laminated steel cores, can be ordered. Also the general design is completed for the modified gun, which will provide a 200-amp electron beam. The contemplated 2-Mev step has been officially approved by the Laboratory and orders are now being placed. The completed accelerator, as well as the Astron facility including the new injection system, is expected to be ready in less than a year.

INTERACTION OF RELATIVISTIC ELECTRON BEAMS WITH A QUASI-NEUTRAL PLASMA

N. C. Christofilos

The study of the stability of the E layer is a very complicated and difficult problem. Consequently the reasonable way to approach this problem is by successive approximations. It is contemplated in successive steps to study:

1. The interaction of finite-sized electron beams of simplified geometry, namely:

a. An infinite-plane slab of electrons parallel to the y-z plane. The stream moves along the z direction. The electron density peaks at x = 0 and decreases smoothly for negative or positive x. The density distribution is an even function of x.

b. A cylindrical axial symmetric beam. The electron distribution is a monotonically decreasing function of the square of the radius.

2. A cylindrical axial symmetric beam, as Case 1b, but with a density distribution in which the density is zero at the origin and maximum at certain radius. The electron velocity is along the z direction.

3. A cylindrical axial symmetric beam, like that in Case 2, but with the electron velocity along the θ and z directions. Two electron streams with their axial velocities opposed will be assumed. This case represents the geometry and velocity orientation of the electrons in an E layer of infinite length.

In all the above cases the electron velocity has been assumed as a δ function. If, during this study, an instability is discovered, it will be necessary to drop the δ-function velocity distribution and consider the actual velocity distribution as it can be derived from the scattering process.

Thus far, only Case 1 has been investigated. The perturbation has been assumed in the form

$$f(x)e^{i(\omega t-kz)}.$$

The equations governing the beam-electron and plasma-electron behavior are

$$\gamma m_0(\omega-kv)^2\,\vec{\xi} = e\left(1-\frac{\vec{v}}{c^2}\cdot\vec{v}\cdot\right)\vec{E} + e\,\frac{\vec{v}}{c}\times\vec{B}, \tag{1}$$

$$\omega^2 m_0\,\vec{\zeta} = e\vec{E}, \tag{2}$$

$$\vec{E} = 4\pi e(n_b\,\vec{\xi} + n_e\,\vec{\zeta}) + \frac{c}{i\omega}\,\nabla\times\vec{B}, \tag{3}$$

$$-\frac{i\omega}{c}\vec{B} = \nabla \times \vec{E}, \tag{4}$$

where $\vec{\xi}$, $\vec{\zeta}$ are the displacements of the beam electrons and plasma electrons respectively, γ is the energy of the beam electrons in rest mass units, $\vec{v}$ is the velocity of the beam electrons, and E and B are the disturbed electric and magnetic fields respectively. Finally n_b, n_e are respectively the beam-electron and plasma-electron density.

In the above equations the hydrodynamic terms $\xi \times B_0$ have been omitted and from Eq. (3) the term

$$4\pi e \frac{ik\vec{v}}{\omega} \cdot \frac{\partial (n_b \xi_x)}{k \partial x} \quad \text{also has been omitted.}$$

The derived dispersion relation is

$$\left[1 - \frac{\omega_e^2}{\omega^2} - \frac{\omega_b^2}{(\omega - kv)^2}\left(1 - \frac{\vec{v}}{c^2} \cdot \vec{v}\right)\right] E = \frac{c^2}{\omega^2} \nabla \times \nabla \times \vec{E} + \frac{\omega_b^2}{(\omega - kv)^2} \frac{i\vec{v}}{\omega} \times \nabla \times \vec{E}, \tag{5}$$

where ω_b, ω_e are the beam-electron and plasma-electron frequency.

The development of this expression (for the particular cases 1a and 1b) and the possible solutions were examined. Solutions were sought in the vicinity of $\omega = kv + \epsilon$, where ϵ/ω is a very small number. The beam distribution in the case of infinite slab is

$$n = \frac{n_0}{\cos h^2 (k_e x)}, \tag{6}$$

where k_e is the inverse half width of the slab.

The derived differential equation is satisfied by Legendre polynomials, namely

$$E = p_n^m \left[\tan k(k_e x)\right], \tag{7}$$

where m^2 is proportional to the plasma density, and $n > m$. This solution exists only for

$$\frac{\omega_b^2}{2\gamma^2 k_e^2 c^2} << 1 .$$

For large values of ϵ/ω no normal-mode solution exists. The derived solution shows no instability. Similar expressions were found for the cylindrical beam.

These results are considered encouraging. However, no conclusions are attempted yet until further approximations are available. The next steps

are (a) to include the term

$$4\pi e \frac{ik\vec{v}}{\omega} \frac{\partial (n_b \xi_x)}{k \partial x},$$

and (b) to include the terms $\xi \times B_0$.

If after the inclusion of these terms still no instability can be discovered, we should abandon the normal mode analysis and seek general solutions of the type

$$f(x, t)e^{ikz}.$$

The only conclusion warranted at this time is that the behavior of the finite-sized beam is decidedly different from the case of the infinite medium. The reason is that no solution is admissible, satisfying the dispersion relation, for $\nabla \times E = 0$. In contrast, if we assume constant density and $\nabla \times E = 0$ we observe that the left-hand side of Eq. (5) is nothing else than the familiar dispersion relation for the two-stream instability. Consequently, because in a finite-sized beam in any solution $\nabla \times E$ is not equal to 0, the behavior of the interaction changes drastically. Hence no inference or conclusion about the stability of the E layer derived by extrapolations of solutions in infinite media is justified. The next step in this study will further clarify the behavior of the E layer.

ASTRON E-LAYER CALCULATIONS

Lewi Tonks*

Results of earlier studies have been reported for publication.[1]

The "slowing down" problem (electrons slowed down but not scattered by the dynamical friction of a uniform plasma) is being explored in the main for three initial energies of electrons, namely, 5, 15 and 40 Mev, at the suggestion of N. Christofilos.

In the earlier problems reversal of field was contingent upon having $G > 2$, where G is the ratio of the external radius of the E layer to the gyration radius of the virgin electron in the vacuum-impressed field. Now, small reversal can occur with G as low as 1.3. It continues to be the low values of G which offer the smoothest transition from unreversed to reversed field with increasing electron injection rate, S.

Two distinct iteration schemes have been developed: Scheme A (including B) and Scheme C (including C'). In Scheme A, electrons to the number established by a fixed injection rate S move in the vacuum field, B_2. Their own contribution to a resultant field is neglected. Their slowing down is calculated and then their own field. The sum of this field and the vacuum field then constitutes the first approximation to a self-consistent field, and is therefore used as a replacement for the vacuum field in the next calculation of electron slowing down, trajectories, and field contribution. The refinement of field continues until the routine has given convergence or until some maximum number of cycles has been run through (15 was the number chosen), and then S is increased by a predetermined amount ΔS to give S_{II}. This number of electrons is now circulated in the final field found for S_I, and so on. This stepwise process continues until the E layer becomes so thin that it includes too few mesh points for a meaningful calculation, and then it is terminated.

Scheme A recommends itself because it constitutes a crude analog of the actual build-up process for the E layer. Its disadvantage is computational, in that the convergence is impractically slow in some cases and can lead to the judgment that convergence has been attained when actually it has not.

In Scheme C it is the magnetic-field strength at a particular radius which is kept fixed, and the iterations converge on a value of S. Here electrons to the number established by a unit injection rate move in a magnetic field which has the value B_2 at the periphery r_2 of the E layer,

---

*Consultant to LRL from General Electric Co. Vallecitos Atomic Laboratory, Pleasanton, California.

[1] Lewi Tonks, The Self-Consistent Field and Motion of Electrons Which Have a Range in Canonical Angular Momentum in a Uniform Magnetic Field (submitted to Phys. Rev.).

adjacent to the vacuum, and the value $B_2/2$ (though some other fraction could be chosen at a lesser radial distance, ρr_2. A field varying linearly with radius is convenient. The field of these electrons is then calculated, and the injection rate S is found which would give a resultant field of vacuum and electron fields which is equal to $B_2/2$. This new field then replaces the previous one as a milieu for the electrons, the next approximation to S is calculated, and so on.

By use of this scheme, behavior has been found that is very similar to that shown by the G = 8 curves of Figs. 7 and 8 in the paper referred to above.[1] This is shown here in Fig. 5 for 5-Mev electrons and G = 4. The internal field is plotted as its ratio to the vacuum field against S. There are 90 radial meshes in the machine computation, and the inner edge of the E layer, in these mesh units, is also plotted against S. Negative values correspond to the circumstance that the individual electron gyrations do not encircle the axis. It is seen that as S increases from zero the E layer thickens and the internal field increases above its vacuum value. Reversal occurs suddenly as the E layer reaches the axis, whereupon the layer shrinks away from it with the electrons now encircling it. In this regime the layer becomes thinner and the reversal less as S decreases.

Naturally the stability of the latter regime was questionable. Scheme B was devised to explore this, since the regime is inaccessible to Scheme A. Scheme B is like A in that S is fixed, but the initial field used is not the vacuum field but a linear one as in Scheme C. The test was to use the linear field corresponding to S = 9.32 and to iterate from it with S = 9.32. This, it was felt, would give very favorable conditions for converging on the corresponding reversed-field configuration found by Scheme C. When this was done the successive iterations gave E layers of increasing thickness with generally less negative internal fields. At Cycle 12 the inner radius of the E layer was 0.25 r_2. For Cycle 13 the layer filled the whole space and the field was unreversed, and Cycles 14 and 15 were consistent with convergence on the unreversed branches of the curves in Fig. 5. It is therefore practically certain that the reversed-field configurations in this case are unstable and unattainable.

Reversed fields which are not associated with an ambiguity of configuration have been found by Scheme A in a number of cases, so that there is no doubt regarding the absence of the just-discussed type of instability in useful ranges of the parameters.

Figure 6 is an example of what is believed to be stable reversal for 40-Mev electrons. A family of trajectories is given for the electrons at various stages of slowing down, namely at 40 times 1, 4/5, 3/5, 2/5, and 1/5 Mev. Since the figure was drawn it has been found that for S = 3.46, one has $B_1/B_2 = 0.63$, and the inner radius of the layer is then at $\rho = 0.82$.

The task of assembling a usefully comprehensive set of results for the three energies--5, 15, and 40 Mev--continues. Another question demanding attention is whether or not a uniform cylindrical E layer may be unstable under certain conditions because of the attraction of neighboring current elements. This could cause "sausage" instability. Axial momentum tends to stabilize. Such an instability, if its degree is controllable, may supplement or replace mirror fields. This is a matter I shall look into as opportunity permits.

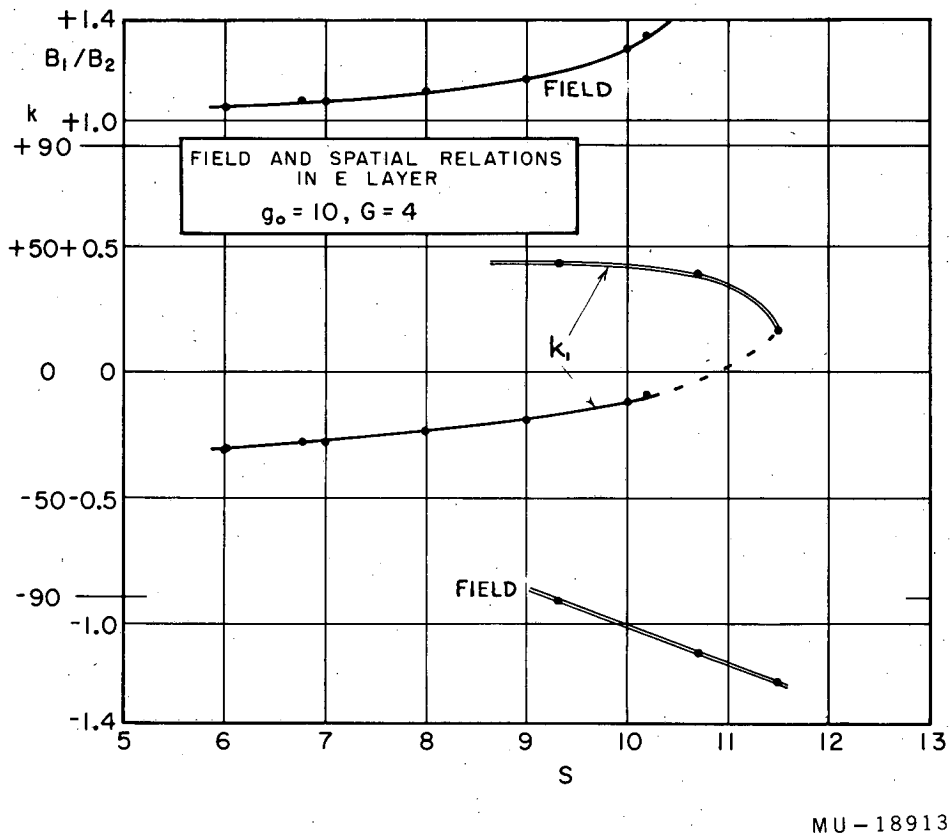

Fig. 5. Field and spatial relations in E layer.

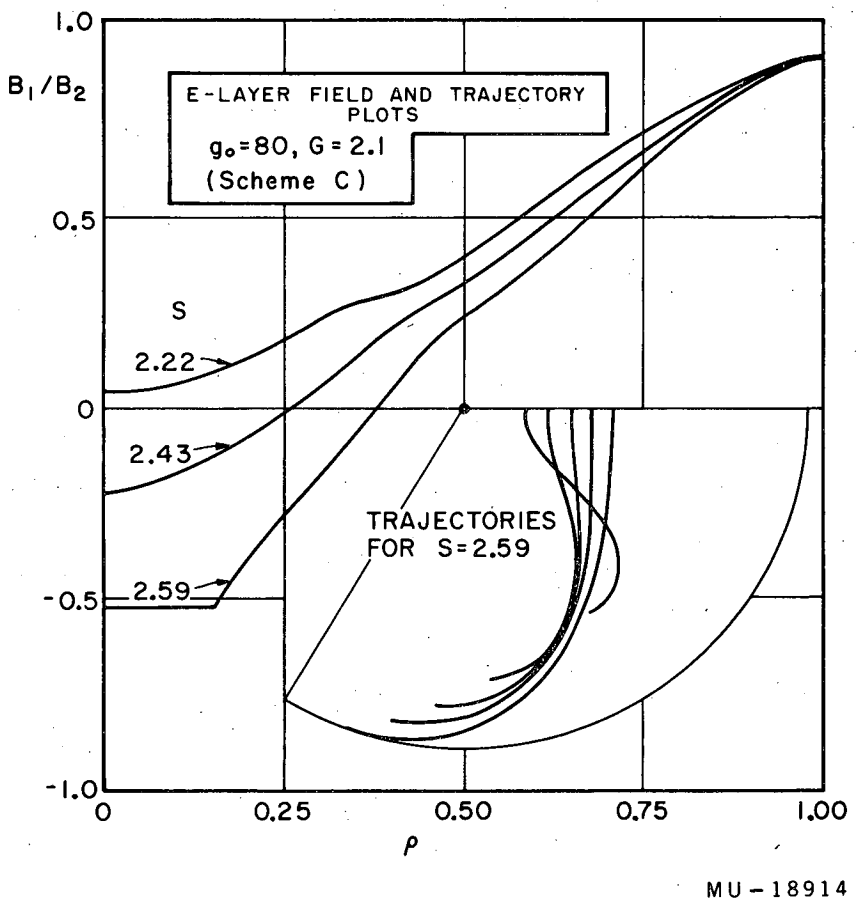

Fig. 6. E-layer field and trajectory plots.

THIN-FIBER SCINTILLATION COUNTERS FOR EXPLORING THE ELECTRON DISTRIBUTION IN THE ASTRON DEVICE

Robert C. Jopson and Hans Mark*

The successful operation of the 800-kev Astron electron gun and E-layer tank has raised the question of how to best diagnose the events in the device which follow the injection of the pulse. In July and August measurements of x-rays emitted when electrons strike the walls of the tank showed that electrons are actually trapped in the vessel for considerable periods (8 msec) after the injection of the pulse. In the following, a counter is described which allows exploration of the electron distribution inside the tank by detecting the electrons themselves, rather than x-rays produced by them.

The counter to be used for this purpose must have the following properties:

1. It must be small enough that its presence inside the machine will not substantially disturb the electron configuration.

2. It must be movable, so that exploration of the electron distribution is possible.

3. It must be essentially insensitive to the background x-rays.

4. The response time of the counter must be fast enough so that information can be obtained about the time sequence of the events occurring in the machine.

The small plastic scintillation fibers (as small as 0.5 mm diameter) recently developed for use in high-energy physics seem to satisfy all the above conditions. (See Fig. 7) The scintillating fibers can be mounted on long flexible glass light pipes (20 feet), which allow considerable freedom of movement inside the tank. The fiber has a light flash for every electron that passes through it, whereas the x-rays must first interact with an electron in the fiber before a light pulse occurs. The interaction mean free path of 100-kev x-rays in the plastic is about 2 cm, and for 10-kev x-rays it is 0.2 cm. This means that a fiber having a diameter of 0.5 mm should have a conversion efficiency of about 1% for 100-kev x-rays and 10% for 10-kev x-rays. Although the 10-kev x-rays have an appreciable conversion efficiency, the pulses produced by these will be so small that it should be easy to discriminate against them electronically. However, care must be taken that there is no pile-up from low-energy x-rays. Finally, the response time of plastic scintillators is of the order of 10^{-8} second, which is very much shorter than the times characteristic of the decay of the trapped electrons.

*Massachusetts Institute of Technology, Cambridge, Massachusetts.

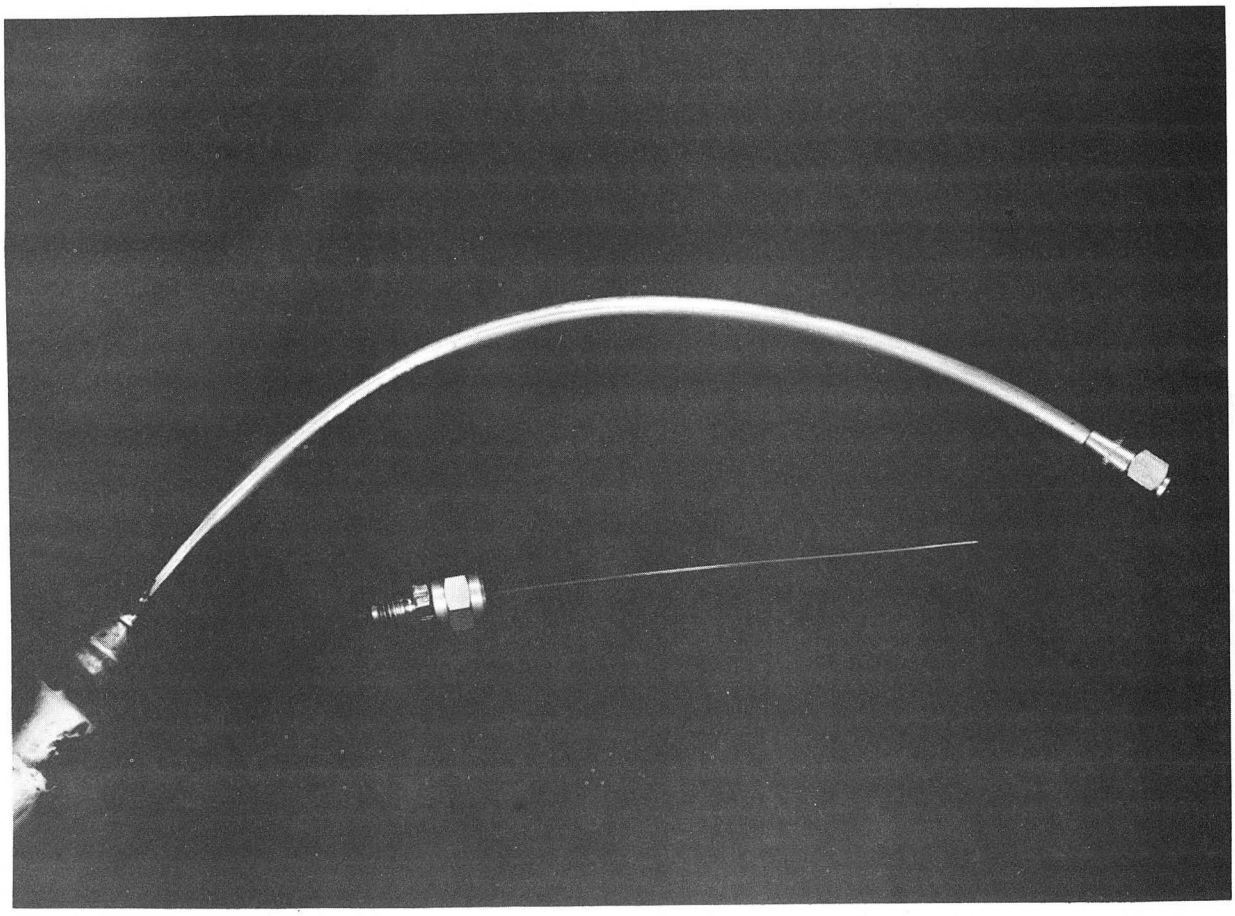

ZN-2298

Fig. 7. Plastic scintillator assembly. Above: the 1-mm glass light tube which carries the light to the photomultiplier tube outside the vacuum, shown just coming out of its assembly. Below: the scintillator and the collet with which it is joined to the glass light tube.

Under operating conditions with the Astron machine, the light pipes are led into the machine through vacuum seals in the end plates. Since the light pipes should not exceed 20 feet in length, it is necessary to operate the phototube inside the main coil extensions in a field of the order of 100 gauss. Several tests were made and it was shown that only moderate magnetic shielding was necessary to operate the RCA 6810 A phototube inside the field. It was found, however, that the phototube had to be shielded with ~ 1 in. of lead to protect it from x-rays, and in addition, had to be electromagnetically shielded so that the characteristic excitation frequency of the cavity was not bothersome. The glass rod going into the cavity had to be shielded from x-ray radiation to prevent rapid darkening of the glass.

DESCRIPTION OF ASTRON EXPERIMENTS

William A. S. Lamb and Robert C. Jopson

Figures 8 and 9 show respectively an over-all view of the Astron dc test facility and a view of the inflection end of the vacuum chamber.

During this period experiments were performed using the scintillation-counter techniques described above. Figure 10 shows diagramatically the typical arrangement of this apparatus in the Astron dc test machine. It should be noted that the scintillator thread either extended radially all the way across the annulus presumed to be occupied by trapped electrons or only a small fraction of this radial distance.

In these experiments coil B (the mirror coil on the end opposite to the beam inflection apparatus) was energized by a dc power supply, and an additional power supply was added to coil A (the mirror coil at the inflection end of the machine) to maintain the mirror field for times greater than a few milliseconds. Briefly coil A was energized by a fast rising pulse (0.1 μsec) to trap the injected beam, followed by a slower-rising pulse (1 μsec) which was crowbarred and maintained until a dc supply could be switched on which could be maintained for several seconds. The A mirror-coil current under these circumstances undergoes fluctuations during the first several tens of microseconds due to the superposition of pulses from these three power supplies, which is doubtless responsible for the loss of many electrons in the initial trapping.

In order to maintain linearity of the counting apparatus it was further required to operate the electron accelerator at greatly reduced current output. Generally these experiments were performed with less than 1 amp peak current. A further effect was a large increase in electrical noise as the current injected was increased. This was believed to be due in part to radio-frequency oscillation of the vacuum cylinder of the machine excited by the introduction of the electron beam.

The first series of measurements was performed with the scintillator thread all the way across the radius of the annular volume occupied by the trapped electrons. Figure 11 is a sketch of a typical oscilloscope trace observed at the output of the multiplier phototube. On the basis of the assumptions that

(a) every electron that hits the scintillator is lost to the system due to energy loss and scattering,

(b) the electrons are uniformly distributed in the volume defined by the two mirrors and the annulus defined by diaphragms at the inflection end,

then the probability per revolution of an electron's hitting the scintillator is

$$\frac{d}{\ell},$$

where d is the diameter of the scintillator and ℓ is the distance between mirrors.

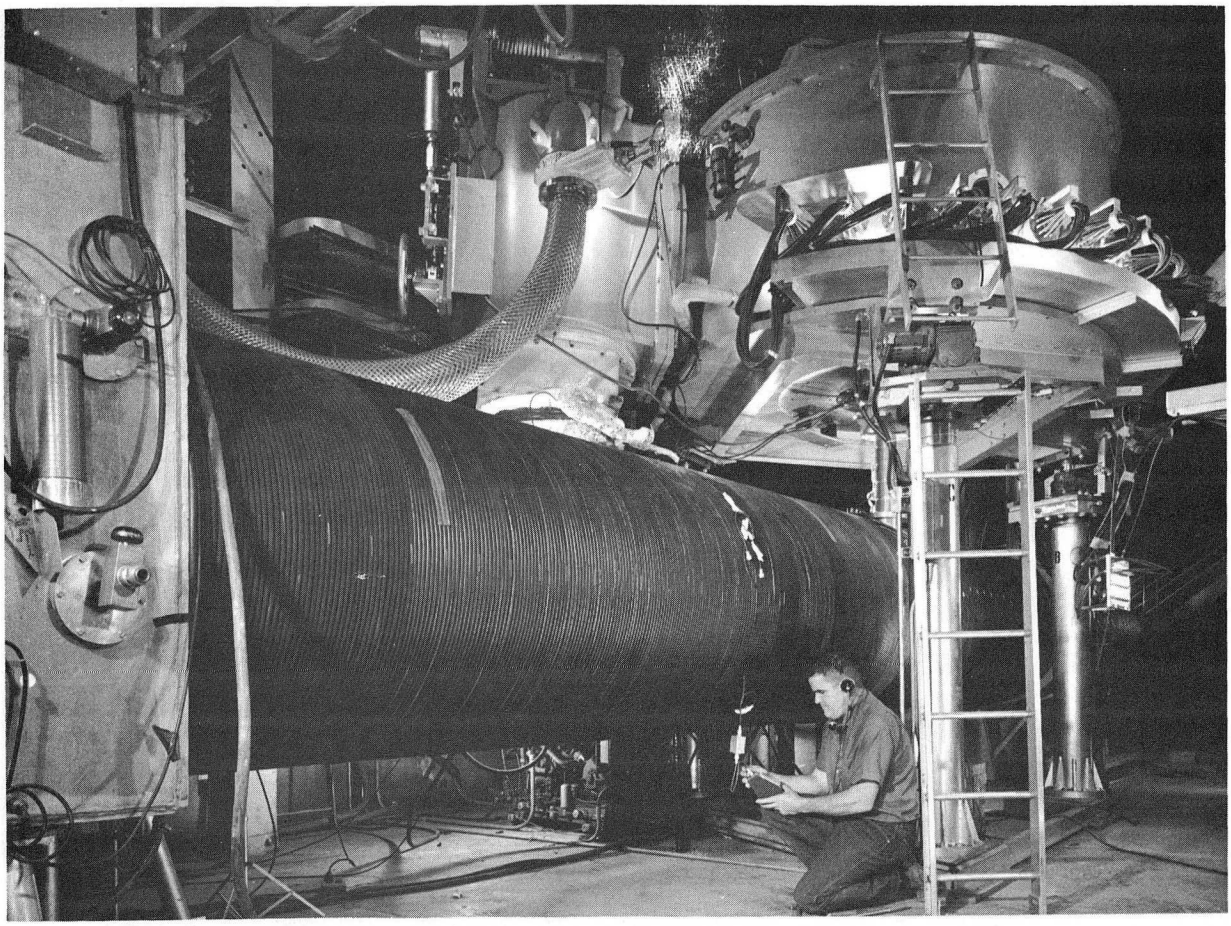

ZN-2297

Fig. 8. Over-all view of the Astron dc test facility. The 750-kev electron accelerator is at the upper right and the vacuum system is shown in the foreground.

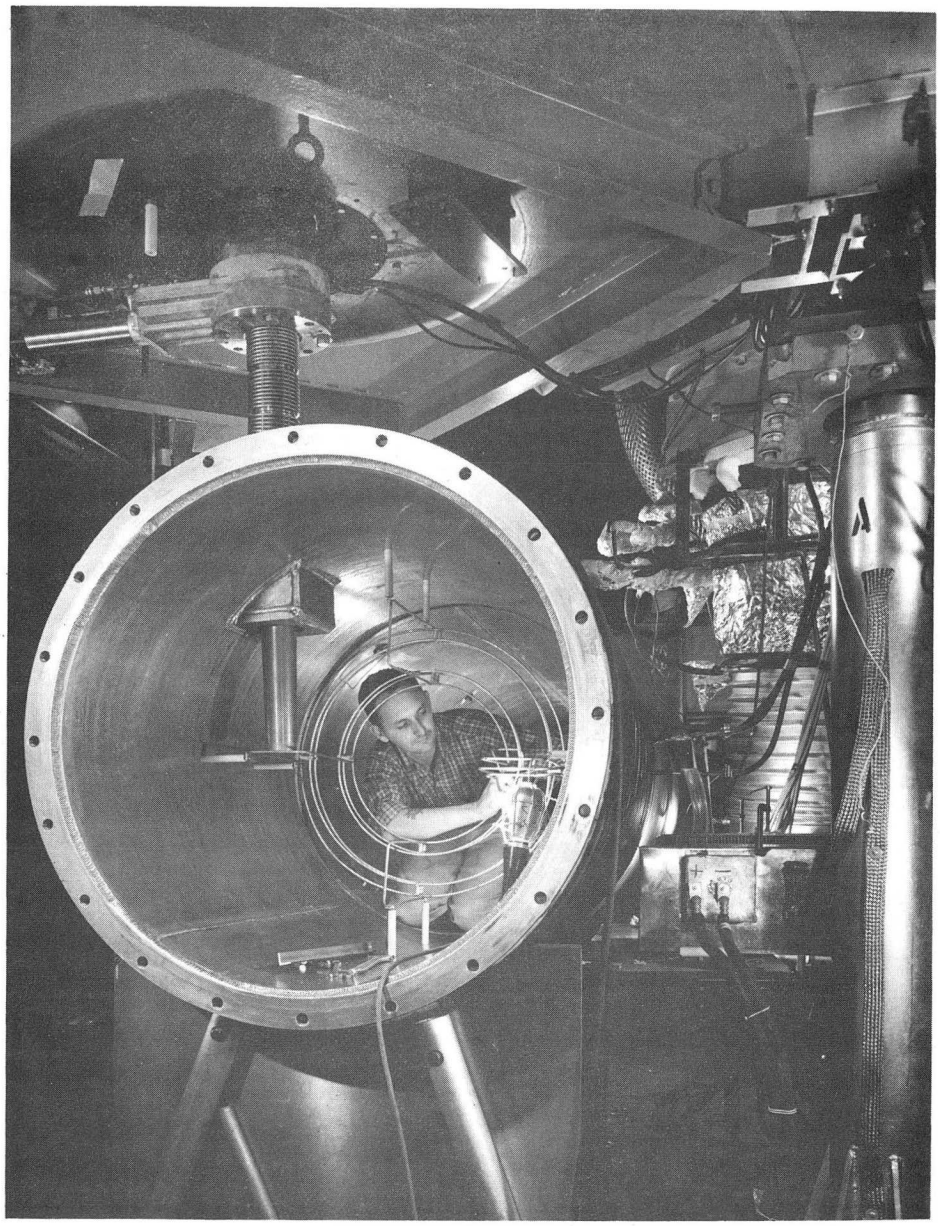

ZN-2296

Fig. 9. A view of the vacuum system from the inflection end showing the mu-metal inflection tube and the coil A structure.

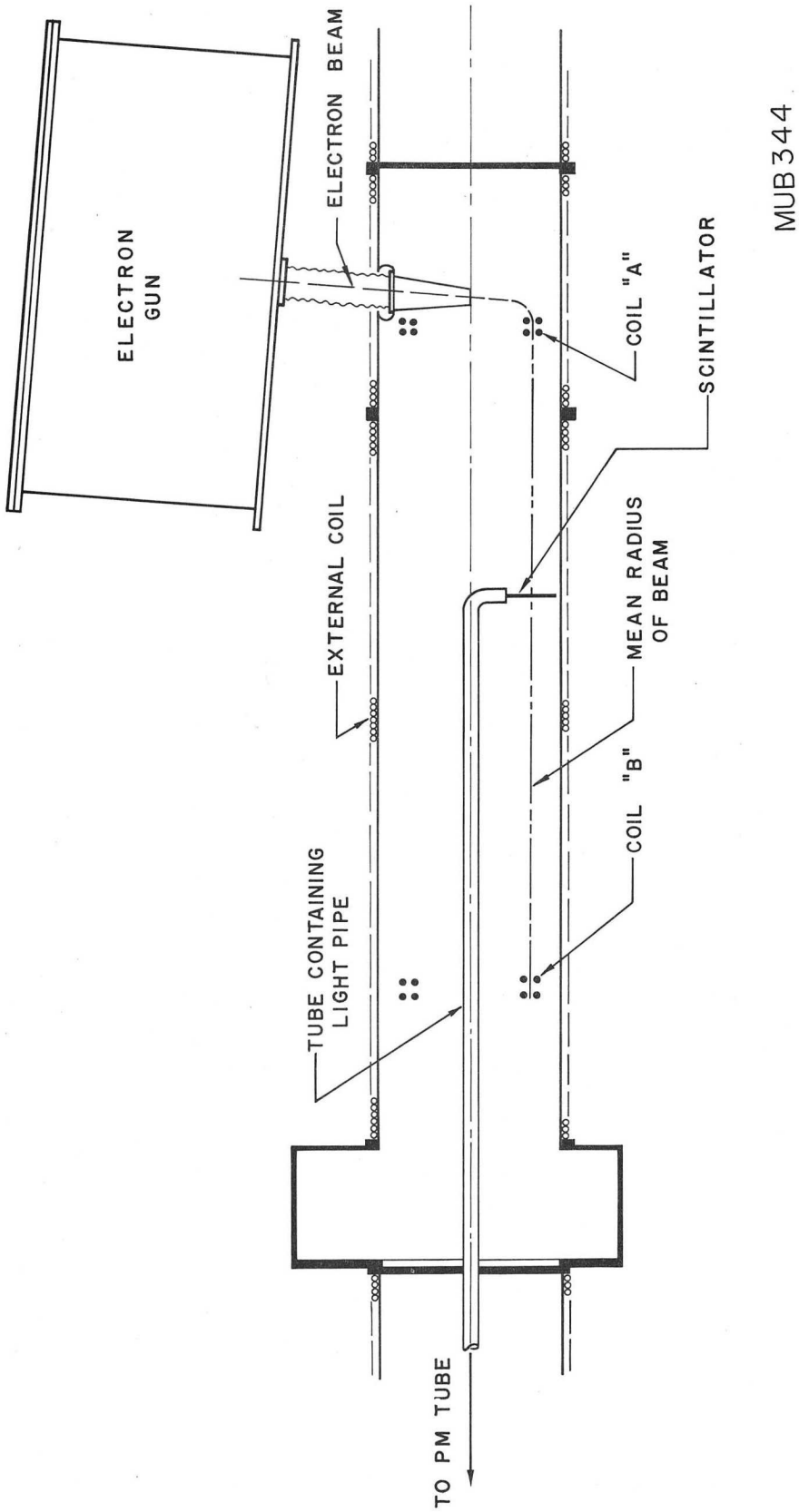

Fig. 10. Experimental arrangement used in counting experiments.

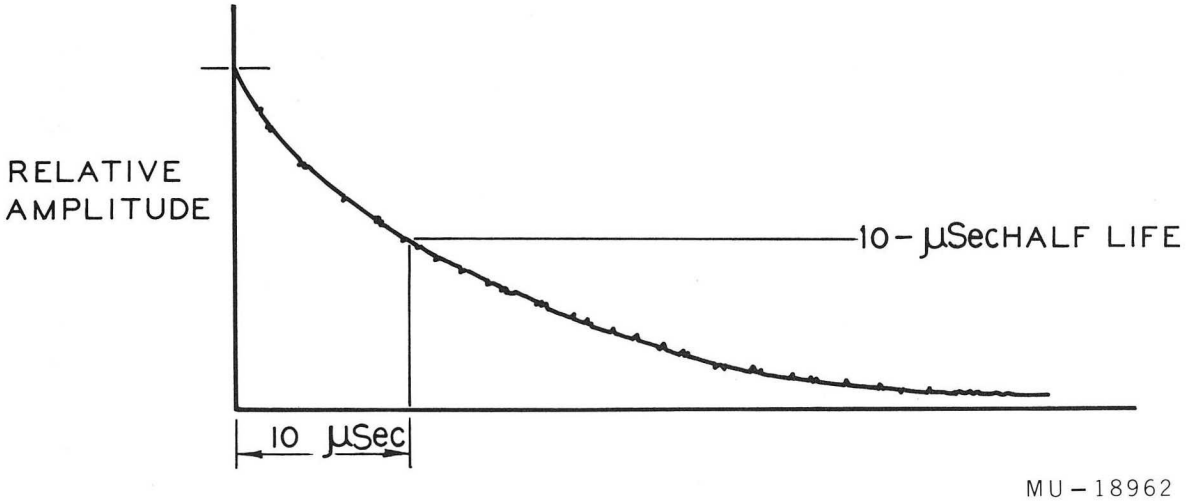

Fig. 11. Oscilloscope trace showing decay of trapped beam.

The time for a revolution is approximately

$$\frac{2\pi\bar{\rho}}{v},$$

where $\bar{\rho}$ is the average radius and v is the velocity corresponding to the energy of the electrons.

Then the e-folding time for the trapped particles is

$$t = \frac{\ell}{d} \cdot \frac{2\pi\bar{\rho}}{v}.$$

Experiments were performed with two diameters of scintillators, 0.5 mm and 1 mm; for these cases

$$t = \frac{200}{10^{-1}} \times \frac{2\times 3.14\times 30}{2.7\times 10^{10}} = 14\times 10^{-6} \text{ second}$$

for $\ell = 200$ cm, $d = 10^{-1}$ cm, $\bar{\rho} = 30$ cm, $v = 2.7\times 10^{10}$ corresponding to 650 kev, and

$$t = 28\times 10^{-6} \text{ second} \qquad \text{for} \quad d = 5\times 10^{-2}.$$

These numbers are in reasonable agreement with the observations on the two diameters of scintillators.

From this one can tentatively conclude that for small currents the loss of electrons from processes other than the presence of the counter itself are slower than 28 μsec.

The next series of experiments was performed with the scintillator tip extending only on the order of a millimeter into the annulus. It was observed that initially the counter output was similar to the experiment described above; however, this was followed by a steady signal. This was interpreted as the counter sweeping out the partial volume defined by the counter and this was followed by electrons scattering into this volume. It was further observed that during the decay of current in the trapping coil A some of the electrons would be forced into the zone observed by the scintillator. Figure 12 is a series of oscillograms taken at different sweep speeds, showing this pulse of particles that coincides with this point in time.

On the assumption that the amplitude of this pulse represents a measure of the number of electrons left in the system an estimate can be made of the lifetime of electrons against scattering and energy loss on the residual gas.

The photographs in Fig. 12 were taken at a pressure 2×10^{-6} mm Hg. Similar measurements were made at pressures varying up to 8×10^{-6} mm, which demonstrated a linear relationship of the time for this amplitude to reach half value, the lifetime being inversly proportional to the pressure. For the case illustrated the time to reach half value is 220 msec. This is not inconsistent with calculations on lifetime of electrons against scattering and energy loss on the densities of gas involved.

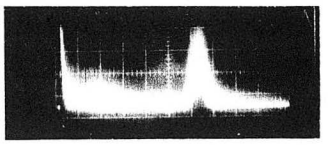

1 msec/cm

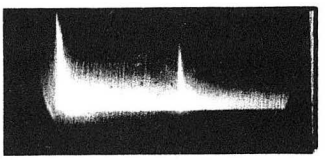

10 msec/cm

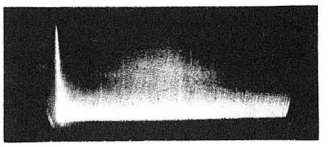

20 msec/cm

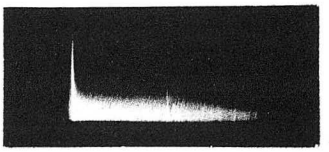

50 msec/cm

MU-18960

Fig. 12. Series of photographs taken at various sweep speeds. The vertical gain is the same in all cases.

Under conditions of somewhat better pressure (3×10^{-7} mm) signals such as this have been observed out to 1.5 seconds.

The results presented above were done with reduced currents; however, they appear to establish the basic soundness of the system but still leave open the question of behavior of the trapped particles under conditions of higher current. This is presently being explored by utilizing magnetic probes to observe the field change due to the trapped electrons.

IV. LIVERMORE PINCH PROGRAM

Dale H. Birdsall, Stirling A. Colgate, Harold P. Furth,
Fred O. Halliday, and Ross Spoerlein

THE LINEAR HARD-CORE PINCH

Two papers on the hard-core pinch were presented at Uppsala.[1] In view of the interest aroused, and of some particular questions that were raised, the linear experiment has been continued for the past three months; it is about to be terminated now.

With regard to the "inverse stabilized pinch experiment" (Fig. 13) the point was made, especially by the Harwell group, that as long as this distribution was achieved by pinching the H_z field outward with H_θ, the H_z lines (which are trapped in the electrodes) would tend to become convex outward [Fig. 14, 2]. This might be argued to lead to hydromagnetic instability, thus weakening our argument that we had shown instabilities in a hydromagnetically stable configuration. To test this point, we have repeated the inverse-stabilized-pinch experiment, programming the initial H_z to be initially fairly concave outward [Fig. 14, 1]. In this case H_r probes show that, during pinching, the field lines remain concave or straight. Nonetheless, instabilities are still observed. Reducing the degree of initial concavity did not seem to have a marked effect on the instabilities.

To confirm this important point further, the inverse stabilized pinch has been assembled by pinching from the outside in with a fast-rising H_z against an initial H_θ. In this case the H_z lines are bound to be concave outward. Instabilities are still observed, especially at low densities (15 μ D_2). Thus we feel quite comfortable in standing on our previous statement that we have demonstrated nonhydromagnetic instabilities in the pinch.[2]

Further experiments have been conducted with configurations having nulls in H_z and H_θ. At sufficiently high power levels, all pinches are found to become slightly unstable, but, as previously pointed out, with a null in H_z and a fairly uniform H_θ, far higher current densities can be supported stably than with a null in H_θ or with the conventional stabilized pinch. Rigorous comparisons have been made, such as that illustrated in Fig. 15, in which distribution (1) is quite stable, (2) is slightly unstable, and (3) is quite unstable. Since even the axial current density in (1) is higher than in (3), the possibility of enhanced instability associated purely with current flow out of the electrodes (discussed in the most recent report) can now be definitely ruled out, and we have a striking confirmation of Alan N. Kaufman and William A. Newcomb's theory of hydromagnetic surface instabilities in

---

[1] Dale H. Birdsall and Harold P. Furth, Hard Core I; Hard Core II, Fourth International Conference on Ionization Phenomena in Gases, Uppsala, Sweden, August 1959.

[2] Dale H. Birdsall, Stirling A. Colgate, and Harold P. Furth, Instability of a Hydromagnetically Stable Pinch Configuration (UCRL-5753-T Abstract), APS Division of Plasma Physics Meeting, Monterey, California, Dec. 1959.

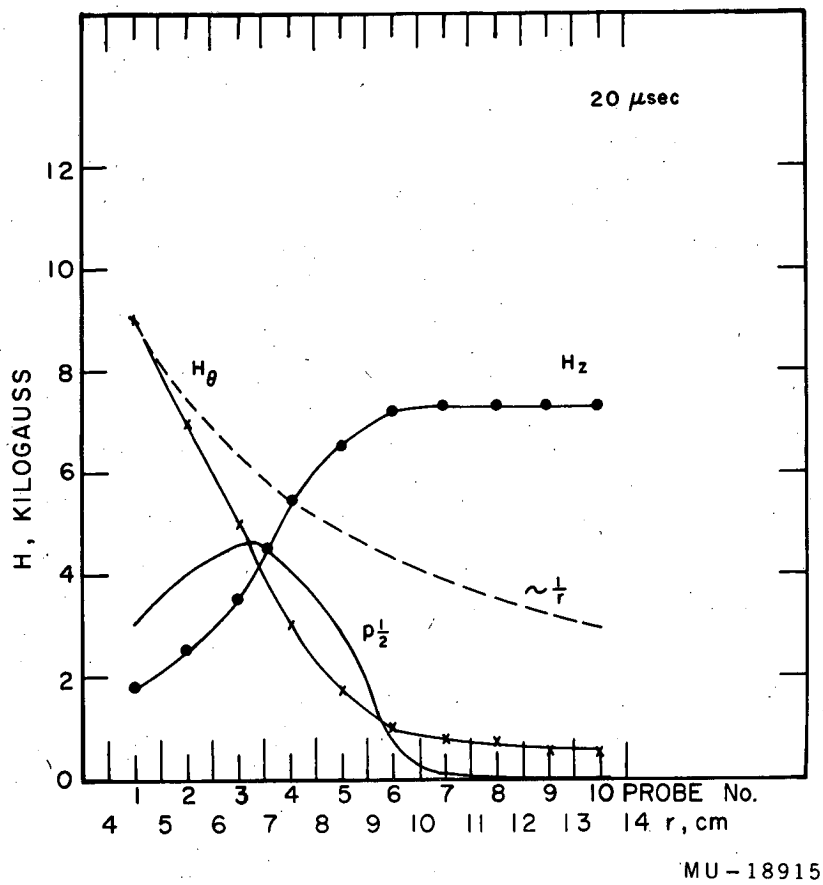

Fig. 13. Inverse stabilized pinch distribution pinching from outside in.

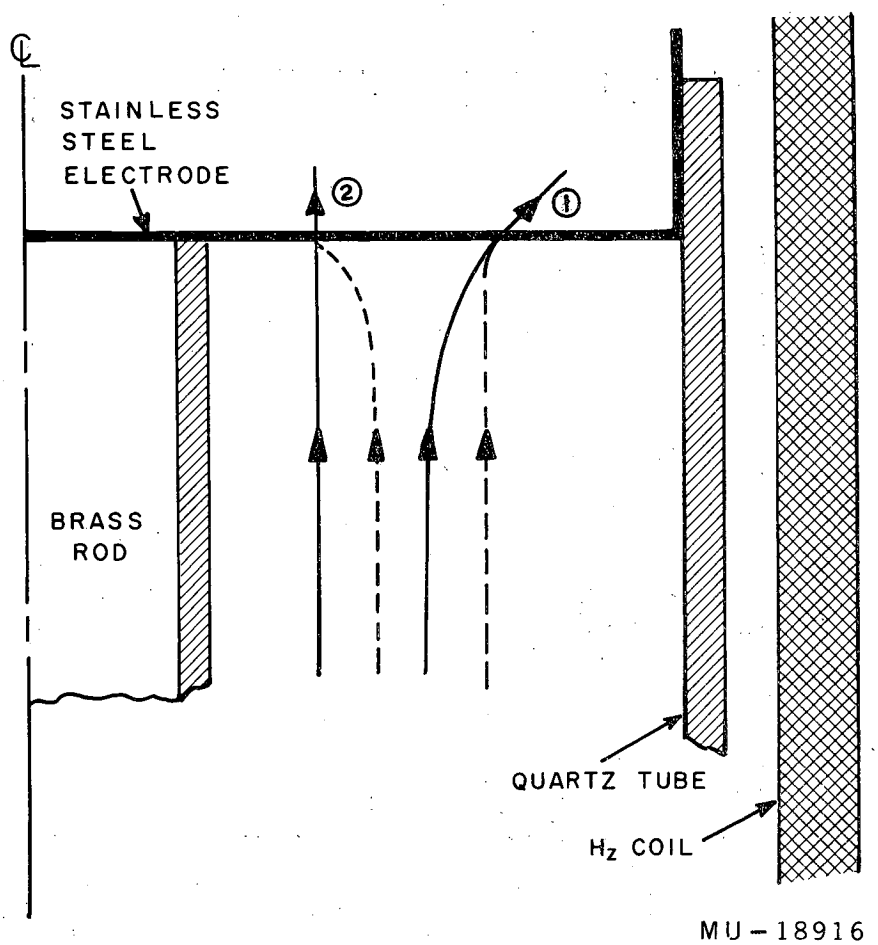

Fig. 14. Entrapment of H_z lines in electrode and bending during inverse pinch.

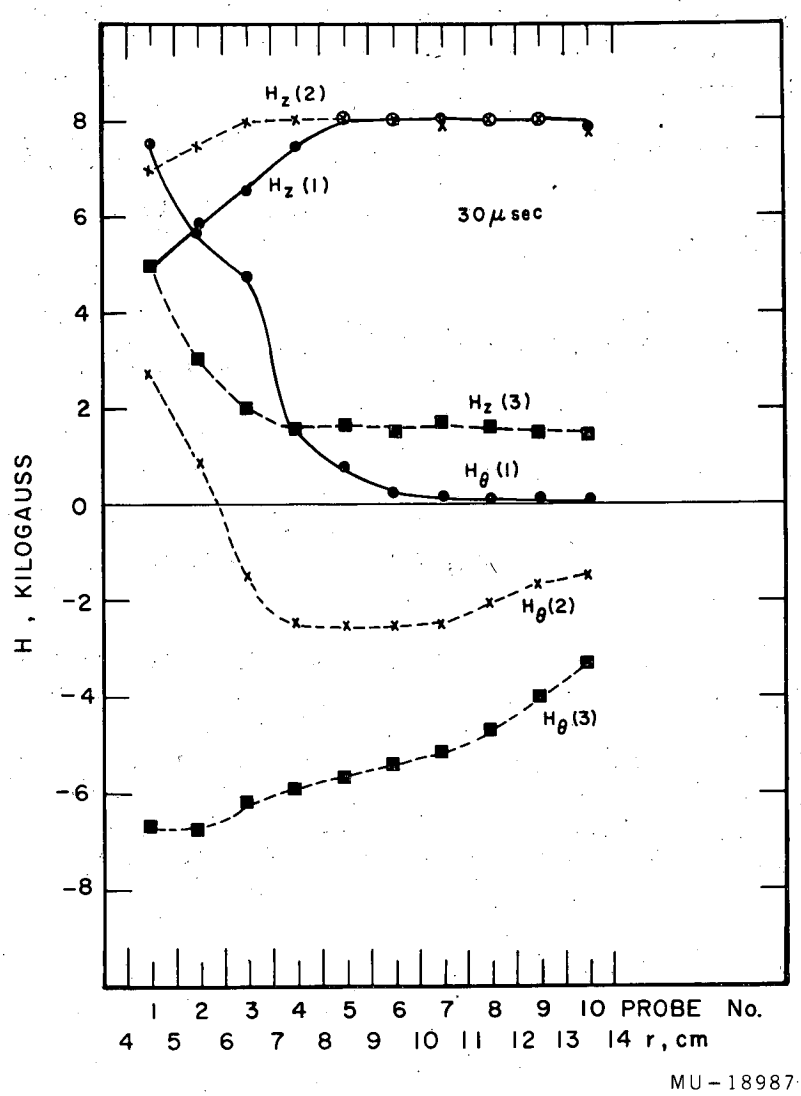

Fig. 15. Inverse stabilized pinch (1); null in H_θ (2); stabilized pinch (3).

a tubular pinch. Thus the results on the linear hard-core pinch can be summarized as proving that the hydromagnetic theory gives a definite index to actual pinch stability, but is not by itself sufficient to guarantee complete stability at high current densities and low particle densities (that is to say, under the conditions usually employed to try to obtain a hot plasma in the pinch). In the demonstration of this proposition, some 20,000 probe traces have been taken over the past 9 months, so that we feel our conclusions have quite a broad data base.

A study of theta pinches has been made in the hard-core tube, demonstrating the importance of initial reverse H_z in forming a sharp front, and giving a measure of plasma density from the pinch dynamics. The effect of a small trapped H_θ has been studied.

Probe data on the triaxial pinch with entrapped H_z have been analyzed, and the relative magnitude of apparent plasma pressure as a function of entrapped H_z has been determined. The occurrence of azimuthally unsymmetric gross instability modes has been noted at the higher values of entrapped H_z.

An experiment with a heated molybdenum cathode (UCRL-8887, p. 71) has been performed,[3] and no appreciable temperature-dependent effect on instability was observed whether the cathode was cold or red hot. The experiment is being repeated with a tantalum cathode, with a view to confirming the previous result and then continuing to the point of thermionic emission from the tantalum. The object is to see whether pinch breakdown can be achieved at very low particle densities (1 to 10μ).

[3] Ross Spoerlein, Stirling A. Colgate, Harold P. Furth, L. Sandy, and O. Twite, Small Levitron (UCRL-5754-T Abstract), APS Division of Plasma Physics Meeting, Monterey, California, Dec. 1959.

SMALL LEVITRON EXPERIMENT

The small levitron[3] of this report was not designed to examine containment but merely to prove the theories of levitating a hard core by induction and creating the desired magnetic field and plasma configurations during the time when the hard core was in the median position. The following figures give an idea of how the machine looked and how it behaved.

Figure 16 is a schematic diagram of the small levitron, showing how the capacitor banks are connected. The rectangular cross section of the bore was chosen for easy, rapid construction. No great effort was made to remove all the contamination sources from the vacuum liner, since, as indicated before, the low L/R time constant of the hard core prevented any appreciable containment. The inner and outer walls of the vacuum liner were sections of pyrex cylinders, and the top and bottom plates were washers machined from Mycalex. The vacuum seals were pressure-contact type with Silastic gaskets in the joints. The outer copper shell was constructed in a similar fashion, with inner and outer copper cylinders and copper washers for the top and bottom plates. These sections were screwed or soldered together where possible, except the joint between the top plate and the outer cylinder, which was an insulated gap to allow penetration of the B_Z field.

Figure 17 shows the actual oscilloscope presentation of the data verifying core levitation and magnetic field compression. The signals are the integrated output of pick-up loops; the top three pictures are the signals from loops intercepting the H_θ field immediately outside the vacuum liner on top and bottom, and the fourth picture is the signal from a probe containing a loop which intercepts the H_θ field near the central core when the latter is in the levitated position. Since the H_θ field resulting from the circulating current induced in the core has the usual 1/r dependence, one can determine the position of the core by comparing the amplitude of the signals from the top and bottom pickup loops. This is the information shown in the top two pictures. In the third picture the oscilloscope trigger has been delayed and the amplifier gain increased in order to examine the fine structure of the signals when the pre-ion bank is used to produce the plasma which is necessary for magnetic field compression. The last picture shows the compression of the magnetic field near the core. The data presented in this figure verify the theories the small levitron was designed to examine, but since the machine was operating more reliably than had been expected, the experimental program was extended to include an examination of some of the stability criteria recently proved on the linear hard-core pinch. For these experiments the core was supported on pins, since the probe necessarily perturbs the field by a comparable amount. In this manner fewer probes were broken because of "overlevitation".

In the so-called "standard stabilized pinch" configuration, the probe traces are found to be nonreproducible early in the pinch cycle. Figure 18 shows the magnetic field profile with B_Z inside and B_ϕ outside the plasma. This magnetic configuration is known to stabilize the m = 0 (or "sausage" mode) instability, but is known to have incorrect shear for complete stability. The pickup-loop signals also show how stability and therefore reproducibility is brought about by having B_ϕ inside and B_Z

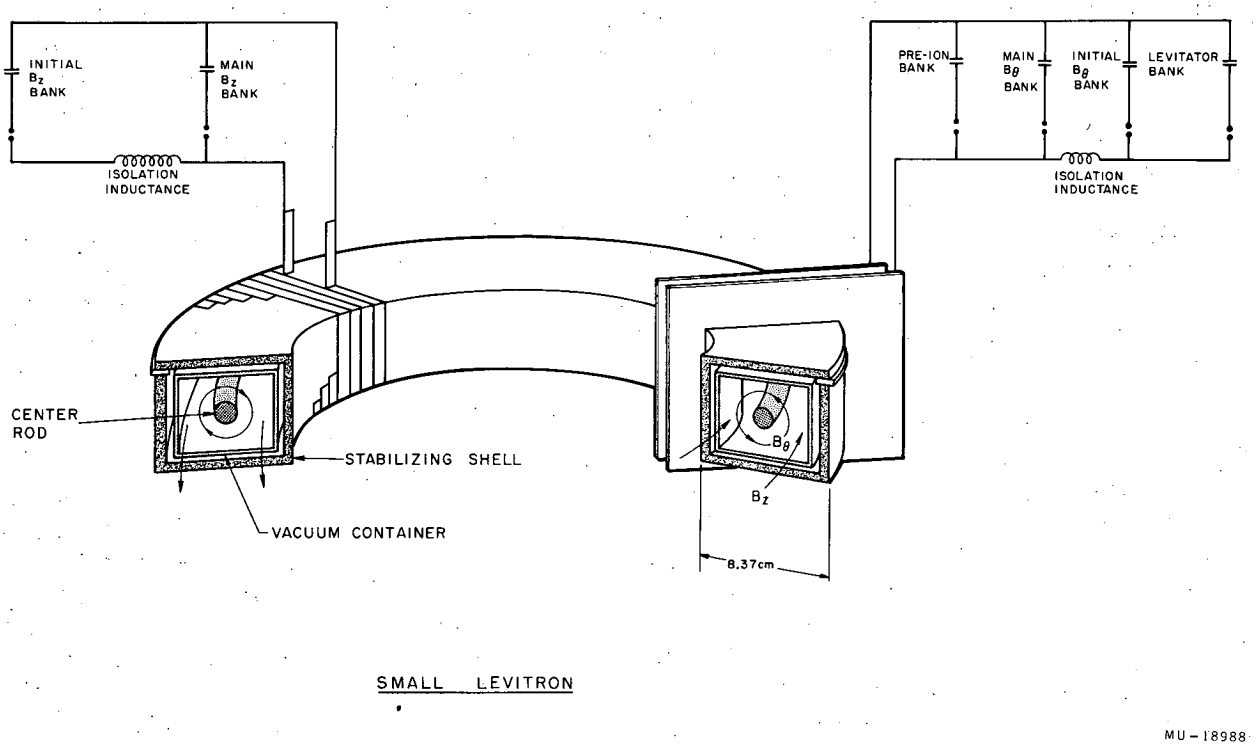

Fig. 16. Small levitron schematic.

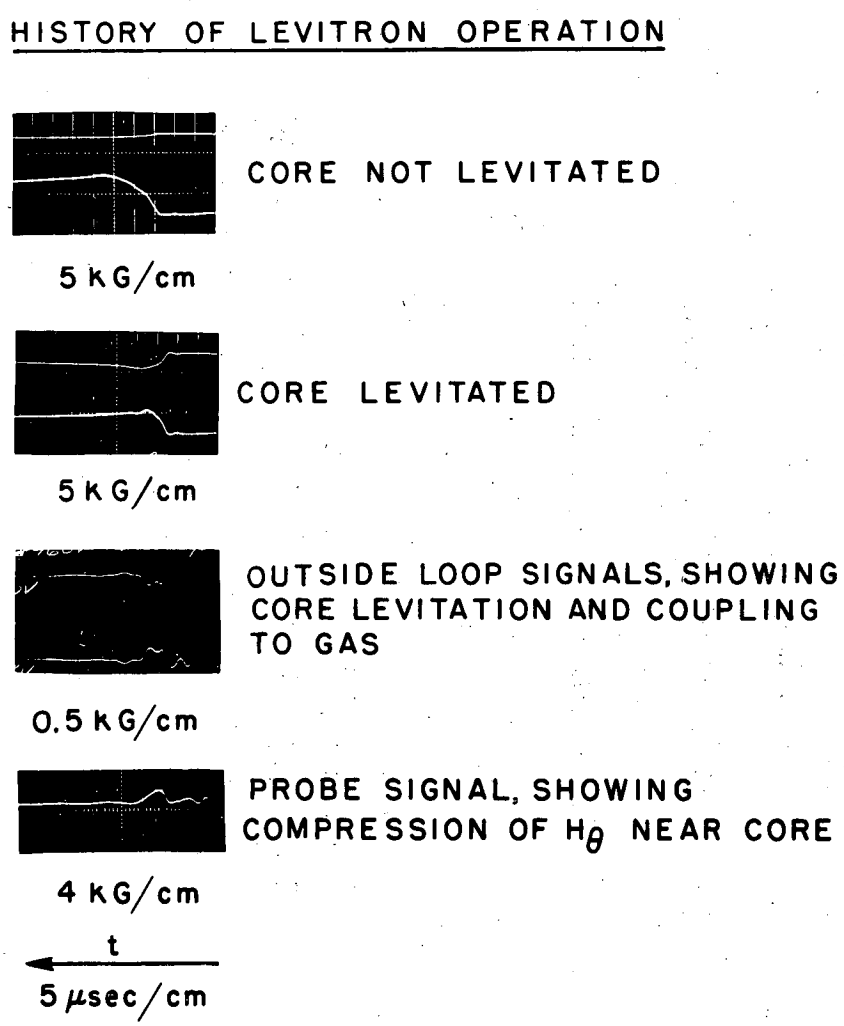

Fig. 17. H_θ monitoring signals from small levitron.

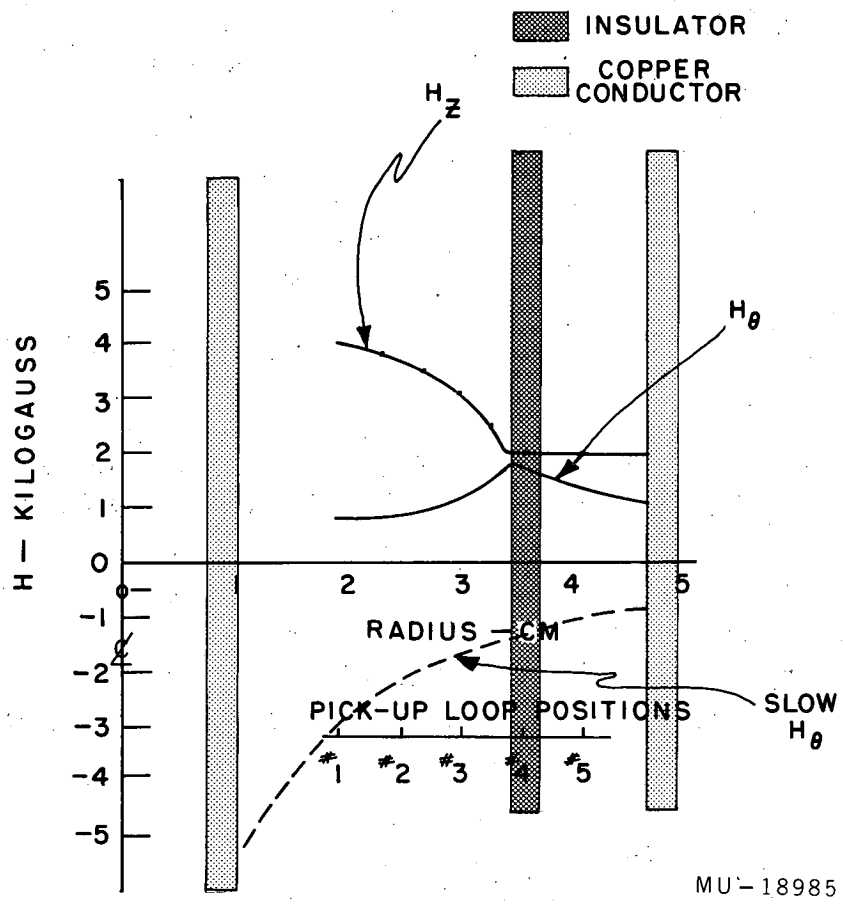

Fig. 18. Stabilized pinch distribution in small levitron. (Field distribution at 12.8 μsec.)

outside the plasma--a magnetic field configuration uniquely possible in the hard-core geometry. Figure 19 shows the corresponding magnetic field profile.

In conclusion one may state that two objectives have been attained. First, the levitron principle has been proved, which allows the design of a larger levitron with a cleaner vacuum and an inherently longer L/R decay time for the core. This will allow the study of plasma heating and plasma energy containment in hard-core pinch configurations. Second, it has been shown that the magnetic field configurations created in the linear hard-core geometry can also be induced in a toroidal hard-core geometry, and that the stability or instability of certain magnetic field configurations demonstrated in the linear hard-core pinch can also be observed in the toroidal system.

ELECTRON-BEAM PINCH

The electron-beam pinch experiment is being resumed, using a 4-in.-diameter pinch tube. The apparatus has been assembled, and the circuit tests are commencing. The possible phenomenological understanding of the role of turbulence in the pinch[4] has further increased our interest in the electron-beam experiment. In combination with the control of hydromagnetic turbulence achieved in the hard-core pinch, the possibility of direct measurements of the properties of turbulence is also of increasing importance.

[4] Stirling A. Colgate, Enhanced Diffusion due to Magnetohydrodynamic Turbulence (UCRL-5734-T Abstract), APS Division of Plasma Physics Meeting, Monterey, California, Dec. 1959.

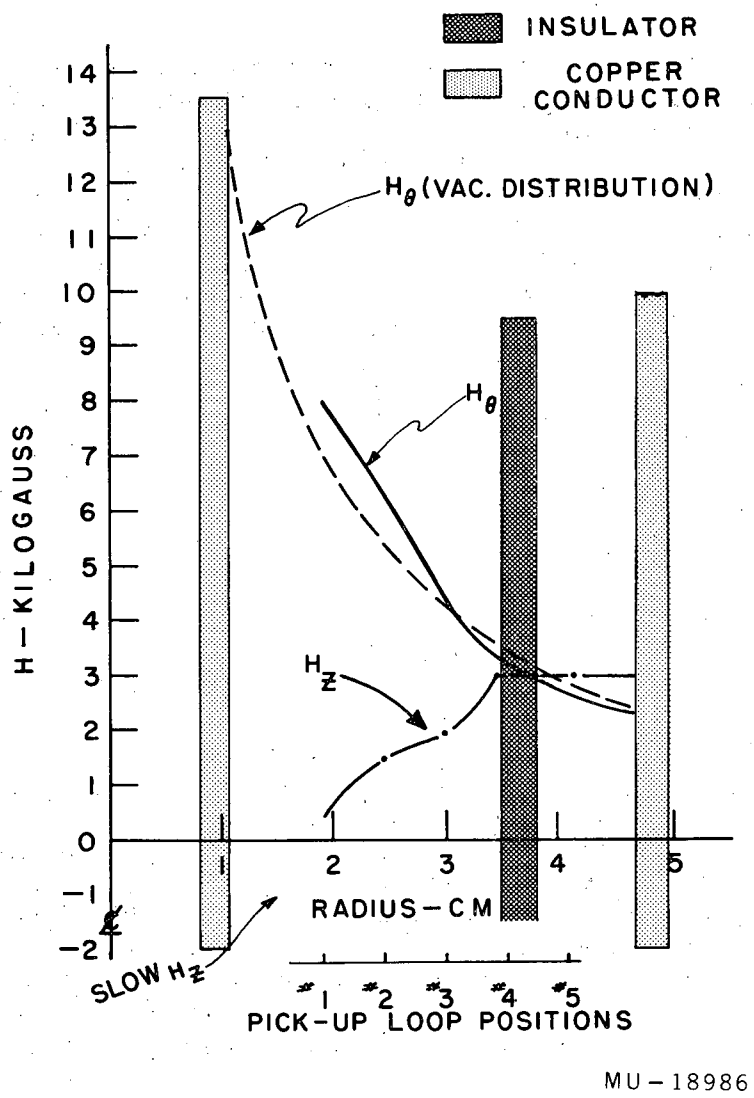

Fig. 19. Inverse stabilized pinch distribution in small levitron. (Hard-core pinch configuration; field distribution at 6 μsec.)

PLASMA ACCELERATION

The simple first-stage design with a button end electrode in a quartz end plate, and tubular outer electrode, has performed satisfactorily at velocities in the range of $5 \cdot 10^6$ cm/sec. A more sophisticated single stage is being tried at present, which consists of a slightly conical insulator tube and normal end electrodes with a central hole in the larger one. The object is to form an m = 0 instability at the narrow end and allow it to advance toward the open end, accelerating the pinched plasma.

The conical pinch is at present limited by gas emission from the pyrex walls of the chamber during pinch formation. A preionization heating cycle, pulsed gas input, and the use of a very fast initial current rise has improved the sharpness of the current boundary layer so that it is less than 20% of the radius, and improved the mass ratio of emitted to initial gas by a factor of 4. These results are obtained by comparing probe signals near the wall and near the axis. With the use of a quartz cone (which is expected this month) and present techniques of boundary-layer formation, the non-linear development of the m = 0 sausage mode of instability should be rapid and predictable.

A small-scale model of the two-stage rail accelerator has been completed for the purpose of mapping the dc magnetic field. Theoretical analysis is also proceeding.[5]

LIQUID SODIUM EXPERIMENT

CW rf of high quality is now available, as well as bursts of 0- to 120-sec^{-1} repetition rate, and the dependence of the growth of Taylor instabilities on pulse rate is clearly documented in the case in which H_θ around a rod creates a funnel-shaped cavity in the sodium (Fig. 20). Using the CW rf and then solidfying the sodium, we have been able to obtain some accurate, smooth castings; these have permitted comparison to theory which is entirely satisfactory.[6]

---

[5] Harold P. Furth and Fred O. Halliday, A Two-Stage Plasma Accelerator (UCRL-5732-T Abstract), APS Division of Plasma Physics Meeting, Monterey, California, Dec. 1959.

[6] Fred O. Halliday, Stirling A. Colgate, and Harold P. Furth, Liquid Sodium Hydromagnetic Equilibrium Measurements (UCRL-5752-T Abstract), APS Division of Plasma Physics Meeting, Monterey, California, Dec. 1959.

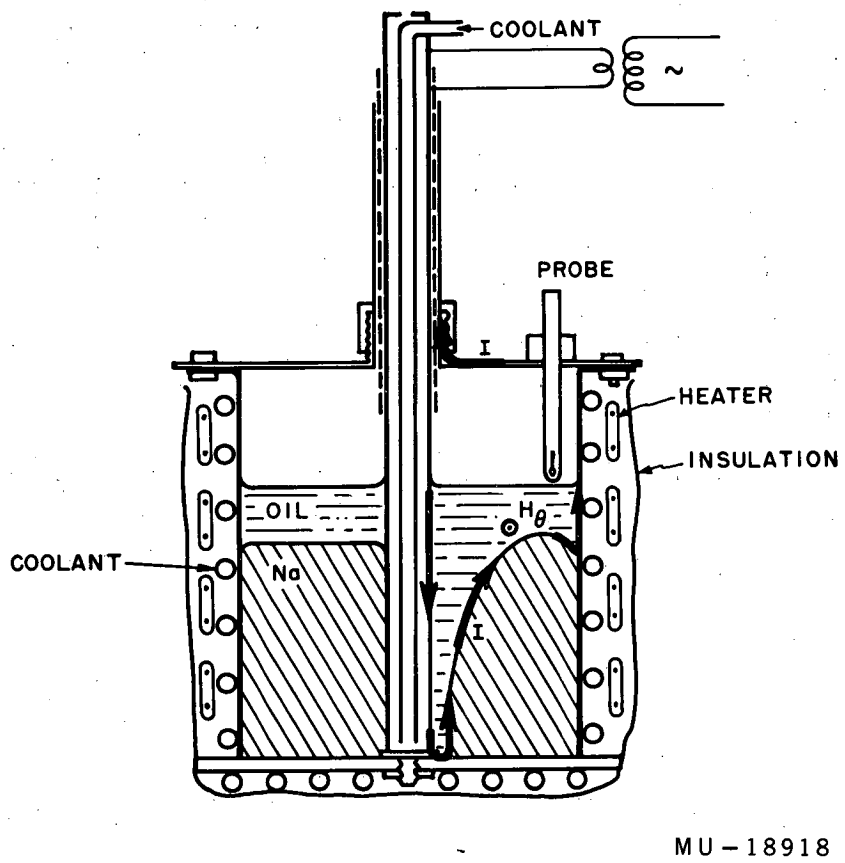

Fig. 20. Sodium rf experiment. Coaxial hard-core geometry.

THE 12-INCH LEVITRON

A mechanical switch for 20 kv and 100,000 amp is partially developed for the levitating circuit. Ion gauges and a mass spectrometer are under development to fit inside the 1/2-in. ports. The circuit connections to the Gamma bank are now planned, and the necessary isolation inductances are being built. The Kanigen coating technique over high-temperature epoxy plastic appears to be developed to a satisfactory state for intial operation.

HIGH-MAGNETIC-FIELD RESEARCH

A note has been published on the construction of the large 200-kilogauss magnet.[7] Meanwhile this magnet has been improved by vacuum impregnation with epon and has been tested and found unimpaired after 30,000 shots at 200 kilogauss, 1000 at 250 kilogauss, and 100 at 300 kilogauss. An ordinary water-cooling arrangement has been perfected to replace low-temperature cooling. A second 200-kilogauss coil, having access transmerse to the field, has been assembled.

These two magnets are currently being used to develop magnetoresistive and Hall-effect probes for plasma research. Commercial units are being tested by the electrical engineering department in our magnets, and special miniature units are being developed by us.[8] It has been relatively easy to achieve quartz probes of 12-mil o. d., containing 3-mil bismuth wires, and giving 1-volt signals at 30 kilogauss on the basis of the magnetoresistive effect. Higher signals at lower fields will be achieved by using indium antimonide, but even present probes are of interest in plasma research.

The applicability of small probes in theta pinch work is obvious. There are also special properties of this type of field detection which make it a valuable adjunct to the ordinary pickup coil in all kinds of experiments. Because the magnetoresistive probe measures the total magnetic field, rather than H_z or H_θ singly, it can be used to obtain highly precise pressure-balance measurements, to study propagation of compression waves, to determine magnetic energy density with a minimum of interference with the plasma, to determine the magnitude of absolute magnetic field fluctuation in a turbulent pinch, etc.

---

[7] Dale H. Birdsall and Harold P. Furth, Pulsed 200-Kilogauss Magnet for Accelerator Experiments, Rev. Sci. Instr. 30, 600-601 (1959).

[8] Dale H. Birdsall and Harold P. Furth, Use of Magnetoresistive Probes to Measure Magnetic Field, Engr. Note UCRL-5794-T, Nov. 1959.

An incidental result of the probe-development studies will be to measure the galvanomagnetic properties of several materials up to 300 kilogauss in the largest and most homogeneous high-field research facility in the world operating at that level.

A spool-type force-free coil with helical wire winding (UCRL-8775, p. 47) has been tested, as has another made of a continuous copper form with a helical slit. The latter was operated repeatedly in the range 100 to 140 kilogauss, though made of unsupported 1/16-in. copper. It failed at 140 kilogauss, owing to a helical instability associated with the widening of the helical slit. This instability can be accounted for theoretically (and is the analog of a similar effect in some hard-core pinches). The wire-wound coil developed a similar instability at 50 kilogauss. Further models are planned in which the helical instability will be geometrically and (or) mechanically inhibited.

THEORY

The understanding of the possible steady-state solutions of the pinch has been extended in a recent paper.[9] Briefly, the paramagnetic solution requires a definite plasma-pressure profile, as well as a nonisotropic resistivity. If by various loss mechanisms (i. e., thermal diffusion, charge exchange, radiation, conduction along lines of force to electrodes), the plasma pressure is kept lower than required, then the convective solution comes into effect. In that case a source and sink of plasma at the wall and axis respectively are required. The convective solution with a negligible plasma pressure has been observed in the hard-core pinch by use of a configuration approximating the conventional stabilized pinch.

[9] Stirling. A. Colgate and Harold P. Furth, The Paramagnetic and Convective Effects in the Pinch, Engr. Note UCRL-5756-T, Nov. 1959.

V. BERKELEY PINCH PROGRAM

SHEET PINCH STUDIES

Oscar A. Anderson

Introduction

New measurements on the large Triax tubes have revealed the sources of certain troublesome phenomena of long standing, including the short life of the pinch at high level[1] and the anomalous behavior in connection with preheating.[2] Modifications are in hand which are expected to correct these conditions, and so far the results are quite encouraging. On the less encouraging side, progress has been somewhat slower than predicted[3] with the switchgear for the high-energy bank; some shortcuts are planned which are discussed below. Early in the quarter the preheating experiments with the 4-inch Triax were finished; the results will be compared with measurements on the large tubes.

Tubular Pinch(Triax)

There are two tubes presently in operation, both employing high-purity alumina insulators and both having outer insulators that are 10 in. in diameter by 8 in. long. The inner insulators have diameters of 4 in. and 8 in. respectively. Thus the nominal radial distance between the insulating walls is 3 in. in one case and 1 in. in the other. These tubes will be referred to as the 4×10 and 8×10 Triaxes, since the inner and outer diameters are the essential features. Drawings of these tubes are shown in an earlier quarterly report UCRL-8682 and in Fig. 21 of this report.

Both tubes were provided with slits in the anode through which the discharges could be observed with a streak camera. Figure 22 shows photographs taken by Willis C. Goss with a Model 100A camera (f:15) at a writing speed of 7-1/2 mm/μsec, magnification 1:16. Although Figs. 22a and 22b, representing the 4×10 Triax, do show the pinch as expected (the thickness oscillations can be followed for several cycles in the original films), the most noticeable feature is the over-all oscillation, which comes dangerously near the inner insulator in Fig. 22a and disastrously so in Fig. 22b. It is certain that this explains some, although perhaps not all, of the peculiar behavior observed at high levels and previously reported. Of course these radial oscillations have been predicted and reported before,[1] but the present photographs show that the amplitude is larger than had been supposed.

---

[1] O. A. Anderson, W. R. Baker, J. Ise, Jr., W. B. Kunkel, R. V. Pyle, and J. M. Stone, International Conference on the Peaceful Uses of Atomic Energy, 2d, Geneva, 1958 (United Nations, New York, 1959), Paper No. 2349, Vol. 32, p. 150.

[2] Oscar A. Anderson, in Controlled Thermonuclear Research Quarterly Report, UCRL-8887, Sept. 1959, p. 75.

[3] Oscar A. Anderson, in Controlled Thermonuclear Research Quarterly Report, UCRL-8775, June 1959, p. 49.

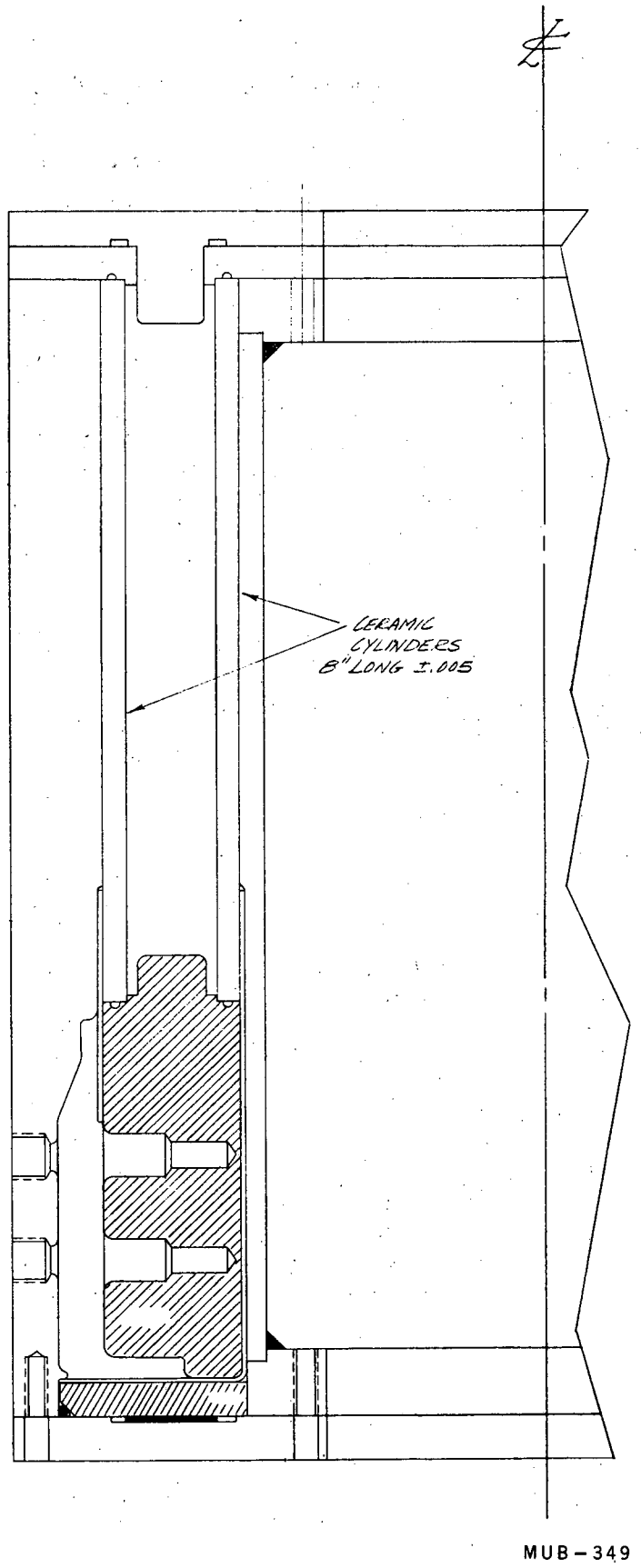

Fig. 21. 8×10 tubular pinch.

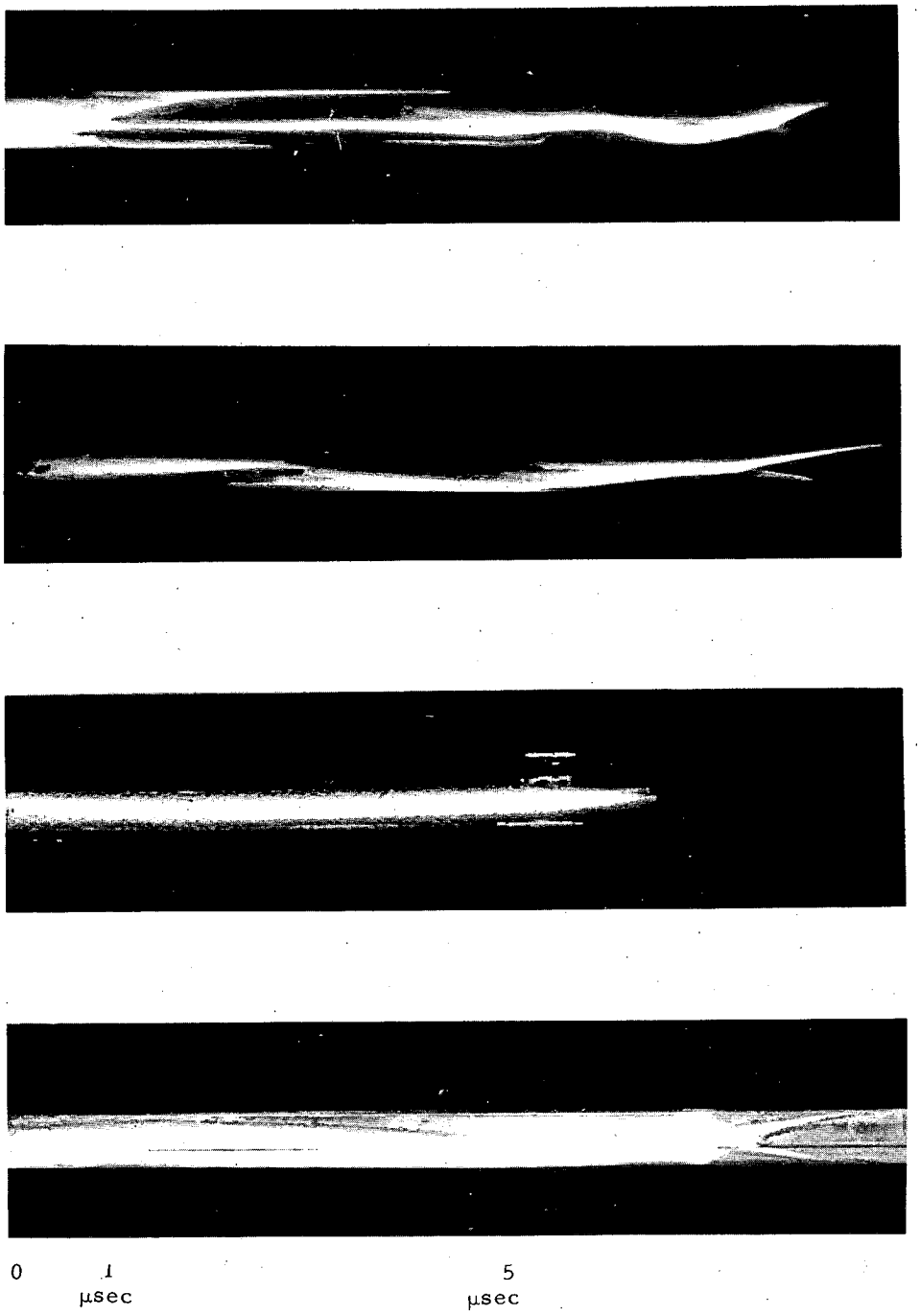

(a)
100 μf
20 kv
250 μ D_2

(b)
25 μf
20 kv
500 μ D_2

(c)
100 μf
15 kv
400 μ D_2
(8×10)

(d)
50 μf
20 kv
500 μ D_2

MUB-348

Fig. 22. Tubular-pinch streak photographs.

The oscillations are more pronounced with the 4×10 tube than with the 8×10 tube, as is seen by comparing Fig. 22c with 22a and 22b. There are two reasons for the 8×10 tube's being different: first, the diameter ratio is closer to unity, and second, the stray inductances are better balanced. Accordingly, the former tube has been modified in a manner planned to compensate for both conditions.

A separate effect which occurs at higher pressures (Fig. 22d) is the bar of light across the tube width at the time of the first pinch. It is not yet certain what this signifies although similar observations have been reported elsewhere. When a streak camera is available again this effect will be given close scrutiny, especially at higher power levels.

There is one satisfying feature in all the streak photographs. It is observed that at least during the first plasma compression period each luminous front appears projected as a sharp line, which indicates that the pinch diameter is uniform over the whole tube length.

The 8×10 Triax, as is seen in Fig. 21, has an accessible inner conductor and for this reason was chosen for a microwave transmission measurement. The idea was to compare this with the reflection measurement already made with the small tube (discussed in a later section). However, it turned out that the results were completely different, and in fact explained the poor behavior previously reported.[2] It was observed, specifically, that the plasma was not being preheated uniformly around the tube. This was confirmed by an optical study. A new preheating bank of the same stored energy but furnishing current at 3×10^{10} amp/sec instead of 3×10^{9} was constructed. After this change was made, the main discharge produced better pinches when preceded by the preheating cycle than without preheating--instead of the other way around.[2] It was also found that the slight variations from shot to shot, which had hindered magnetic probe studies, could be essentially eliminated.

Switches and Other Devices

Because of certain delays in the high-energy bank switchgear program an alternative plan has been initiated. This is to make at least temporary use of the old switches by adding the silastic insulation feature[2] planned for the new ones. This should make it possible to start the high-energy experiments planned for the large Triax tubes much sooner than otherwise. Synchronization tests with two of the old switches showed that an improved triggering system was necessary, since the jitter time was of the order of 0.5 μsec. Internal and external modifications are being carried out.

Parts for the large ribbon pinch have been machined, but it has not been possible to obtain the insulator originally planned. It remains to be decided whether to try to fabricate one from flat plates, using cement.

Preheating Study

Since the role of the preheating cycle has never been fully understood, occasional experiments have been carried out in this connection. For example, several experiments were designed to determine the cooling-off time after the preheating current was turned off. It was found by optical and electrostatic probe methods, among others,[3] that the characteristic cooling time was as long as 50 microseconds, contrary to expectation. This research was concluded in September with a microwave-reflection measurement performed by Ferdinand Voelker (see another section of this report) which again indicated this same order of magnitude for the cooling time.

It should be noted that with a preheating bank about the same as used with the 10-inch Triax (see above), uneven current flow was not observed. This, of course, is partly due to the smaller diameter, which makes the magnetic field stronger, but still it is felt that part of the difference may arise from the use of quartz insulation rather than alumina. The smooth surface maintained by quartz absorbs less gas, obviously an advantage. It has been noticed that quartz seems to take much less operating time to clean up after having been exposed to the atmosphere.

Future Plans

The inductance-balancing modification is complete and further streak-camera observations will be made soon. The ratio of inner to outer inductance is adjustable and it is intended to find the optimum value experimentally. After this, further changes in the preheating arrangements may lead to still further improvements. By the time the high-current bank is ready things should be in very good order, except for one problem: The insulation arrangement on the high-pressure part of the large tubes is essentially the same as that on the switches and is known to be unreliable. Hence some work needs to be done on adapting the silastic insulation principle to these tubes.

A recently proposed experiment is of some interest. O. Buneman has suggested that the large "resistive bump" sometimes occurring at high currents[1] might be explained on the basis of a two-stream instability and that further measurements might establish whether this is the case. At first this idea seemed to fit the known facts, since on the basis of his theory the electric field observed was about right. However, a computation shows the critical current density[4] to be at least an order of magnitude higher than actually present. It may be that Buneman's values for the critical field can be brought into agreement with his critical current (which is probably correct) by taking into account small-angle collisions. At any rate, no specific experiments of this type are planned until this situation is a little clearer. The theory should also be modified to include the effect of the transverse magnetic field present in the Triax.

---

[4] O. Buneman, Phys. Rev. 115, 503 (1959).

HOMOPOLAR PROGRAM

Homopolar II

Melvin J. Bernstein and Wulf B. Kunkel

The acoustic probe, developed by Alan W. DeSilva,[1] was employed in careful measurements of the velocity distribution. Previously, the velocity distribution had been deduced through the use of an analog[2] from measurements of the radial (diamagnetic) component of the magnetic field, the measurements lying along a radial line just outside the insulator boundary of the rotating plasma. The agreement is very good under the assumption that the acoustic probe measures ρv^2, whereas the magnetic field gives $\rho v^2/r$. The ratio of the two distributions, giving $1/r$ very accurately, establishes considerable confidence in the acoustic probe.

Homopolar III

William R. Baker, Alexander Bratenahl, William S. Cooper, and Wulf B. Kunkel

This device, described fairly completely in UCRL-8682, was designed with the notion that, by placing the insulators parallel to the axis of the machine and perpendicular to the magnetic field, centrifugal force could be relied on to remove plasma from this critical region. Previous experience with Homopolar I and II and calculation of viscous effects showed that in these flat machines possible stimulated breakdown across insulators might account for the observed limitation in energy that could be imparted to the plasma. Unfortunately, a similar energy limitation appears to persist even in this modified design, but some progress has been made in understanding it.

During the period of this report, a large number of diagnostic techniques have been employed which, together with several calculations, have considerably advanced the general understanding of Homopolar III's behavior. In the interests of brevity, only the conclusions drawn from these experiments will be discussed here.

When the source bank is switched on to the Homopolar (no preionization) there follows a delay time, $\tau = B^2/V^3 \ln V/p$ (purely empirical), up to 200 μsec with ~ 5% jitter during which a feeble discharge exists (a few amperes). At the conclusion of τ the impedance suddenly drops four orders of magnitude and ~ 100 ka flows in a 40-μsec pulse. The plasma becomes essentially fully ionized, accelerates into rotation, and collapses into a ring at the equator within 10 to 15 μsec. The time to collapse and the thickness of the ring agree well with theory, assuming an ion temperature of the order of 10 ev.

---

[1] Alan W. DeSilva, in Controlled Thermonuclear Research Quarterly Report, UCRL-8887, Sept. 1959, p. 81.

[2] W. R. Baker, A. Bratenahl, A. W. DeSilva, and W. B. Kunkel, Viscous Effects in Highly Ionized Rotating Plasmas, in Proceedings of the Fourth International Conference on Ionization Phenomena in Gases, Uppsala, Sweden, Aug. 17-21, 1959 (North Holland Publishing Co., Amsterdam, The Netherlands.)

If a β is derived for the "centrifugal pressure" it is found that in many cases it is of the order of 0.5, which means that there should be a moderate to strong pressure gradient in the radial direction and a corresponding perturbation of the applied magnetic field which, in vacuum, falls very nearly inversely as the minor radius of the torus. This behavior of the vacuum field should result in a fairly sharp transition between a condition of no radial pressure gradient and a condition of a large radial pressure gradient. The corresponding increase in the capacity in the extreme limiting case should theoretically be by a factor of 2.2 for this machine. As the voltage is raised from 4 kv to 5 kv the undistorted capacity--i. e., for no pressure gradient--is observed, and is independent of voltage. Above 5 kv, however, the capacity increases steadily and very rapidly with voltage, reaching a value of five times the initial capacity at 7.5 kv. At the same time large current flashes (3 ka) have been observed across the insulator by means of a differential magnetic probe. In addition, the inductance of the discharge decreases and more and more charge passes through the system in excess of that required to charge the enhanced capacity to the equilibrium voltage. Unquestionably, insulator breakdown occurs in this machine just as it did in the earlier models. This happens despite the fact that the pressure near the insulator should be reduced by a factor of 1000 by the centrifugal pumping. The enhanced capacity must be due to very large amounts of material being stripped or outgassed from the insulator. Surely an engineering problem of fundamental importance in Sherwood is the proper understanding of the behavior of insulators in or near a hot plasma.

The bands of current seen on the anode have been probed in the interior and it is found that they correspond to pressure ridges in the radial direction of amplitude $\Delta p/p \sim 15\%$. Since they are of constant and finite amplitude one hesitates to call them instabilities. They may be described as an $m = 12$ to $m = 13$ mode, and as such the number seems reasonable, since their wave length is about equal to the thickness of the plasma in both the radial and axial directions. Although the effect is quite similar to the $m = 1, 2, 3$ modes reported recently in the Stellarator, the latter seems to be due to quantizing the rotational transform according to Kruskal's theory, whereas the former must have a different origin. The current belief is that two types of boundary-layer flow exist simultaneously and may be related to the transient and localized formation of an anode sheath.

By operating the external dc coils[3] as either an antimirror or a mirror, not only is the plasma ring thickness strongly modified in the expected direction but also the bands are suppressed, as expected, for about 100 μsec. This does not necessarily mean, however, that the plasma ridges are suppressed. The probe experiment to determine whether they are has not yet been performed.

One real mystery is beginning to manifest itself in these experiments. It has always been observed that the decay constant of the voltage seems to be independent of the capacity of the machine, but the significance was overlooked. In fact even in the earlier Homopolar models, with gases ranging

[3] A. Bratenahl and Wulf B. Kunkel, in Controlled Thermonuclear Research Quarterly Report, UCRL-8775, June 1959, p. 54.

from hydrogen to iodine vapor, the decay constant was remarkably constant and did not behave like 1/RC. If the explanation is forthcoming, one might suspect that the apparent energy limitation observed in the Homopolar experiments is related in some way.

VI. ION MAGNETRON

J. Donald Gow and Robert W. Layman

INTRODUCTION

To increase the efficiency of any apparatus it is necessary to understand the nature of its losses. The efficiency of the ion magnetron is dependent on the rate of loss of the circulating ions. Circulating ions are defined as those ions which are born in and ejected from the sheath.[1]

Circulating ions can be lost by one of several methods: charge exchange, recombination, scattering, and leakage out the ends of the discharge by axial migration. Of these, losses by charge exchange and axial leakage undoubtedly dominate. Liner power dissipation and liner current as a function of axial position at various magnetic field configurations were measured to study these processes of ion loss.

This experiment has not been completed, because of failure of the magnet power supply; however, preliminary information gathered to date has proved interesting and is presented below.

EXPERIMENTAL GEOMETRY

A set of 27 aluminum rings, 7 in. in diameter and 1 in. wide, extending axially from 3 in. outside the north end of the solenoid to 1 in. beyond the axial center concentric with the liner, was installed in the machine. The rings, spaced 1/16 in. apart, are thermally and electrically insulated from each other and the liner. Each ring is equipped with a copper-constantan thermocouple, the copper leg being used to measure the ring current. The rings are cooled by radiation and conduction through the support assembly. An aluminum false liner of the same diameter as the rings was installed in the south half of the machine. The anode is a 1-in. o. d. hard-drawn copper tube, supported at both ends under 700 to 1000 pounds tension.

A Leeds and Northrup Speedomax is used to record ring temperatures. Ring currents are measured by either an oscilloscope or milliameter. Separate measurement of current and temperature permits separation of effects due to ionic and neutral (charge-exchange) impingement.

---

[1] J. Donald Gow, Lloyd Smith, and John M. Wilcox, The Ion Magnetron, UCRL-8579, Feb. 1959.

EXPERIMENTAL PROCEDURE

With the magnetic field, high voltage, and D_2 pressure set to chosen values, the machine was pulsed and the ring currents and rates of temperature rise recorded. The pulse length and pulse rate were set so that the rings receiving the most power would reach temperature equilibrium at around 100°C, thus a temperature rise on the rings receiving relatively small amounts of power could be detected. This procedure was followed for two magnetic-field configurations. Magnet power-supply failure has temporarily interruped this experiment.

RESULTS

Figure 23 shows liner power and current as a function of axial position for a slight mirror field at 12 kv and 0.3 μ. This demonstrates quite clearly the loss of circulating ions by charge exchange. Axial containment even at this mirror ratio is also evident.

Figure 24 shows power and current for a mirror ratio of two at the same voltage and pressure. Here there is no evidence of charge exchange. At the axial center the magnetic field is below magnetron cutoff, therefore a large percentage of the higher-energy circulating ions is intercepted before charge exchange can take place. Towards the end of the discharge there is evidence of electron dumping on the liner. This is not yet clearly understood.

The data so far collected give further confirmation that the machine is running as an ion magnetron. A complete discussion of the conclusions of this experiment will be presented when all the data have been collected.

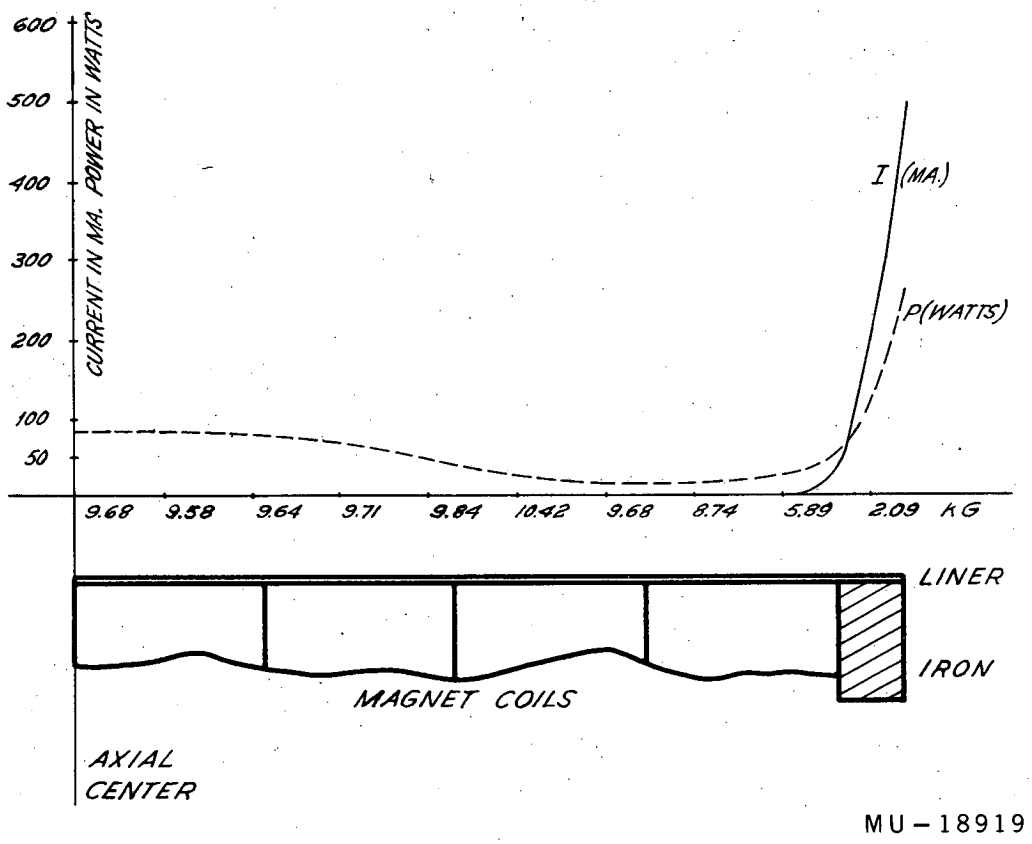

Fig. 23. Liner current and power dissipation vs axial position; slight mirror field.

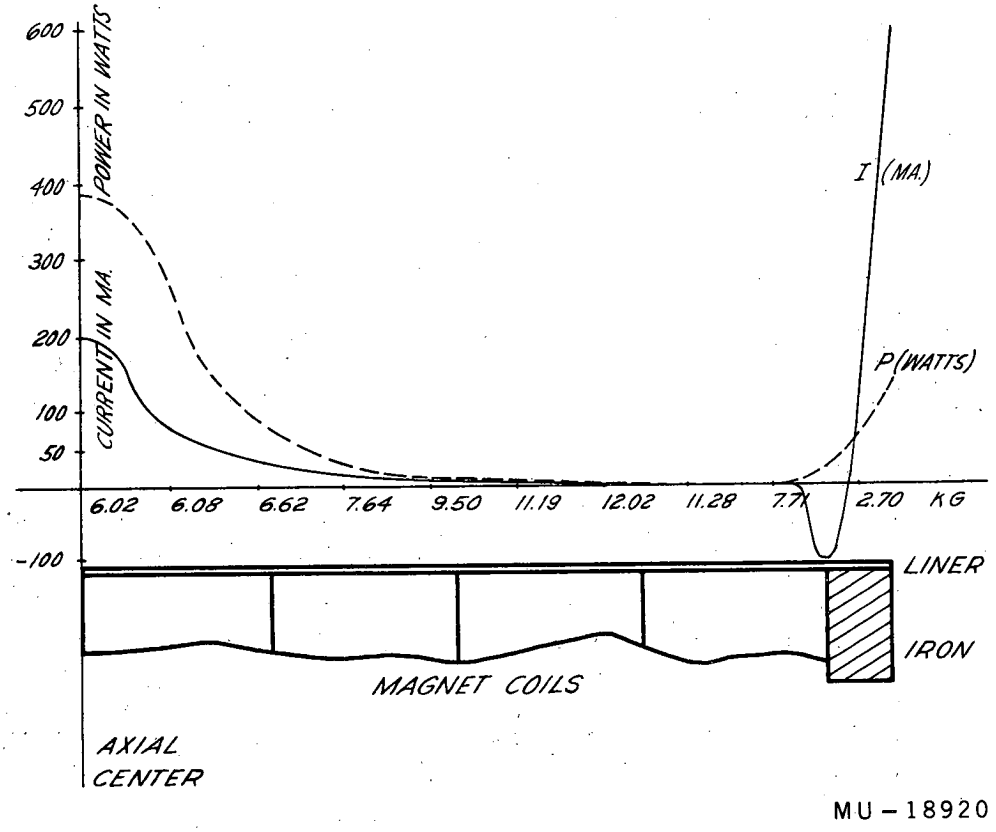

Fig. 24. Liner current and power dissipation vs axial position; mirror ratio 2.

VII. THEORETICAL RESEARCH

THE HEATING UP OF ELECTRONS IN A PLASMA

Warren Heckrotte and John Killeen

The IBM 709 code, DION,[1] for solving the plasma Fokker-Planck equation has been completed for one species of particle. As a check on the code several examples of the relaxation of an electron or ion component of an ionized gas to a Maxwellian distribution have been run. In addition a beginning of the two-component problem has been made. The equation for the electrons when both electrons and ions are being considered is

$$\frac{\partial f_-}{\partial t} = \frac{\Gamma e}{2} \left\{ \frac{\partial^2 f_-}{\partial v^2} \left[A(f_-, v, t) + A(f_+, v, t) \right] \right.$$

$$+ \frac{\partial f_-}{\partial v} \left[B(f_-, v, t) + B(f_+, v, t) + 2 \frac{m-M}{M} \int_0^v f_+ \frac{v^{1^2}}{v^2} dv^1 \right.$$

$$+ 2 f_- \left[f_- + \frac{m}{M} f_+ \right] ,$$

where

$$A(f, v, t) = \frac{2}{3} \left[\frac{1}{v^3} \int_0^v f v^{1^4} dv^1 + \int_v^\infty f v^1 dv^1 \right] ,$$

$$B(f, v, t) = \frac{4}{3v} \left[\int_0^\infty f v^1 dv^1 - \int_0^v f v^1 \left(1 \frac{v^1}{v}\right)^2 \left(1 + \frac{v^1}{2v}\right) dv^1 \right] ,$$

$$\Gamma e = \frac{4\pi e^4 \ln\Lambda}{m^2} .$$

[1] Warren Heckrotte and John Killeen, The Slowing Down of Fast Ions in a Plasma, in Controlled Thermonuclear Research Quarterly Report, UCRL-8887, Sept. 1959, p. 86-90.

If in the beginning we neglect the energy loss of the ions we can solve for the heating up of the electrons by means of the above equation, keeping f_+, the ion distribution function, fixed in time, i.e., $f_+(v, t) \equiv f_+(v, 0)$. This problem has been solved, where the ions are deuterons at 200 kev and the electrons are initially at 10 ev and heat up to 1 kev. The results will be presented in a forthcoming report.

SCATTERING LOSS RATE IN MIRROR GEOMETRY

David J. Berkowitz

The basic calculations for the problem of scattering from mirrors with actual spatial variation have been previously outlined.[1] To this end, two approaches were taken.

In the first approach, the scattering effects were approximated by a modal expansion. The results permitted a rather convenient expression for the behavior of the angular distribution in velocity space as a function of time:

$$\frac{dA_j}{dt} = \sum_k a_{jk} A_k + \sum_k \sum_p b_{jkp} A_k A_p, \tag{1}$$

where A_j is the amplitude of the normalized symmetric Legendre function corresponding to the jth mode in a mirror system whose over-all loss-cone cosine is

$$\mu_c = \sqrt{1 - \frac{B(z=0)}{B(z=z_{max})}} . \tag{2}$$

In the report cited,[1] it was stated that computations were in progress. This work is now essentially complete and the results are being analyzed. One important result of the calculations has already been found. In Fig. 25 the relative loss rate for the lowest mode as a function of mirror configuration for two mirror ratios (R = 1.5 and 3.0) is plotted. These configurations are specified by means of the parameter $\Delta L/L$. Here ΔL is the length of the straight section (B = constant) between mirrors, and L is the total length between mirrors (see Fig. 25 insert). For $\Delta L/L = 0$, the mirror system is essentially that given by

$$B = B_0 \left(1 - \alpha \cos \left[\frac{2\pi z}{L}\right]\right).$$

For $\Delta L/L = 1.00$ the mirror system is a square well. Transition between the two cases is made by progressively decreasing the relative length of the mirror region, keeping the mirror ratio constant.

It can be seen that the loss rate for a mirror system with $\Delta L/L = 0$ is considerably greater (~ 2 to 2.5) than that for the square-well mirror of the same ratio. This result implies that mirror systems must of necessity be built quite long to overcome this difficulty.

---

[1] David J. Berkowitz in Controlled Thermonuclear Research Quarterly Report, UCRL-8887, Sept. 1959, p. 83.

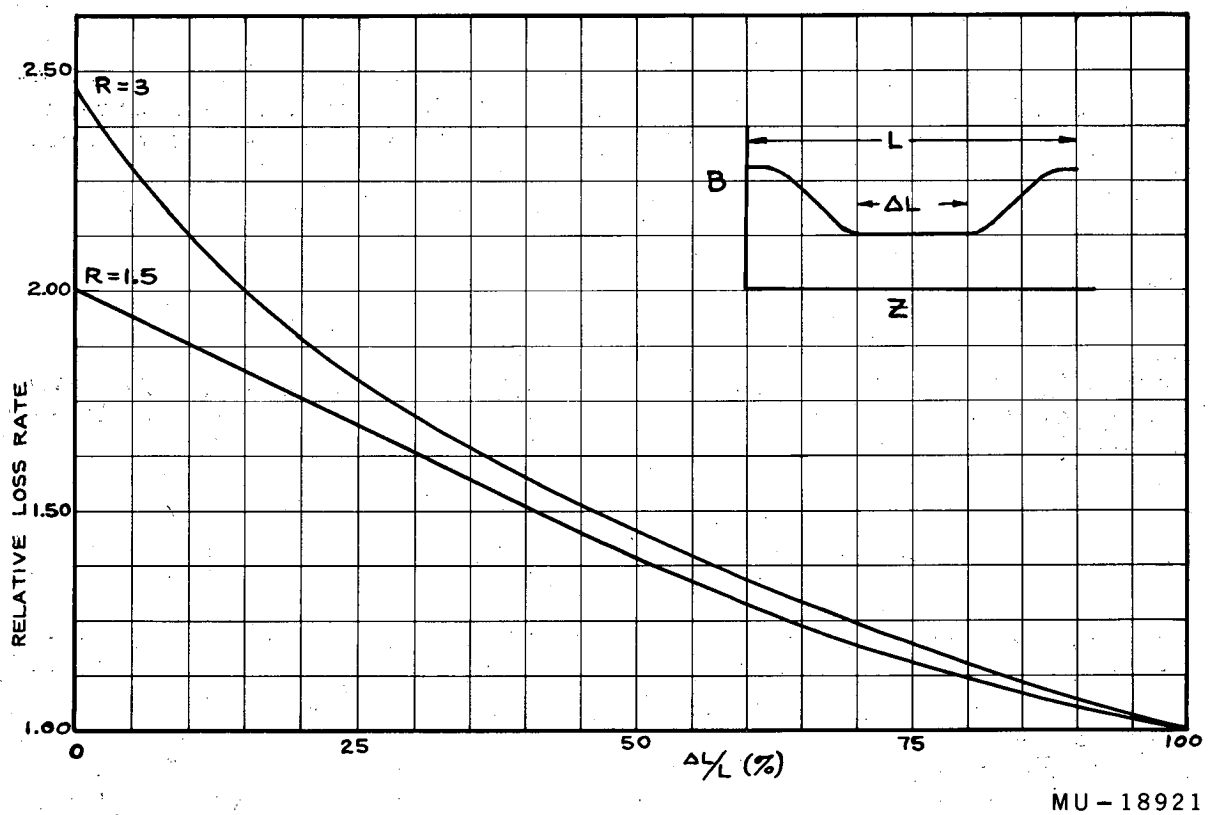

Fig. 25. Relative loss rate vs percentage flat region for spatially varying mirrors.

The effect of this greater loss rate is based upon a fixed number of ions in the confined plasma. The modified shape factor results in the corresponding ion density's being generally somewhat greater for the fields tapered at the ends than for the square well, so that the resulting thermonuclear reaction rate would be somewhat increased and partially compensate for the increased loss rate out the ends.

In the second approach the same problem is being solved with the scattering effects being treated more or less exactly in the form of direct numerical integration of the Fokker-Planck equation. This procedure takes considerable computer time despite numerical simplications on the computation procedure. The results to date indicate a loss rate somewhat greater than in Fig. 25 for $\Delta L/L = 0$.

HYDROMAGNETIC STABILITY OF A TUBULAR PINCH

William A. Newcomb

I have been carrying out numerical calculations on the hydromagnetic stability of a tubular pinch under the assumption of an infinitely thin current layer.[1] The instabilities are divided into two categories: Type I, in which the current layer moves as a whole, and Type II, in which the displacement has a discontinuity at some point in the layer. The Type I stability criterion depends on the following variables: the angles ϕ_i and ϕ_e between the magnetic field and the z axis at the inner and outer edges of the layer, the radius α of the central conductor (in units of the layer radius), and the radius β of the outer wall. It is shown that $m = 0$ displacements are stable, and that $m = 1$ displacements (kink instability) are the least stable of those with $m \neq 0$. The numerical calculations are therefore restricted to $m = 1$. The results are shown in Fig. 26 for the least stable case, where $\alpha = 0$ and $\beta = \infty$. The regions marked "s" are stable, those marked "-" are unstable for right-handed helical displacements (i.e., displacements proportional to $\exp(i\theta + ikz)$ with $k < 0$), those marked "+" are unstable for left-handed helical displacements, and those marked "±" are unstable for both types of displacement. Roughly speaking, the pinch tends to be stable if ϕ_i and ϕ_e have opposite sign, or if they have the same sign but with $|\phi_i| > |\phi_e|$. If α and β are finite, the unstable regions are smaller, but they never disappear entirely, even if α and β are very close to one; a pinch is always unstable if $|\phi_i|$ is very slightly less than $|\phi_e|$. (See Fig. 27 which is only a rough sketch, since the numerical calculations have not been completed.)

The Type II stability criterion depends not only on the variables mentioned above but also on the detailed structure of the current layer. Specifically, it depends on the functional relation between the plasma pressure P and the angle ϕ as one passes through the layer. As before, the $m = 1$ displacements turn out to be the least stable. We assume that ϕ is a monotonic function of r throughout the layer. It is shown that the pinch is unstable whenever $|\phi_e - \phi_i| \geq 180^\circ$. Thus the field cannot rotate through more than 180 deg as we pass through the layer. The pinch is also unstable if $\sin^2\phi$ is an increasing function of r at the outer edge of the layer. Thus the only possible stable cases are the following, if we choose a coordinate system with ϕ_i in the first quadrant: (1) ϕ decreases with ϕ_i to ϕ_e with $0 < \phi_e < \phi_i$, (2) ϕ decreases from ϕ_i to ϕ_e with $\phi_i - 180^\circ < \phi_e < -90^\circ$, and (3) ϕ increases from ϕ_i to ϕ_e with $90^\circ < \phi_e < 180^\circ$.

Case 1. This case obviously has Type I stability, as is seen from Fig. 26. The necessary and sufficient condition for Type II stability is that

$$P < P_{max}(\phi, \phi_e, \beta)$$

[1] Allan N. Kaufman and William A. Newcomb, UCRL-5434 (in preparation).

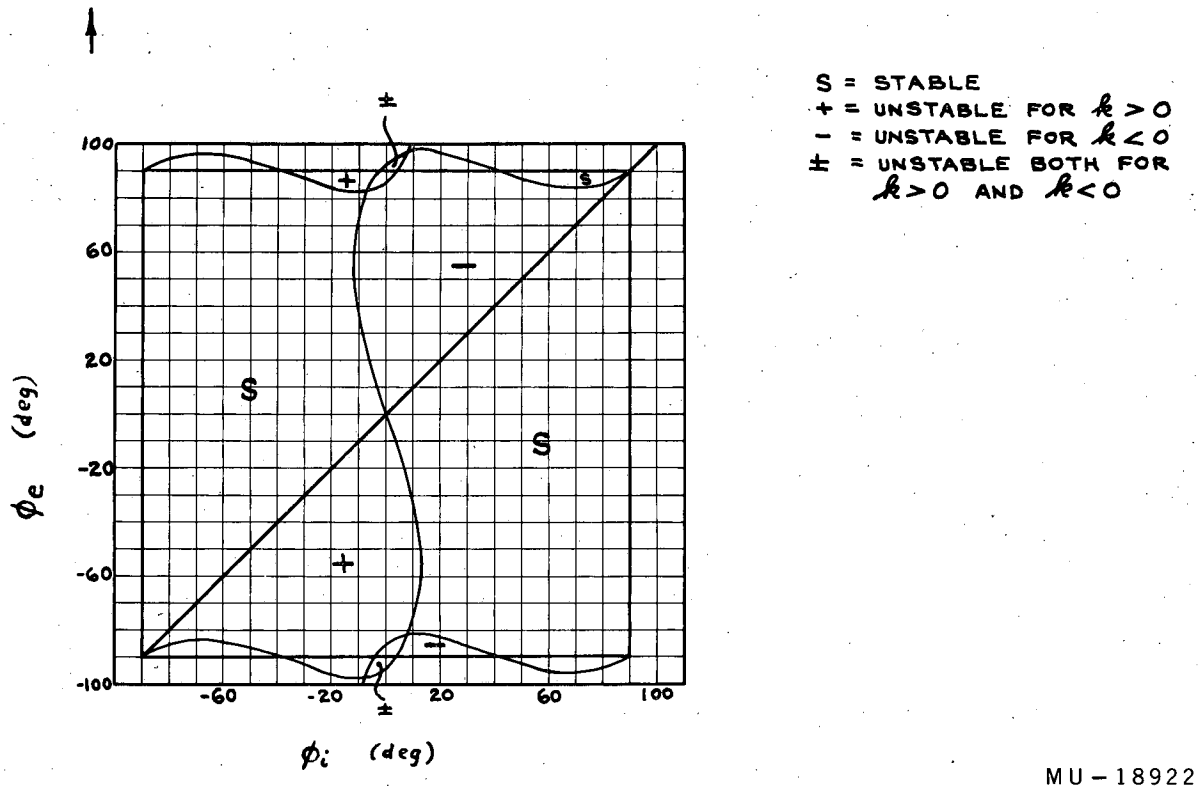

Fig. 26. Type I stability diagram for $\alpha = 0$, $\beta = \infty$; displacements of the form $\exp(i\theta + ikz)$. S = stable; + = unstable for $k > 0$; - = unstable for $k < 0$; ± = unstable for both $k > 0$ and $k < 0$.

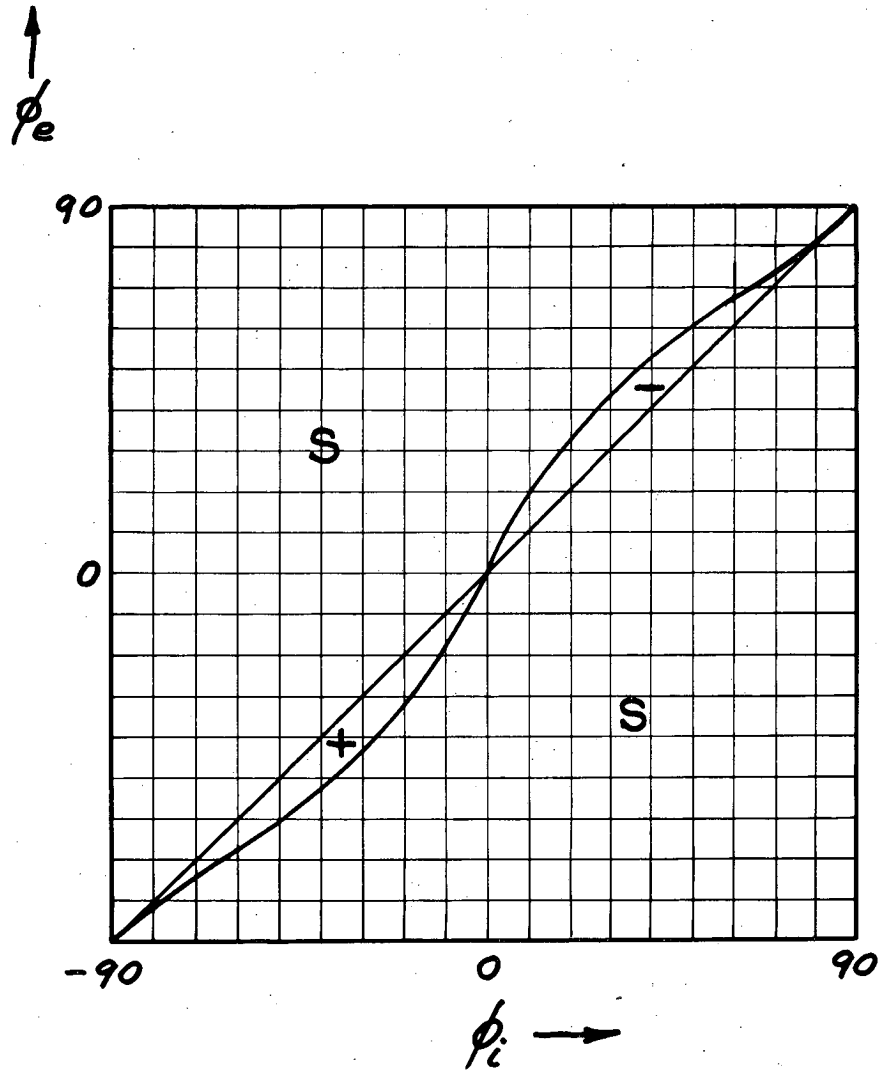

MU-18923

Fig. 27. Type I stability diagram for α and β both close to unity.

at every point in the layer for which

$$\phi_e < \phi < \phi_0 (\phi_e, \beta),$$

where P_{max} and ϕ_0 are certain functions of the indicated arguments. The function P_{max} increases from 0 to $(1/2)B_0^2$ as ϕ goes from ϕ_e to ϕ_0, where B_0 is the magnetic field at either edge of the layer. (B has the same magnitude at each edge because of pressure balance.) Suppose that $\phi_i > \phi_0$. Then the layer is divided into two parts: the inner part $\phi_0 < \phi < \phi_i$, where P can have any value consistent with pressure balance $(P < (1/2)B_0^2)$, and the outer part $\phi_e < \phi < \phi_0$, where there is a certain maximum pressure consistent with stability. If, on the other hand, $\phi_i < \phi_0$, then the "outer part" consists of the entire layer, and P must be kept below P_{max} at every point; ϕ is plotted as a function of ϕ_e for $\beta = \infty$ (the least stable case) in Fig. 28.

Cases 2 and 3 may or may not have Type I stability, as is seen from Figs. 26 and 27. Also, they are subject to an m = 0 Type II instability unless

$$P_0 \quad \frac{1}{2} \quad B_0^2 \cos^2 \phi_e \frac{\beta^2 + 1}{\beta^2 - 1} \quad ,$$

where P_0 is the plasma pressure at the point where $\phi = \pm 90^\circ$. We have not yet completed the investigation of m = 1 Type II stability for these two cases; we do know, however, that the stability criterion will have the form

$$P_{min} (\phi, \phi_i, a) < P < P_{max} (\phi, \phi_e, \beta),$$

where $P_{min} < P_{max}$ if and only if the pinch has Type I stability.

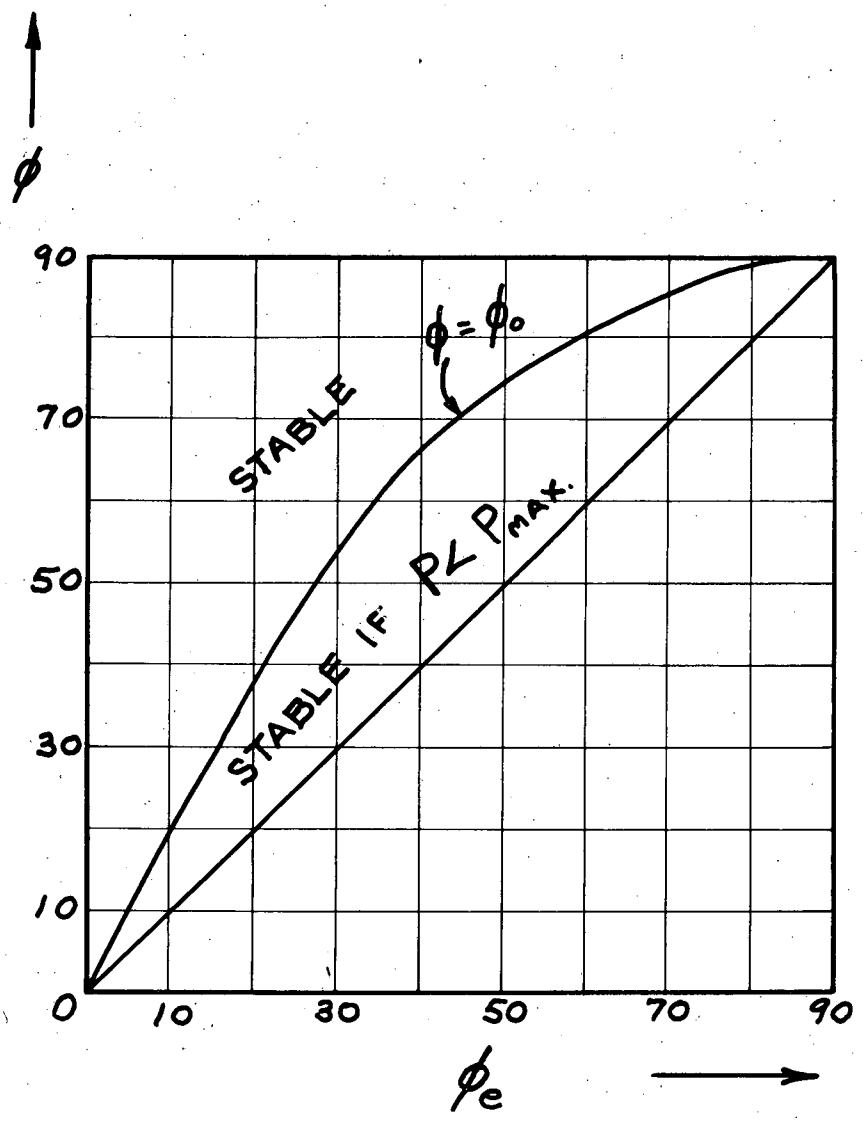

MU-18924

Fig. 28. Type II stability diagram for $0 < \phi_e < \phi_i < 90$ deg.

VIII. BASIC EXPERIMENTAL RESEARCH

PLASMA PHYSICS AND MICROWAVE DIAGNOSTICS

T. K. Allen,* M. C. Horton, George A. Paulikas, Robert V. Pyle, Henry F. Rugge, J. Warren Stearns, and Ferdinand Voelker

Diffusion of Plasma Across a Magnetic Field

The extension of the "enhanced diffusion" experiment of Lehnert (UCRL-8887, p. 92) has been continued with better diagnostic apparatus, but the previously reported phenomena are not yet understood.

Although it has been argued that the moving striations that are observed under most conditions in this experiment do not appreciably affect the theory of a positive column, striations have remained a source of concern and further efforts have been made to eliminate them by adjusting the external resistance and by striking auxiliary discharges in the anode structure. These approaches were unsuccessful. However, striationless regimes do exist at the lower pressure (~ 250 μ in He) and the fact that the curves of critical field change smoothly between the striated and unstriated conditions is perhaps an argument that these effects are not important.

Several other qualitative checks for possible sources of confusion have been made, e.g., a misalignment of the tube axis with respect to the magnetic field by a few degrees does not affect the critical magnetic field, B_c, but makes the radial potential measurements dependent on the direction of the magnetic field (the variations are of a quantitative rather than qualitative nature). A modest spectrographic effort did not reveal any identifiable impurity lines, and the insertion of an activated charcoal trap at liquid nitrogen temperatures in the gas supply line does not affect the data. The importance of preventing the magnetic field lines from linking the electrodes (which should produce Simon-type diffusion) has been estimated by putting one or both of the electrodes in the uniform part of the magnetic field. The critical field vs. the pressure is shown for various configurations in Fig. 29. It would appear that under normal operating conditions the critical phenomena are not influenced by the length of the tube except, perhaps, for pressures below 400 microns. This is approximately the pressure region in which ambipolar diffusion should change to Simon diffusion. Conditions are presumably better at the lower pressures when the electrodes are not linked by magnetic field lines, and many measurements were made at pressures of a few hundred microns, at which the critical phenomena are sharpest.

A clue to the behavior of the critical field was obtained by measuring the time-resolved light output with three photomultipliers looking near the top, center, and bottom of the discharge tube. It was found that below the critical field the distribution of light is roughly that of a normal positive column (precise measurements were not attempted). Above the critical field the luminous column was constricted and rotated within the tube 10^4 to 10^5 times per second. A streak camera was built to show this effect more clearly. Figure 30 was obtained with an 8-msec pulse at 4 amperes of 220 μ of He.

*Visiting Lawrence Radiation Laboratory from AERE, Harwell.

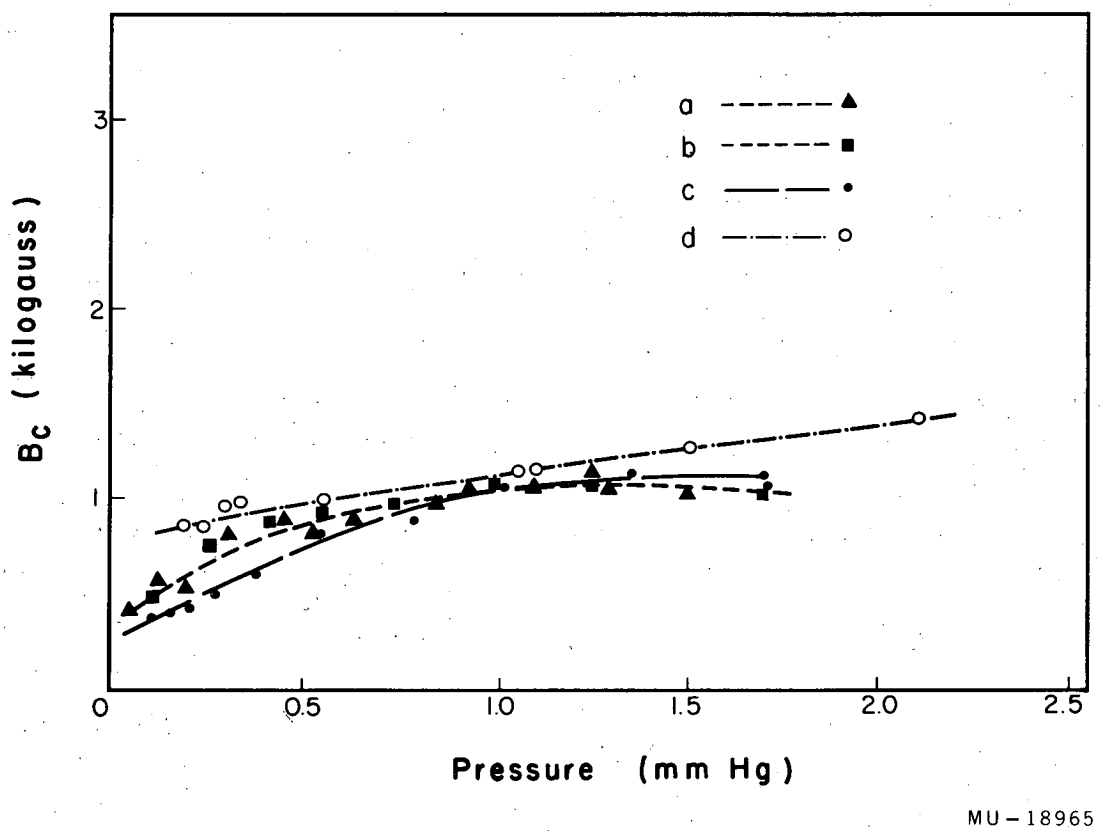

Fig. 29. The critical magnetic field vs pressure for various electrode configurations; He gas. (a) and (d), electrodes outside magnetic field (normal condition); (b), anode in magnetic field; (c), both electrodes in magnetic field. (a), (b), and (c) at 50 to 300 ma dc, (d) at 5 amp pulsed.

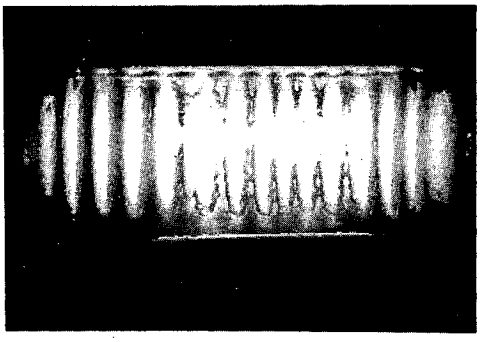

(a)

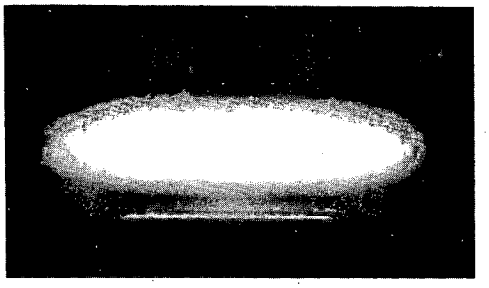

(b)

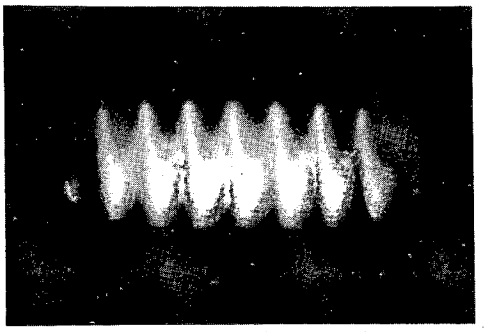

(c)

MUB-347

Fig. 30. Streak-camera photographs for a 4-amp current in a 6-cm-diam tube at 260 μ He. (a) B = 0, (b) B = 710, (c) B = 1075, B_c = 910 gauss.

As the magnetic field was increased the appearance changed from a striated to a uniform column and then, at the critical field, to a constricted rotating column. Slightly above B_c the rotating column becomes quite irregular. A close inspection shows that the previously discussed breaks in the longitudinal electric field and noise curves do not occur at exactly the same magnetic fields, the former being associated with the change from a uniform to a constricted rotating column and the latter with the onset of irregularities in the rotating column.

Various Langmuir probe measurements have been made in the dc discharges. The potential with respect to a second probe fixed at 6 mm from the tube wall shows a reversal in the radial electric field as the magnetic field is increased (Fig. 31), although there is no quantitative agreement with predictions. It has been suggested that the changes associated with the critical magnetic field may be due to this field reversal. Temperature measurements have been attempted with single and double probes. The single-probe measurements were not really to be depended on, as large-amplitude electrical oscillations were found to be present, which probably interfered with the measurements. For example, the apparent temperature, which below B_c is about 5 volts, increases rapidly above B_c to more than 30 volts.

Double-probe temperature measurements appear more reasonable, although there is once more an increase above B_c (Fig. 32). The temperature is independent of radius (as predicted) below B_c. The electron density is shown as a function of radius and magnetic field in Fig. 33. With increasing field the distribution becomes more peaked; the measurements above the critical field are of dubious value but show a more uniform distribution.

A remarkably close agreement between the cyclotron frequency and the calculated average plasma frequency at the critical field was observed over a wide variation of parameters for the dc case, leading us to suspect an interaction between these two oscillations. However, we have recently raised the plasma density to about 3×10^{12} electrons/cm^3 with pulses of several amperes and a few milliseconds long, and the magnetic fields at which the critical phenomena occur are unchanged. The average densities are measured by displaying the phase shift in an 8-mm microwave transmission path. At these higher current levels the moving striations, when they occur, perturb the plasma density by about 10%. This is a much smaller perturbation than was observed in the lower-current dc case.

Present measurements are concerned with detailed studies of the electromagnetic frequency spectrum below the critical field, the decay of the plasma after the current pulse, time-resolved probe measurements, and pulsing to still higher currents.

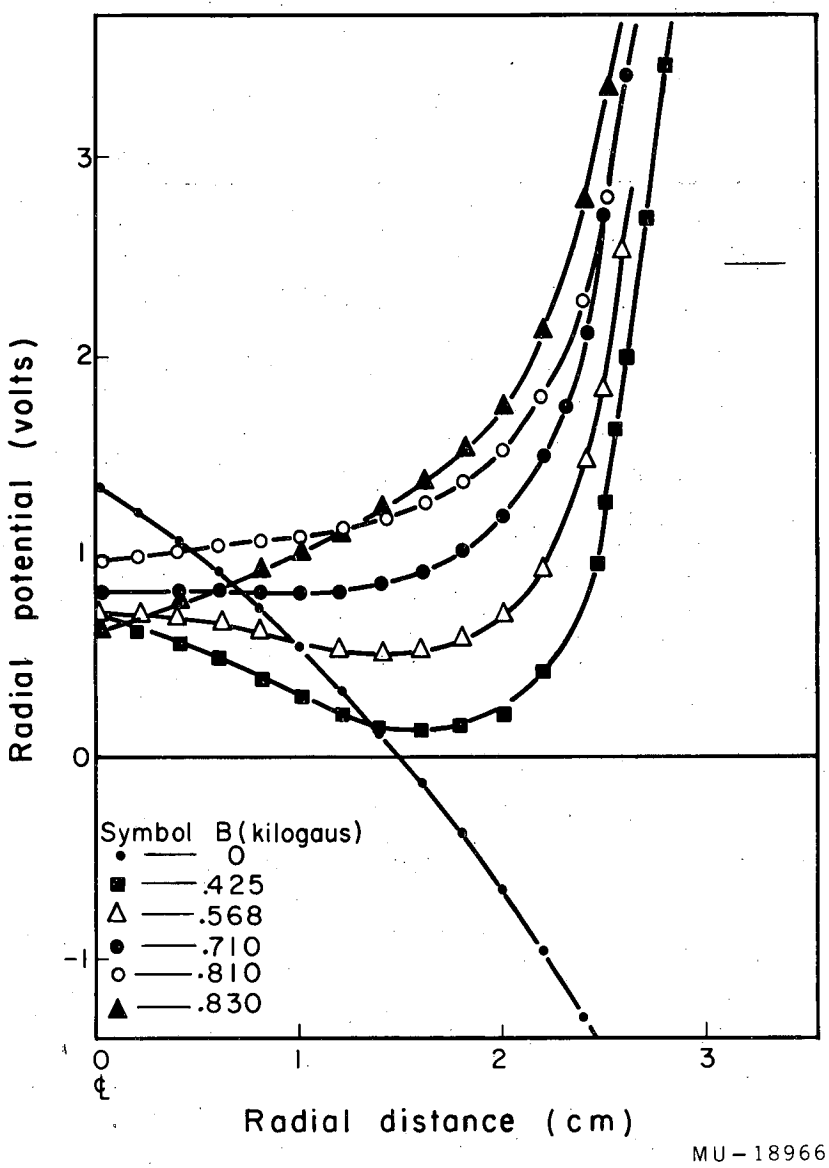

Fig. 31. Potential as a function of radius and magnetic field with respect to a probe fixed at 6 mm from the tube wall; p = 210 μ, I = 200 ma; He gas.

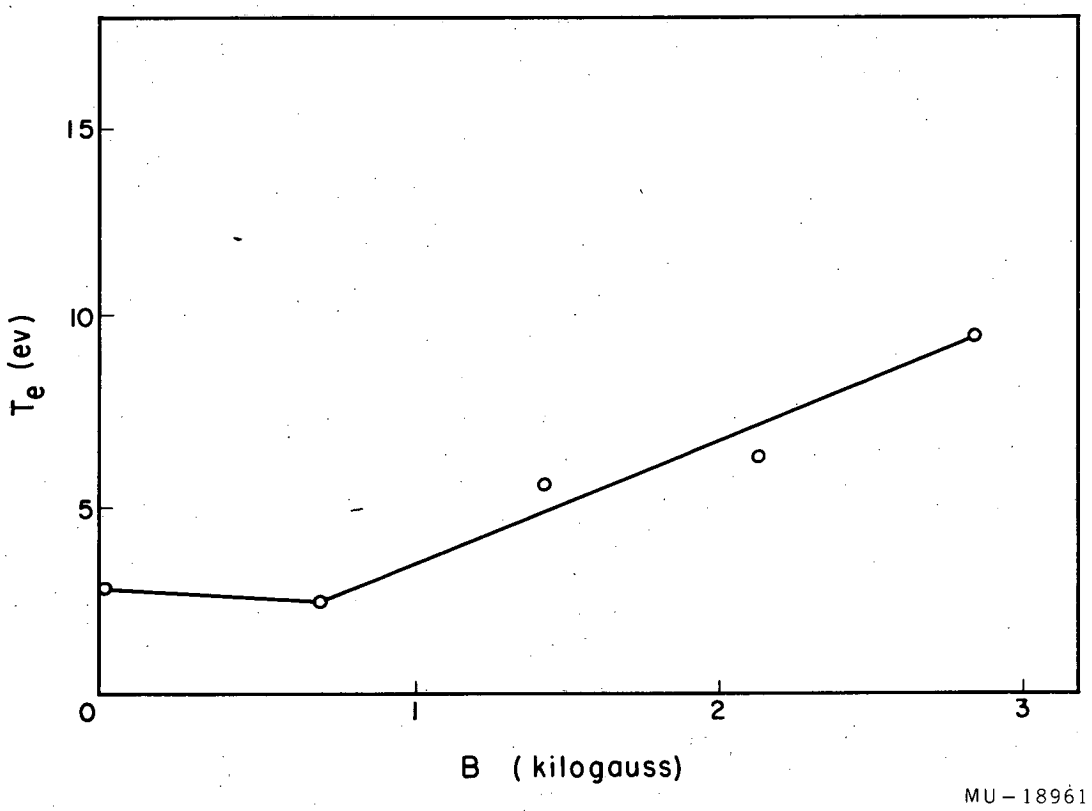

Fig. 32. Temperature near the tube center vs B; p = 220 μ, I = 200 ma; He gas.

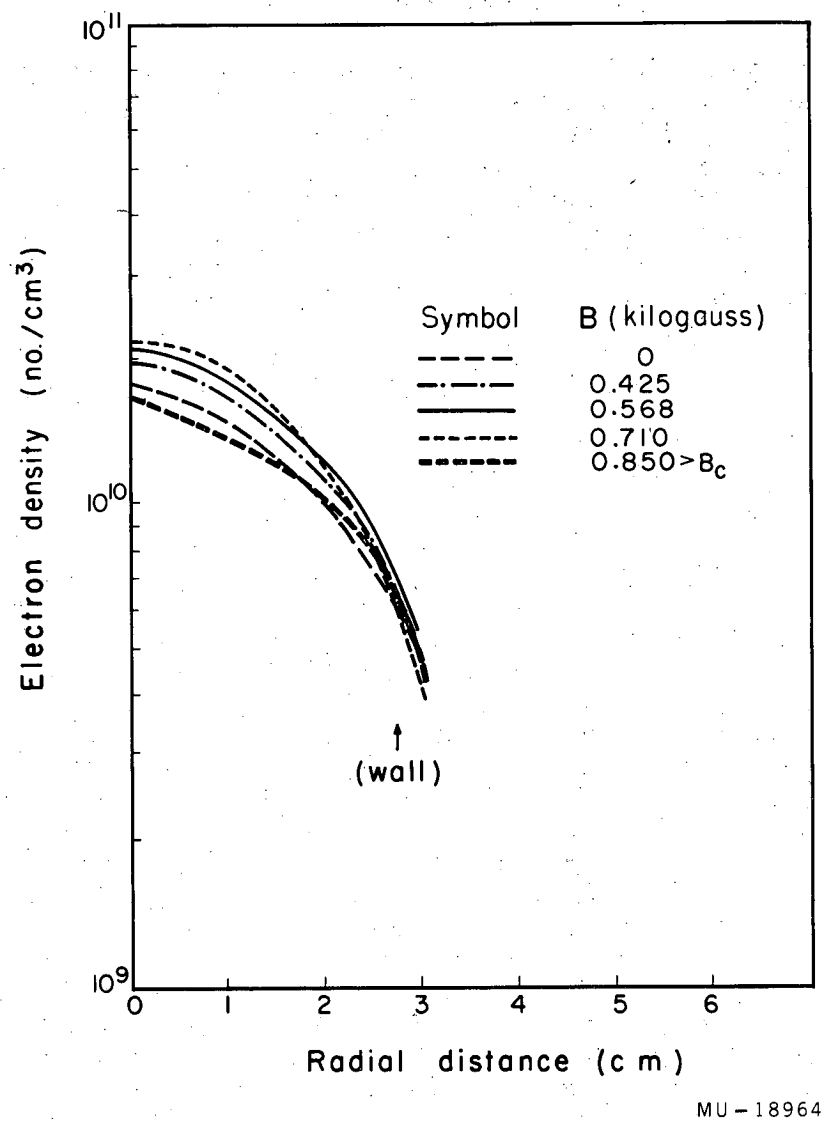

Fig. 33. Electron density vs radius and magnetic field; p = 220 μ, I = 200 ma; He gas.

Plasma Oscillations

An experiment is in progress to observe the growth and decay of large-amplitude electrostatic oscillations in a 1-in.-diameter low-energy electron beam passing through weakly ionized mercury vapor. The beam is intercepted by a repeller electrode that can be biased and moved with respect to the cathode. The oscillations are picked up by dipping a small movable probe into the beam. Measurements will be made with an axial magnetic field to reduce the transverse scattering by the high rf electric fields, with the main region of interest near $\omega_p = \omega_c$.

Experiments with a PIG Discharge

Several experiments have been done on a PIG discharge, using microwaves and Langmuir probes for diagnosis. An anode with a rectangular hole and an anode with a square hole have been used in our PIG in an effort to obtain slabs of plasma. Our feeling was that if we could obtain a reasonably sharp boundary on the plasma it would be much easier to correlate density measurements made with microwaves with those made with probes. Several interesting properties of PIG discharges were observed during these experiments.

There seems to be a critical magnetic field for the PIG discharge above which the plasma becomes unstable and noisy. Probe and photomultiplier signals indicate that a rotational mode may exist. Above this critical field the microwave signal becomes more and more obscured by the noise. For currents below 1 amp the B_c becomes larger as the current becomes smaller; for currents from 1 to 5 amp the B_c was more or less constant with increasing current, and also seemed independent of pressure from 6 μ to 60 μ of He. The discharge is relatively quiet below 500 gauss and the microwave signals are quite clean; this was the region we operated in when trying to relate microwave densities to probe densities. Our first measurements were made with microwaves and probes at different times, although with the same current, magnetic field, and pressure. Our next attempt has been made with a square defining hole in the anodes, so that the probe can be introduced from the top at the same time as the microwaves pass through the discharge horizontally. Here we assume that symmetry causes the density profile to be the same for the probe as for the horns.

With a 0.5-mm wire in a 2-mm glass rod there is a change of several per cent in the microwave measurement when the probe is inserted directly between the horns. The probe measurements show a profile that is almost a Gaussian distribution instead of being a rectangular slab. The current through the discharge is a sinusoidal pulse, and so the measurements are made point by point from an oscilloscope at the time of peak current. There is some doubt about how good the probe measurements are in the magnetic field, but at 300 gauss the electron Larmor radius is about 10 times the sheath thickness, so that the probe measurements may be all right. The density distribution as determined by the probe was used for a numerical integration to determine by means of microwave measurements the phase shift to be expected. The integration gave an expected phase shift of 2.9 radians, while the microwaves indicated 6.28 radians. (This was for helium at 16 μ with a field of 500 gauss, a current of 2.5 amperes, and an anode

aperture of 2×2 in.) The peak density was about 3.4×10^{12} electrons/cc as determined by the probe.) The microwave density is within a factor of 2 of the probe density.

Another curious phenomenon that we observed is that for certain conditions in the PIG discharge the amplitude of the microwave signals goes through maximums and minimums with increasing density, and at the same time the phase shift and attenuation change more rapidly than one believes the density is changing. This could be explained by the reflections from a rectangular density distribution. If one assumes that the density distribution is more nearly rectangular than is indicated by the probe measurements and that the nulls occur when the thickness of the slab is an odd number of wave lengths, the results are consistent with densities of 8×10^{12} and indicate that the plasma increases in thickness with the arc current. Looking at the discharge in a rotating mirror indeed shows that the luminous width of the discharge increases with arc current. This phenomenon was for argon at 8 μ at fields of about 250 to 300 gauss. Probe measurements made not at the same time but under the same conditions indicate that the density profile is similar to a Gaussian distribution and not abrupt enough to cause reflections of the microwave signal, casting doubt on this explanation.

We plan next to make density profiles with the probe and microwave measurements simultaneously in argon and at several pressures. We hope, then, to explain the conflicting evidence which seems to exist now.

Measurements on Triax Pinches

Two very simple microwave experiments have been made on Triax pinches. The first consisted of a klystron operating at 33 kMc, a slotted line, and a horn looking through the wall at the pinch. Photographs of the voltage at the slotted line probe vs. time were made for a number of positions along the slotted line. The position of null and the standing-wave ratio were determined as a function of time during the discharge. These showed that the microwave energy did not penetrate beyond the glass wall after the first 5 μsec and did not again begin to penetrate until 50 μsec later, even though the current lasted a few microseconds.

The second experiment consisted of a klystron operating, at 33 kMc, a pair of horns looking through the pinch and with a matched crystal detector terminating the receiving horn. The object of this experiment was to determine how long the microwave signal remained cut off. The results are discussed in the section on pinches.

Phase-Lock Servo System

This is a system for presenting phase shift in one arm of a microwave bridge circuit as a voltage signal varying in time. An EMI 9521 klystron operating at 33 kMc is used as the rf source. This signal is divided in a "magic tee," half through a short arm of a bridge circuit and half through a long arm. The long arm consists of a waveguide to and from the plasma, a pair of horns looking through the plasma, and a calibrated phase shifter. The two arms of the bridge are brought together in a balanced mixer.

If the frequency of the klystron is changed, the signal out of the balanced mixer varies sinusoidally with frequency because of the difference of length in the bridge arms. If there is a continuous phase shift in one of the bridge arms this also causes a sinusoidal output from the balanced mixer.

The signal from the balanced mixer is amplified and applied to the repeller of the klystron. If the loop gain is high enough and the polarity of the correct sign, the frequency will be servoed to hold the signal from the balanced mixer constant regardless of phase shift between the horns. The voltage applied to the repeller will be linear with phase shift for small changes in frequency.

The unit we have in operation enables us to measure a phase shift of about π radians before the servo runs out of range. This is a function of the length of the long arm of the bridge; the long arm cannot be lengthened indefinitely, however, because of the attenuation in the waveguide. The minimum phase shift measurable is a function of the signal-to-noise ratio of our amplifier. This is now about 0.1 radian, and can certainly be reduced with more care in the amplifier circuitry.

The phase-lock servo system is being used to measure the decay of low densities of about 5×10^{10} electrons/cc as now used. The frequency response of the present system should be from 50 to 100 kc, although this has not been measured yet.

Microwave Components

The development of components for producing circularly polarized waves has been completed, but any further development of components has been suspended because of budget reasons. A simple apparatus for propagating 33 kMc on a Goubau line has been tried and seems to work as predicted. (A Goubau line is a waveguide consisting of a dielectric coated wire. It has low losses and shows promise of guiding microwaves through a plasma under conditions whereby an insulated rod can be tolerated in the plasma.)

HYDROMAGNETIC WAVE PROPAGATION

John M. Wilcox and Alan W. DeSilva

No new results of fundamental interest have been obtained during this quarter; instead, the experimental equipment has been revised and, we trust, improved. Installation of the cyclotron resonance heating experiment has been completed and vacuum tests have been begun; experimental results should be available soon.

An experimental technique that illuminates the magnetic lines has been developed to make possible accurate alignment of the vacuum chamber walls with the magnetic field. A copper cylinder 36 in. long and 5-3/4 in. in diameter is to be aligned with a uniform axial magnetic field of approximately 10 kilogauss. One end of the cylinder is closed off with a copper plate, and the other end is closed off with a pyrex plate which is pierced by eight short wires, 1/16 in. in diameter and extending out for 1 in. on each side of the plate. The wires were 45 deg apart on a 4-in. -diameter circle and were welded in place by a glassblower. The chamber was filled with 150 microns of hydrogen and a negative voltage of about 1200 volts was applied to the wires. From each wire we observe a sharply defined line discharge which runs along the magnetic field lines that pass through the wire. Attached to each wire one can observe a glowing thread which traces out the magnetic field lines. With the aid of a telescope the vacuum chamber position could be aligned to within 1/32 in. or less.

A number of small magnetic probes have been constructed and calibrated. These will be used to measure the wave velocity and attenuation and the spatial variation of azimuthal, radial, and axial components of the wave magnetic field.

Ionization has been produced by a 45-μf condenser bank which oscillated several times as it discharged (see Fig. 34). This condenser bank has been replaced by a square-wave pulse line such that the ionizing current flows for 100 μsec and then stops, leaving a quiescent plasma with no external currents flowing through it. Wave propagation can still be observed when the wave is induced several hundred microseconds after the ionizing current has stopped.

The 2-in. -diameter (2-in. -long) electrodes were replaced by 0.5-in. -diameter (0.5-in. -long) electrodes in an effort to have a closer approximation to a point source of radial current. The transmitted wave under these conditions was rather hashy, and when the vacuum chamber was taken apart the molybdenum electrodes were observed to be badly pitted, and bits of molybdenum were driven into the insulators. Therefore we have returned to the use of 2-in. -diameter electrodes.

In one series of experiments the tube was ionized by discharging the square-wave slow bank between one center electrode and the outer cylinder. This produces a spinning plasma somewhat similar to the Homopolar or Ixion experiments. A large-amplitude semisquare hydromagnetic wave can be driven by then shorting out or crowbarring the electrode to the outer cylinder. Since this can be done with a very low inductance circuit, a larger

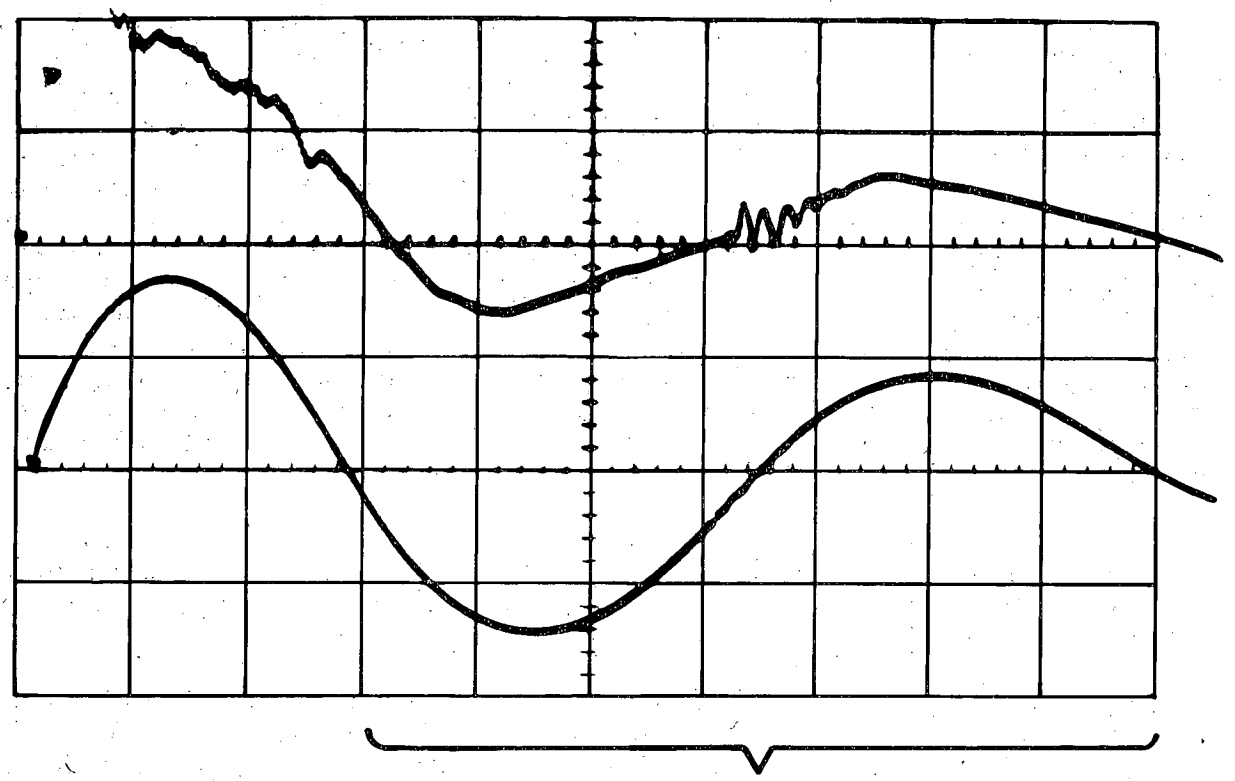

MU-18302

Fig. 34. Slow-bank voltage and current. Horizontal scale 10 μsec per large division. Top trace is voltage between the center electrodes at 100 v per large division. Bottom trace is current at 40 ka per large division.

signal is possible than can be conveniently obtained from an active drive such as a condenser or oscillator. This square wave was observed to travel down the tube at approximately the Alfvén velocity. The received wave form was more rounded than the driving wave form. This may have been caused by the attenuation of the frequency components above the ion cyclotron frequency. In the theoretical discussion of Alfvén-wave propagation a small-amplitude treatment is not needed for the case in which a wave is propagating in only one direction along the magnetic field.

It was noted during the course of the preceding experiments that the ionization proceeds down the tube with a well-defined front and at a measurable velocity, which depends upon various experimental parameters. Although not directly related to the hydromagnetic wave phenomena, this "ionization wave" is of interest in establishing the initial conditions in the tube. The velocity with which this disturbance travels was determined by measuring the current that flows in a copper strap short-circuiting the receiving electrode to the liner. In most cases the current in this line rises quickly from a sharply defined point in time after some delay representing the time for the ionization to proceed from one end of the tube to the other. It would appear that ionization takes place in a fairly restricted region at the front of the ionization wave, leaving behind it a region of warm, rotating plasma. Once rotating, the plasma generates a back emf which would prevent further radial current flow. Hence, most probably the radial current flows mostly at the front face of the "ionization wave." The velocity varies rapidly with applied voltage, going roughly as V^2. Increasing the magnetic field causes the velocity to increase linearly with B. The velocity decreases with increasing pressure up to a point at about 100 microns and then increases slowly.

AXIAL TRANSFER OF RADIO-FREQUENCY ENERGY TO THE CENTER OF A "MAGNETIC MIRROR"

Edmund S. Chambers

A 20-ampere deuterium discharge, in the form of a uniform hollow cylinder, has been obtained. By applying a radio-frequency electric field radially through the plasma, at one end of this discharge, axially propagating waves were excited. Energy transfer to ions at the center of the machine was detected by axial magnetic-field-detecting coils. The measured impedance across the rf gap was about 1 ohm. This impedance has had an inductive component in some experiments and a capacitive component in others. In most experiments the impedance has increased linearly with static magnetic field, as expected from theory. The impedance decreases with increasing pressure, as expected. So far, for ease of measurement, the rf current has been limited to 5 amp.

Experiments are being continued in which hydromagnetic waves are directly excited at one end of a magnetic mirror machine by an alternating radial electric field. These waves propagate axially toward the center of the machine, where at ion-cyclotron resonance the energy of the waves is transferred to ions of the plasma by a damping process. In this way energy can be continuously "poured" into one end of the magnetic mirror to be utilized in the form of transverse ion motion at the center of the machine without requiring material electrodes at this point. One of the crucial requirements of such a scheme is that the rf voltage be applied in such a way that it is not shorted out at the end of the machine by conducting walls that shunt electrons across the magnetic lines. In the experiments to be described this is accomplished by utilizing the insulating character of a cathode sheath. Such a sheath is formed at the end of the reflex (PIG) discharge used in forming the initial plasma.

T. H. Stix[1] has developed the theory of and used a similar type of waves in the stellarator geometry. Harold P. Furth[2] proposed utilizing these waves in the mirror geometry, and has made many helpful suggestions as these experiments have progressed. Earlier experiments concerned with more direct but limited methods of employing ion-cyclotron resonance are described by Edmund S. Chambers et al.[3]

Figure 35 indicates how the ions and electrons gain energy from the radial electric field. Then through the influence of the magnetic field both are deflected in the same azimuthal direction. This constitutes a mass motion of the plasma that propagates axially along the magnetic field in the manner of whirl rings described by Alfvén.[4] Figure 36 shows how the

[1] T. H. Stix, Phys. of Fluids 1, 308 (1958).

[2] H. P. Furth, Ion-Cyclotron Waves in Mirror Geometry, UCRL-5423-T, Feb. 1959.

[3] E. S. Chambers, A. A. Garren, D. O. Kippenhan, W. A. S. Lamb, and R. J. Riddell, Jr. Cyclotron Resonance Heating of a Plasma in a Magnetic "Mirror," UCRL-5286 June 1958.

[4] Hannes Alfvén, Cosmical Electrodynamics (Clarendon Press, Oxford, 1950), p. 88.

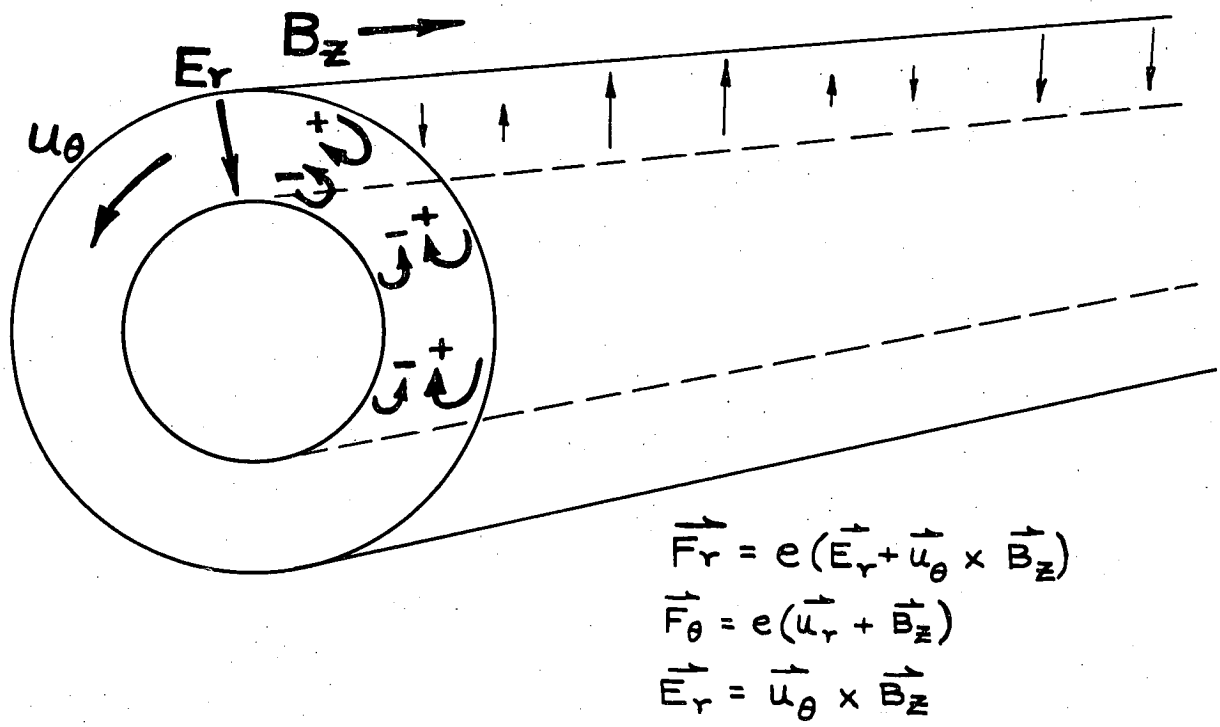

Fig. 35. Hydromagnetic wave excitation.

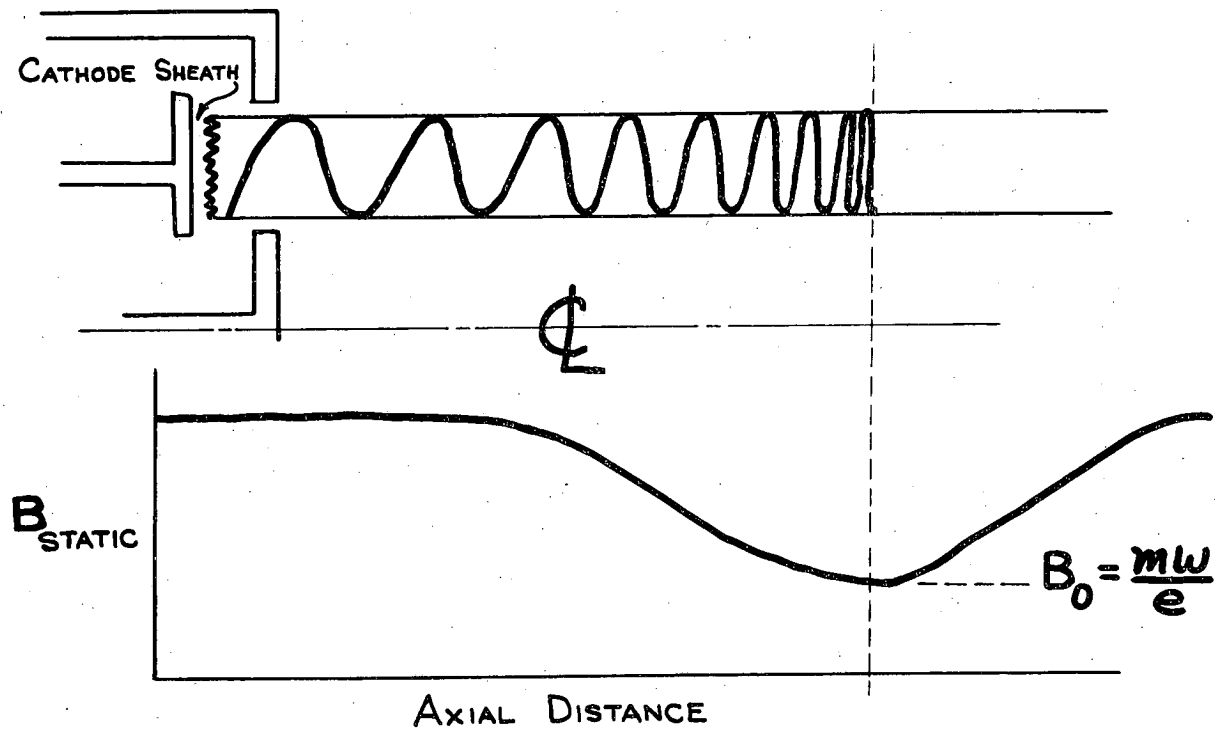

MU-18926

Fig. 36. Axial variation of hydromagnetic wavelength.

wave length of the waves is believed to vary with decreasing static magnetic field. As the waves propagate into regions of lower magnetic field the wave length becomes shorter and shorter, until at ion-cyclotron resonance the wave length decreases to zero. At such a point the wave may be reflected or it may be strongly attenuated by "ion cyclotron damping."[5] Another way to look at it is to consider the plasma cylinder as a coaxial transmission line. The propagating azimuthal motion, u_θ, of the plasma carries with it a radial electric field, $E_r = u_\theta \times B_z$. When this field reaches a region of ion-cyclotron resonance the ions take up energy somewhat in the manner of a cyclotron. Indeed, from this standpoint the machine may be considered to be a plasma cyclotron. Figure 37 indicates in a rough way the type of energy transfer that may take place. This picture of the damping mechanism may be too simple. For instance, at the resonance point the phase velocity of the wave has dropped to zero, and the ion on successive turns may encounter fields of varying phase. In spite of this it seems clear that to the extent the wave is attenuated the ions of the plasma will pick up energy. Just as a rapid change in refractive index reflects on electromagnetic wave, a rapid decrease in the static magnetic field may reflect the hydromagnetic wave. This problem has been studied by Stix,[5] but his results have not yet been applied to this case.

Figure 38 illustrates the equipment being used. The magnet coils provide a static magnetic field of 4345 gauss at the center of the machine, for resonance, with a mirror ratio of 2.2. The driving electrodes are placed at one end of the mirror with one of the reflecting cathodes of the reflex discharge just outside them filling in the gap. The cathode at the driving end is made of tungsten sheet and is self-heated by ion bombardment from the discharge. Observing its color temperature serves as a sensitive means for determining the uniformity of the discharge around the cylinder. In recent experiments, after careful adjustment, the uniformity has been excellent. This is important because at ion-cyclotron resonance, at which the ions are gyrating away from their neutralizing electrons, a uniform ring of plasma ensures that no undesirable azimuthal polarization will form. At the other end of the discharge a white-hot tungsten rod filament supplies about 95% of the electrons. The two driving (rf) electrodes form the anodes for the discharge. Figure 39 shows how the circuit is arranged so that both are at dc ground potential. The discharge current divides approximately equally between the inner and outer anode electrodes.

Earlier experiments[6] and some of the current ones have been aimed at detecting effects produced by the hydromagnetic waves as they pass through the plasma. Ions gyrating in planes perpendicular to the magnetic axis are equivalent to magnetic dipoles. When the energy of such ions changes, the dipole strength changes correspondingly, and if this magnetic flux links another coil a voltage is induced. In the earlier experiments a tuned multiturned coil was used for this purpose. This was placed parallel

[5] T. H. Stix, Absorption of Plasma Waves MATT-3, June 1959.

[6] E. S. Chambers, Ion Cyclotron Resonance Heating, in Controlled Thermonuclear Research Quarterly Report, UCRL-8887, Sept. 1959, p. 113.

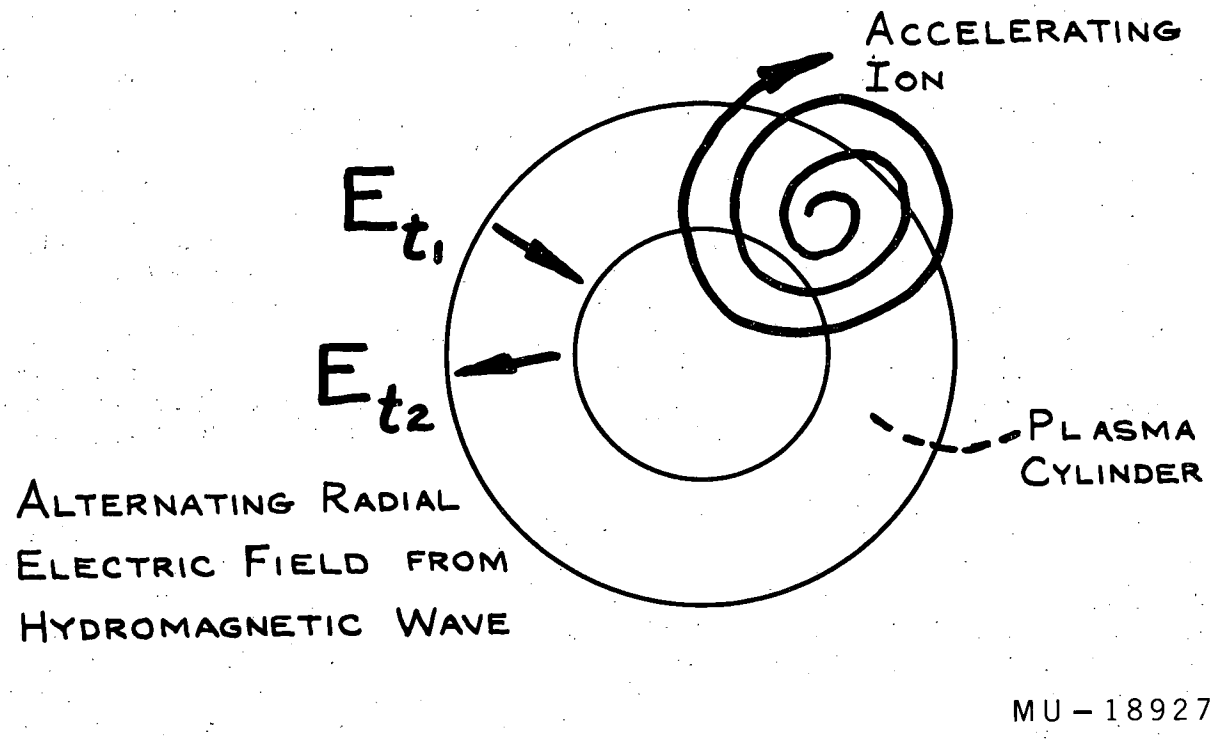

Fig. 37. Ion acceleration by ion-cyclotron damping.

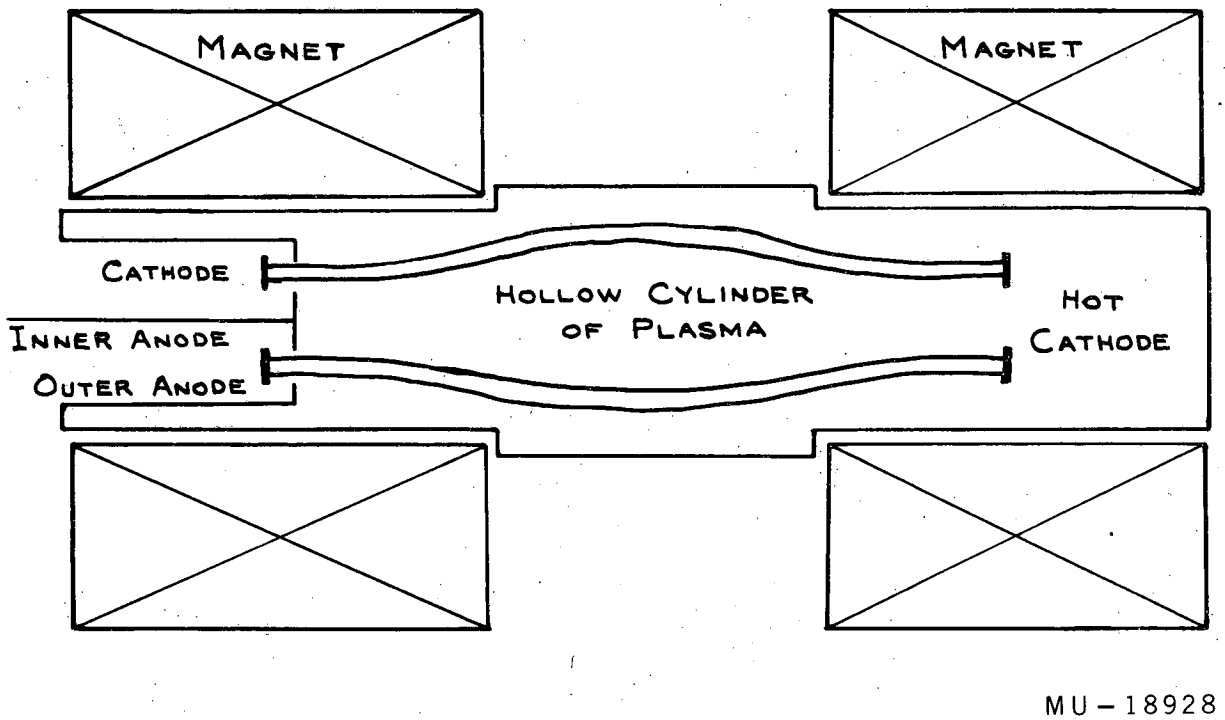

Fig. 38. Magnetic "mirror" and electrodes.

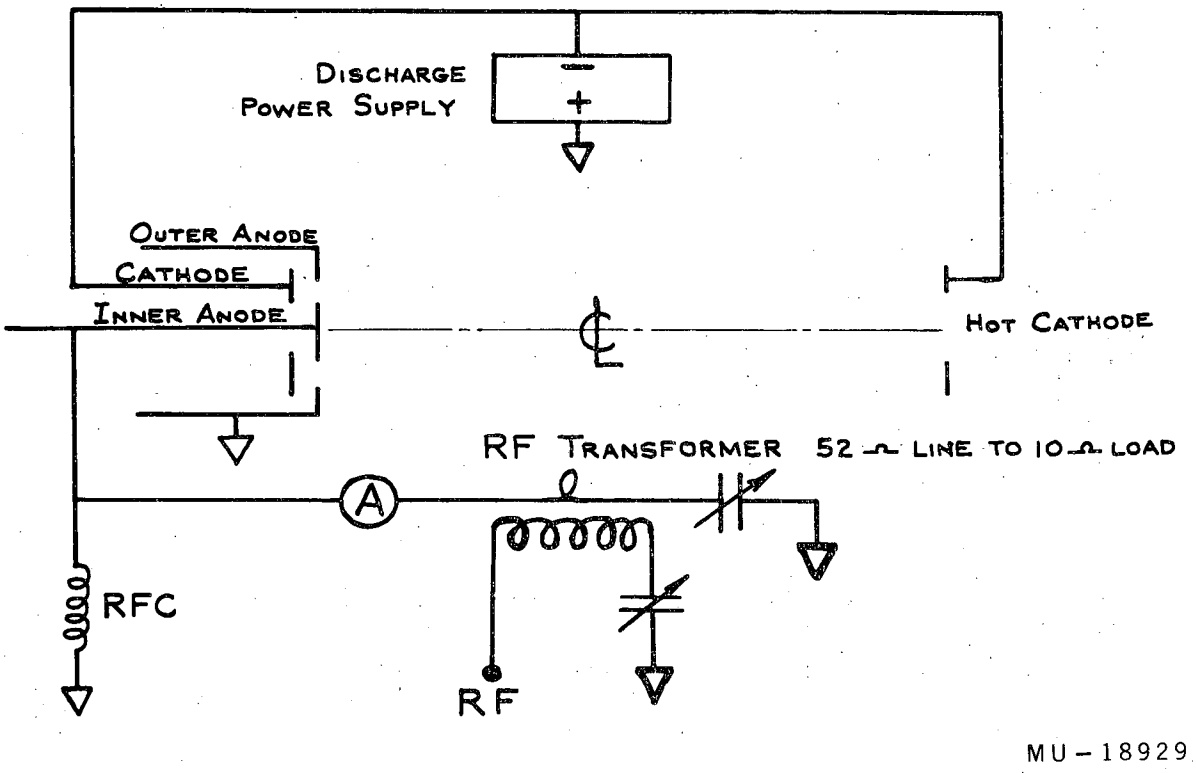

Fig. 39. Electrical circuit.

to but offset about 1/2 inch outside the plasma cylinder. In recent experiments a coaxial single turn was used, with a diameter about 2 in. larger than the beam. In both cases signals of several volts have been obtained. Such signals show decided peaks at the times when a resonance region is close to the coil. This, to me, clearly indicates that energy is being transferred to the ions as predicted by the theory. As the static magnetic field is raised above the level for cyclotron resonance at the center there will no longer be a resonance region in the machine and the waves will propagate through to the far end. This has been observed experimentally by a sharp dropoff in voltage of the central pickup coils. A corresponding rise in voltage was noted on a coil placed at the far end. A rough sketch of the results obtained is shown on Fig. 40.

Other indications of wave activity have been obtained by using a radial probe with its end about 1/2 in. from the plasma. At times, when a resonance region was adjacent, the probe voltage rose.

Another important phase of the problem being investigated is the transfer of energy between rf electrodes and the plasma. The impedance of the rf gap is being studied by measuring its circuit characteristics. The gap is first short-circuited with a copper strip. The tuning capacitor (see Fig. 39) in the secondary of the rf transformer is then tuned so that the capacitive reactance balances the inductive reactance of the conductors leading to the gap. At this condition the current in the secondary circuit is wholly dependent on its resistance and the voltage applied. The current is measured by an rf ammeter and the voltage by a diode and dc meter or a vacuum tube voltmeter. During a run with plasma between the gap the tuning capacitor is again adjusted for maximum current and voltage and current read again. The plasma load has been found to be capacitive in some experiments and inductive in others. The impedance has usually been about 1 or 2 ohms. A recent experiment, in which the cylinder of plasma was uniform, is summarized: filament power, 2.4 kw; deuterium pressure, 1 μ; reflex discharge voltage, 200; current, 20.8 amp. With B_{static} adjusted for cyclotron resonance at the center of the machine, 4345 gauss, an rf current of 4.8 amp, 3.3 Mc, was passed through the plasma. An accurate absolute measurement of the gap voltage could not be made in this particular run, but the impedance was of the order of 1 ohm. The characteristic impedance of a transmission line is

$$Z_0 = \sqrt{\frac{L}{C_0 K}} ,$$

where C_0 is the vacuum shunt capacity per unit length of the line and K is the dielectric constant. Where K is large, we have

$$K = \frac{4 \pi \rho C^2}{H^2} ,$$

where ρ is the mass density of the plasma. It was found that the impedance decreased with increasing pressure, as predicted by the equations. The equivalent series capacity of the plasma was 0.03 μf, indicating $K = 10^4$.

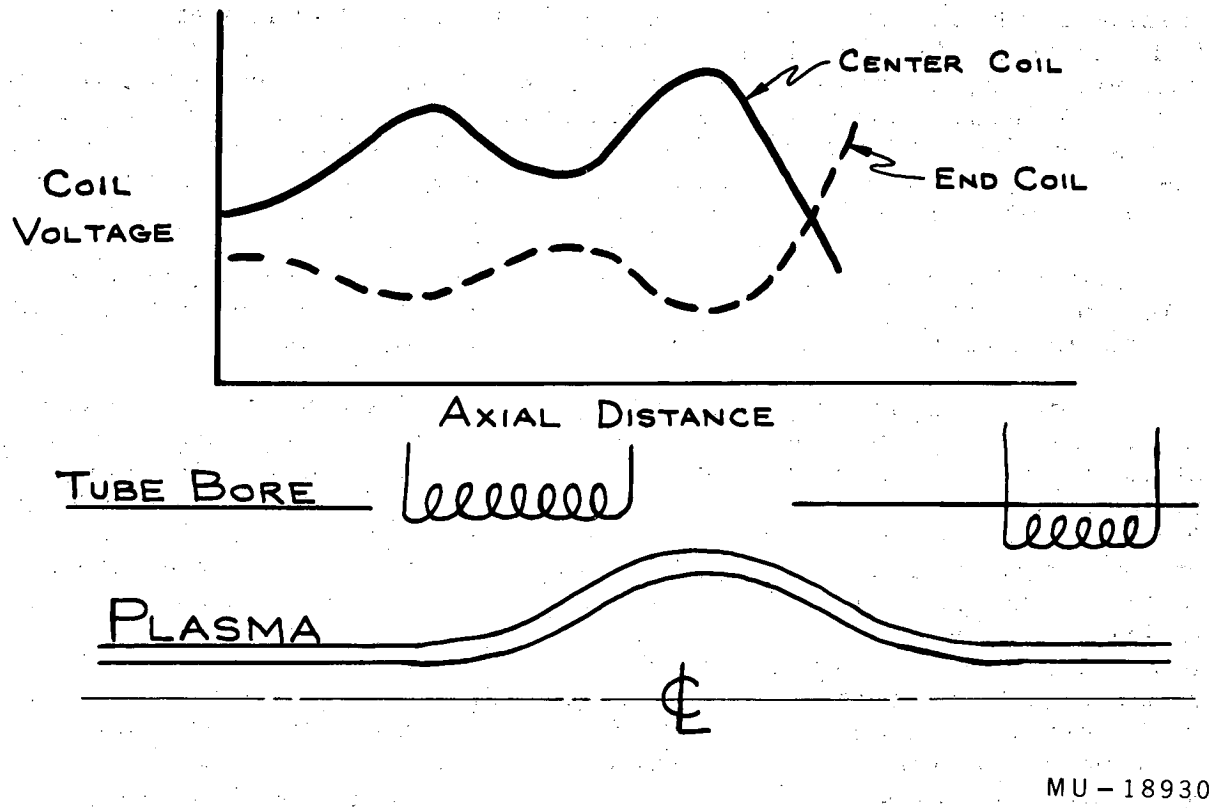

Fig. 40. Wave detection.

In this particular run the impedance appeared to decrease with increasing field. This is opposite to what the equations predict. It would be understandable if the plasma density increased sufficiently at the same time. The discharge current remained substantially constant during the change in magnetic field.

In most experiments, the rf impedance varied linearly with magnetic field, as predicted by the equations. This result strongly suggests that the rf voltage is not being shorted out around the electrodes and that it is being used effectively in influencing the plasma. The electrical capacity exhibited by the plasma is probably an example of the hydromagnetic capacitor discussed by O. A. Anderson et al.[7] The flywheel effect is caused by the azimuthally rotating plasma. From the standpoint of a transmission line, however, if all the energy were utilized at the far end, the line would appear to be "flat" and completely resistive. Thus at least a part of the wave appears to be reflected. With the proper static axial magnetic field gradient, strong damping of the waves should take place, accompanied by strong heating of the ions.

[7] O. A. Anderson, W. R. Baker, A. Bratenahl, H. P. Furth, J. Ise, W. B. Kunkel, and J. M. Stone, Study and Use of Rotating Plasma, in International Conference on the Peaceful Uses of Atomic Energy, 2d, Geneva, 1958 (United Nations, New York 1959) Paper No. 373, Vol. 32, p. 155.

ATOMIC AND MOLECULAR BEAM RESEARCH

Gilbert O. Brink

The crossed-beam machine for the measurement of collision cross sections is still under construction. Because of strikes and various delays the vacuum tank has not yet been received. It is supposed to be delivered sometime within the next month. The electronic equipment is being installed in the new laboratory in Building 180 and should be ready before the vacuum system is completed.

During the last quarter considerable thought has been given to the type of mass spectrometer to be used with the machine. At present it appears that some form of time-of-flight spectrometer may be the best. Since this type uses no magnetic field it can be self-calibrating, as one needs to know only the geometry and the voltages applied in order to know the mass number. Also, the transmission in this type can be made larger than in the magnetic type.

A vacuum system is being set up to try out a time-of-flight spectrometer. The system should be completed within the next two weeks, and some preliminary measurements made to determine the operating characteristic. The type of spectrometer chosen is that described by Wiley and McLaren.[1] It is a particularly simple type that makes use of oscilloscope display. It makes possible the continuous monitoring of the abundance ratio of two isotopes, a feature that is of considerable importance for cross-section measurements.

[1] W. C. Wiley and I. H. McLaren, Rev. Sci. Instr. 26, 1150 (1955).

ION-SOURCE DEVELOPMENT

John A. Fasolo

The Von Ardenne-type sources described in previous reports have not been operated during this quarter because the 100-kv source test facility is no longer available for this purpose.

The Model III source has been dismantled and will be reassembled with a water-cooled z electrode designed for efficient cooling of the electrode.

A new source, CS II (Source II, Series C) has been designed and will be built to provide maximum cooling of the anode and trapping-chamber structures.

A new ion-source test facility is being assembled in the area adjacent to that in which the apparatus for Gilbert O. Brink's atomic- and molecular-beam cross-section measurements will be located.

This facility will be used initially to test an rf ion source of the type developed at Saclay by Contant, Prevot, and Vienet.[1] A source of this type has been built and will be used to provide an atomic ion beam for Brink's cross-section measurements.

[1] J. Contant, F. Prevot, R. Vienet, Etude et Realisation d'un Cannon à Ions du Type Haute Frequency à Debit Elevé, Service de Physique Appliquée du Centre d'Etudes Nucleaires de Saclay, Report No. PA/7737.

IX. ENGINEERING AND TECHNOLOGICAL DEVELOPMENT

ULTRAHIGH-VACUUM DEVELOPMENT

Norman Milleron and Leonard L. Levenson

Estimate of Progress in 1959

Our goals were (and continue to be):

To pump away thermalized gas and directed beams of particles at "black hole" pumping rates.

To repeat,[1, 2] a "black hole" for thermalized gas implies

$$S = Avk/4 \times 10^{-3} \text{ liters/sec},$$

where A = area of a hole (perhaps the entire area of a chamber),

v = average velocity for a Maxwellian gas,

S = maximum possible speed associated with area A,

$k < 1$, an efficiency factor.

A black hole for a beam of gas implies disposing of the entire beam, perhaps many equivalent NTP/cm^3/sec.

Believing diffusion pump systems to underlie any satisfactory solution to the black hole problem, we set out to optimize a diffusion pump system comprising a bakable valve, trap, and baffle, and an oil diffusion pump.[1]

The work can be divided into four mutually dependent problems:

1. A theoretical[3] and experimental[4] study of conductances of optically opaque trap geometries is nearly complete. Progress here was very encouraging because of the firm agreement between experiment and Monte Carlo type of calculation by Donald H. Davis,[3] who has also given us very valuable theoretical advice. The best theoretical and experimental value to date gives $k = 0.38$. One gross bounce on a trapping surface is deemed necessary and sufficient for capture.

---

[1] Norman Milleron and E. C. Popp, Gettering Hydrogen at Ultralow Pressures by Evaporated Metal Coatings, UCRL-5258, Nov. 1958.

[2] Norman Milleron and Leonard L. Levenson, in Controlled Thermonuclear Research Quarterly Report, UCRL-8682, March 1959, p. 65.

[3] Donald H. Davis, A Monte Carlo Calculation of Molecular Flow Through a Cylindrical Elbow and Other Shaped Pipes, (to be submitted to J. Appl. Phys.)

[4] Leonard L. Levenson and Norman Milleron, Optimum-Speed Oil Diffusion Pump Systems for Ultrahigh Vacuum, (to be submitted to Rev. Sci. Inst.)

2. A bakable valve is being worked on. A most promising solution incorporates an all-metal valve and trap in a single unit (k = 0.38).

3. Baffle studies--or, more properly, studies to eliminate baffles--are nearing completion. The backstreaming rate has been reduced nearly to the rate at which a pool of oil, at room temperature, will backstream owing to the room-temperature vapor pressure of the oil (see below).

4. The diffusion pump itself might be improved by reducing the length of its barrel[2] above the top jet and by increasing the mass flow in the top jet.

We feel confident enough to conclude that the optimization of a bakable oil diffusion pump system is within reach, and to predict that a completely oil-free diffusion pump (DP) system may quite possibly be made with a system pumping efficiency of 0.3. In light of this prediction, our original goal of 20,000 l/sec of deuterium at 1×10^{-9} mm Hg for a 32-in. NRC pump seems reasonable, since this implies a system pumping efficiency of only 0.13 on a 32-in. orifice.

Clearly, even an efficiency of 0.3 does not satisfy the "black hole" concept. Accordingly, we have conjectured in our previous reports[2, 5] about other pumping methods in series with diffusion pumps (see below).

In conclusion, the exchange of information with Westinghouse, Oak Ridge, and Princeton has helped our program very much. We are especially grateful for several ideas we have found useful: room-temperature trapping of oil,[6] jet cap heaters and covers,[7] and--above all else, perhaps--the chance to discuss ideas.

Work this Quarter

Of the three areas of investigation implied by our goal,

(a) black hole pumping and beam catching,

(b) clean pumping with diffusion pumps, and

(c) complementary techniques,

only (b) and (c) have been pursued experimentally this fourth quarter.

A few remarks about the possibilities of (a) are included.

---

[5] Norman Milleron and Leonard L. Levenson, in Controlled Thermonuclear Research Quarterly Report, UCRL-8775, June 1959, p. 76.

[6] M. A. Biondi, in Westinghouse Research Laboratories Quarterly Progress Report, Ultrahigh Vacuum Techniques, NYO-2616, July 1959.

[7] C. E. Normand, Tests of Oil Diffusion Pumps, part 4.3, p. 70, ORNL Thermonuclear Project Semiannual Report ORNL-2693, January 31, 1959.

Black Hole Pumping and Beam Catching

Our previous report suggested pumping with a PIG type discharge supported on metallic vapor.[2] We now wish to offer the same general PIG idea as a way of establishing a check-valve action at the orifice to a DP system. The notion offered is to change the probability of a particle's going back out of an orifice once it has entered. The feasibility of our scheme probably rests on the attainment of a pumping efficiency of 0.2 or better for a DP system. If a curtain of electrons can discriminate between slow particles and fast particles, then a solution to the problem of handling directed beams and accompanying thermal gas is at hand. If an electron curtain can reflux slow particles and pass fast particles, a check-valve action can be achieved in front of a DP system. This idea assumes the DP system has a probability > 0.2 of removing particles refluxed by the curtain. The curtain must operate as an efficient refluxing device. That is, particles can freely enter the curtain from both sides and are not returned to the plasma side, being instead refluxed to the DP through the edges of the curtain.

Specifically, curtains could be maintained on both the entrance and exit sides of a chamber pierced by a high-velocity directed beam. The beam would pass through both the curtains. Room-temperature gas coming with the beam could be excluded from entering the system through the first curtain by redirecting these slow particles to a DP system. On the exit side of a horizontal beam two DP's would be placed side by side, the beam passing over the first and into the second. A large orifice connecting the first DP with the plasma system would have a curtain, and a small orifice would connect the first and second pumps. The beam would largely be disposed of by the second DP. It may be worth remembering the Simpson linear jet pump[8] for use as the second DP with its long axis parallel to the beam axis.

An estimate of these ideas of using PIG's as curtains and (or) pumps will be given in a forthcoming report, by Norman Milleron and Leonard L. Levenson, Preliminary Pumping Results with a Penning-Type Discharge Supported on Condensible Metal Vapors, UCRL-5598-T.

Clean Pumping with Diffusion Pumps

4-Inch-Diameter Angle Trap

The base pressure observed on the tungsten filament GIC-100 B-A gauge rose steadily with time. After 2 weeks of operation the pressure was $\sim 6 \times 10^{-10}$ mm Hg. After 3 months of operation, the indicated pressure was 1×10^{-8} mm Hg, which may not yet be an upper limit. Our question is: Is this pressure rise caused by the typical spectrum of cracked hydrocarbons

[8] E. R. Lind and J. F. Steinhaus, Development of a Large, Linear Jet, Mercury Diffusion Pump Having High Pumping Speeds in the 10^{-6} mm Mercury Absolute Pressure Range, MTA-14, March 1953.

usually associated with pump oil? From similar work at Westinghouse on copper-trap life[9] it does not appear that typical cracked-oil products are responsible for our observed pressure rise. Not having a mass spectrometer, we tried to get an estimate of the lifetime

$$\tau = \tau_0 \exp Q/RT$$

of particles on the surface. We also looked for multilayer adsorption. Using these two methods, we hope to discriminate between heavy and light gases as follows: By leaving the B-A gauge off for progressively longer periods of time at room temperature and then turning it on, we can compare the amount of gas picked up on the filament and glass envelope in each time period. This surface pickup can be done from liquid nitrogen temperature up to 400°C. This desorption method of assessing the amount of material collected on filament and envelope surface at a given temperature can give a good indication of whether or not multilayer adsorption is occurring. Multilayer adsorption at room temperature indicates a higher heat of physisorption than possible with very light hydrocarbons and inorganic gases. The wall temperature of the B-A gauge was lowered to liquid nitrogen temperature. It was also raised to 400°C by placing an oven around it. Our results will be given in a future report.[4]

Conductance Measurements

Conductance tests have been made on several models. The models included chevron and single-louver geometries with slats inclined at 30 deg and 45 deg; a 90-deg cylindrical elbow with equal arm lengths, and a cylinder provided with end openings smaller than the i. d. of the cylinder. This last model contained a thin disc of diameter equal to the diameters of the end openings. This disc was centered between the end openings, was parallel to them, and was coaxial with the cylinder. Both the 90-deg cylindrical elbow and the cylinder were opaque to any direct line of sight through them. The slats in the single-louver models barely overlapped in such a way that no line of sight existed between two slats when they were viewed along a line vertical to the plane of the orifice between them. The chevron model had its slats bent into V's with apex angles of 90 deg. This chevron model was opaque from all directions of view.

In all the louver and chevron models tested to date, the ratio of the length of the slats to the normal distance between them was 5.33.

For the 90-deg cylindrical elbow the ratios of the arm lengths (measured from the centerlines) to the cylinder radius were 3.0.

The opaque-cylinder models had dimensions such that the inside radius of the cylinder was 1.5 times the radii of the end openings and the center disc. The inside lengths of the models were 2.0 and 3.0 times the radius of the end openings.

---

[9] J. H. Carmichael and W. J. Lange, The Use of Copper Foil Isolation Traps with Ultra-High Vacuum Systems, in Transactions, Fifth National Symposium on Vacuum Technology (1958), p. 137.

The results of the tests on these models may be expressed in terms of the geometrical factor P, such that

$$F = P F_0,$$

where F_0 is the conductance (liters/sec) of the orifice area, and F is the conductance of the model as a whole. For the 30-deg and 45-deg louver models, P was found to be 0.20 and 0.32 respectively. For the 90-deg chevron model, P was 0.13. The factor P for the 90-deg elbow was 0.30. The opaque cylinders had values of P of 0.38 and 0.37 for the models with ratios of axial length to the radius of the openings of 2.0 and 3.0 respectively.

The experimental values of P given above are accurate to within 10%. The geometrical factors, P, have been calculated by Donald Davis[3] of the theoretical group, for the 90-deg cylindrical elbow and the opaque cylinder. For these cases, the experimental and calculated values agree within the accuracy of the experimental values.

This work is continuing and will be reported in more detail at a later date.[4]

Large Diffusion Pump Test System

In this quarter, we have been able to appreciably reduce the rate of backstreaming from a NRC H-10-P (10.5-in. i.d.) oil diffusion pump. This reduction was made without the use of baffles.

A combination of devices was used. One device was an electric heater attached to the top jet cap. With this electric element, the top jet cap could be superheated to temperatures as much as 150° C higher than the boiler temperature (~ 200°C).

The other device was a water-cooled copper cylinder which was fitted over the top jet cap. This cylinder could be raised or lowered while the pump operated. Its bottom edge could be lowered below the bottom edge of the top jet cap so as to be impinged on by the vapor jet.

It was found that the backstreaming rate remained high (relative to the lowest obtained rate) when either of these devices was used without the other. If the bottom edge of the cooled cylinder was raised above the lower edge of the top jet cap, backstreaming was greatly increased; this was the case even for temperatures as high as 300°C on the top jet cap. Furthermore, even when the bottom edge of the cooled cylinder was 3/4 in. below the lower edge of the top jet cap, backstreaming could be kept very low only if the heater supplied enough power to keep the temperature of the top jet cap at least as high as the boiler temperature (~ 200°C). However, even with the jet cap heater off, the backstreaming rate could be much reduced by use of the cooled cylinder alone.

The amount of oil vapor that condensed with time on the inside surface of a plexiglas plate over the mouth of the diffusion pump was used as a qualitative measure of the backstreaming rate. The working fluid was

Narcoil-40. The o. d. of the lower edge of the top jet cap of the H-10-P pump is 4-1/8 inches. The i. d. of the water cooled-cylinder was 4-7/16 in.

The backstreaming rate of the NRC H-10-P oil diffusion pump has been reduced almost to the amount of oil vapor which would arise due to the oil vapor pressure at room temperature. However, more work needs to be done to refine the techniques described above. Furthermore, research must be done to determine the dependence of pump speed on various arrangements and operating conditions of the devices we have described.

We are indebted to researchers in England[10] and at Oak Ridge[7] from whom we have adopted several of our techniques and ideas.

[10] B. D. Power and D. J. Crawley, Sources, Measurement, and Control of Backstreaming in Oil Vapor Vacuum Pumps, Vacuum 4, 415-37 (published 1956).

CRYOGENIC PUMPING

Gordon Gibson,* Willard C. Jordan,† Eugene J. Lauer, and J. Ralph Ullman

The purpose of these tests and a description of the apparatus are given in previous progress reports.[1,2] Figure 41 presents an additional run with liquid-helium-cooled charcoal. The charcoal sample and other conditions were the same as on previous runs.[2] The hydrogen leak was adjusted so that the pressure at the high-pressure end of the 1-in.-diameter, 20-in.-long cylindrical hole increased from the base pressure up to a steady value of about 6×10^{-6} mm Hg (which could be maintained by diffusion pumps in the high-energy injection analogy). The ion-gauge reading at the low-pressure end did not rise significantly above the base pressure of about 2×10^{-8} mm Hg for 70 minutes, which is very encouraging. Following this run an air leak was found, which may explain the base pressure of 2×10^{-8} mm Hg. It is expected that if this leak were stopped the base pressure would be less than the observed 2×10^{-8} mm Hg.

It would be interesting to see the results of the following runs:

(1) conditions the same as above, but with the air leak stopped,

(2) with the 1-in.-diameter charcoal wall replaced by a 1-in.-diameter metal wall,

(3) with a 0.5-in.-diameter charcoal wall,

(4) with different absorbents.

Work on this test has stopped, in conformity with the decision not to develop the technology of high-energy injection.

---

*Consultant from Westinghouse Corp., Atomic Power Division, Pittsburgh, Pennsylvania.

†Consultant from Bendix Aviation Corp., Research Laboratories Division, Detroit, Michigan.

[1] Gordon Gibson, Eugene J. Lauer, and John R. Ullman, in Controlled Thermonuclear Research Quarterly Report, UCRL-8775, June 1959, p. 83.

[2] Gordon Gibson, Willard C. Jordan, Eugene J. Lauer, and John R. Ullman, in Controlled Thermonuclear Research Quarterly Report, UCRL-8887, Sept. 1959, p. 118.

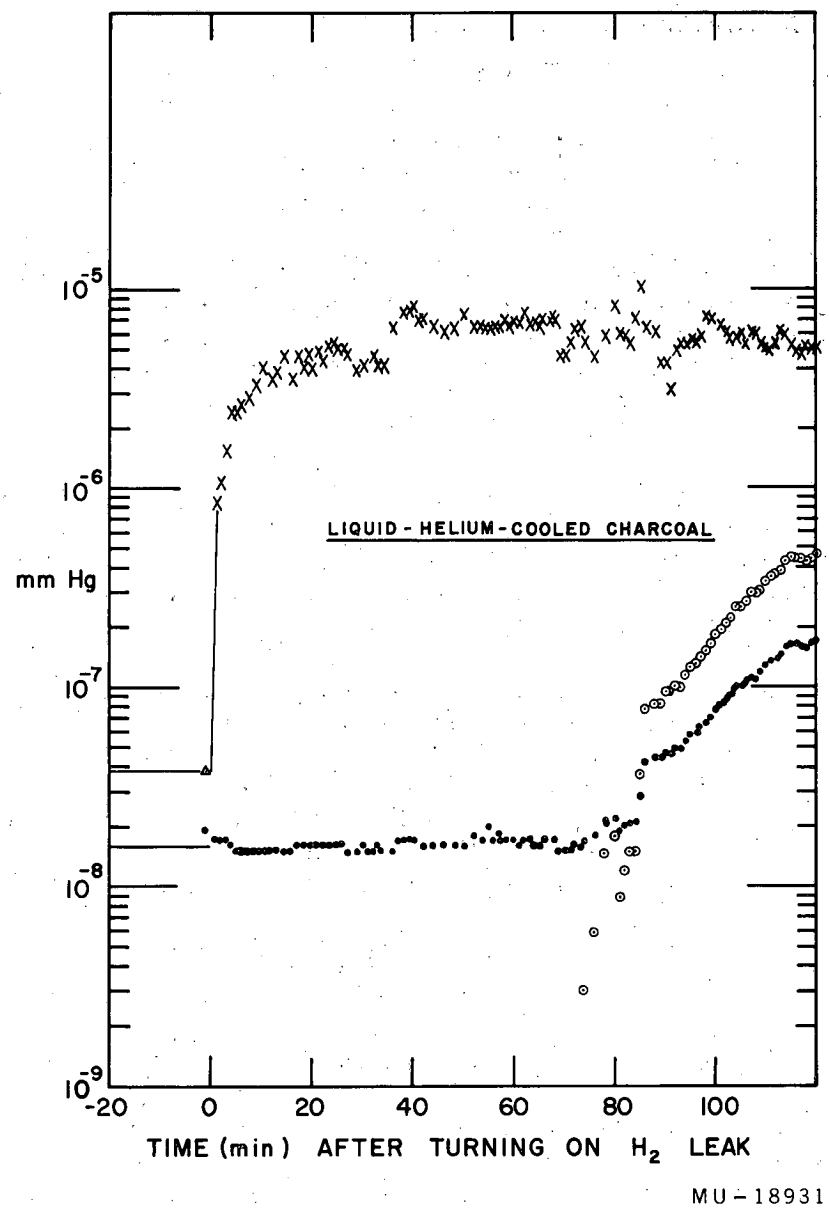

Fig. 41. Liquid-helium-cooled charcoal.

MECHANICAL ENGINEERING DEVELOPMENT

Thomas H. Batzer

Beta-Ray Experiment

J. Ralph Ullman

To facilitate adjustment of the 6500-lb mirror coils on their support structure, a pair of nonmagnetic coil jacks was fabricated and installed. Also fabricated and in use are new aluminum coil spacers. These are replacements for the original cumbersome wooden dunnage. Use of the new equipment permits individual coil displacements to ± 6 deg about a horizontal or vertical axis.

A compensating coil placed around the phototube in the counter at the mirror loss cone permits mirror-coil bias to be increased from 30% to 100% while maintaining the central field between the two mirrors at 1.3 kilogauss. The coil is 29 in. long by 8.2 in. o.d. by 6.2 in. i.d., fabricated from 1/4-in.-square hollow conductor.

To increase the mirror fields by using existing power supplies the large Waldo magnet coils will be replaced with smaller coils. Each mirror will consist of two 36-in. i.d. 6-in.-long modular coils. To carry and position the new coils two aluminum magnet supports have been designed and are being fabricated. The supports permit coil displacement up to 12 deg in a horizontal plane. A slight modification on the existing aluminum coil spacers permits their use with the new magnet supports.

Cryogenic Pumping Experiment

J. Ralph Ullman

After a 250-300°C charcoal bake-out a fourth run was completed. The liquid helium was transferred successfully through a new vacuum-jacketed transfer line. Two carbon resistors coupled to a Wheatstone bridge served to bracket the liquid helium level. Total liquid helium used during the run was 101 liters. The exhaust helium gas was gathered by a gas holder floating on the line. A total of 2383 ft^3 was recompressed into cylinders at 1700 psi with approximately 117 ft^3 lost to the atmosphere.

A leak from the outer vacuum chamber (held at 10^{-3} mm Hg) into the high-vacuum volume, (held at 10^{-8} mm Hg), which contained the charcoal, was noted after the run. This leak had been suspected from the beginning of the test runs. Unfortunately, the magnitude of the leak had not been determined. The amount of charcoal contamination between the time of bake-out and the completion of the run, a period of about 4 days, can only be a matter for speculation. The results of this run are reported elsewhere in this quarterly report (p. 121).

The cryogenic pumping experiments have been dropped and future plans cancelled. The pumping stand and liquid nitrogen trap will be salvaged.

Dissociation of D_2^+

The D_2^+ analyzer, a device for measuring the break-up of a D_2^+ beam from the Cockcroft-Walton accelerator on thin films, was assembled and the vacuum system roughed down.

The protype target arc was placed in operation. The machine was being made ready for placement in the Cockcroft-Walton pit. Plans for this experiment included obtaining operating data to be used to direct the final design of the target arc.

The target arc progressed from layout to detail and fabrication stage. The design is approximately 90% complete, with the deflecting magnet yet to be done. Major parts of the vacuum system, including the 20-in. valve, have been received from the vendor. This portable apparatus would permit studies to be made on a dissociation of D_2^+ versus D_2^0 in ionized deuterium. Again, the D_2^+ beam would be provided by the Cockcroft-Walton accelerator. The auxiliary pumping system was designed to pump hydrogen at 2000 l/sec at 10^{-5} mm Hg.

In the latter part of October all phases of the work on dissociation of D_2^+ were discontinued.

P4 Probe Rotator

A probe rotator for use in the P4 plasma has been designed and more than half the parts have been received. Specifications call for a drive speed of 0 to 1800 rpm. The shaft will be closed to atmosphere through a differentially pumped labyrinth seal. Since the success of the probe depends on the seal, a preliminary assembly will be made in the Mechanical Engineering Laboratory to insure performance before it is delivered to the P4 group.

Hard-Core Torus

Raymond E. Keyes

The contract for a corrugated liner has been let to Precision Sheet Metal of Los Angeles. Their present schedule is to produce the first liner elbow section about December 14, and the first completed liner halves by January 7, 1960 or sooner. A Kanigen nickel liner will be coated on the external copper shell halves and tested as a possible replacement for the thin sheet metal corrugated liner. It is somewhat of a compromise in that it will not be as clean a system and it will be limited to a lower bake-out temperature. A number of specimens have been made and tested in order to arrive at the best method of securing the nickel to the copper liner. The Electrical Department has conducted resistance tests of the specimens. The results indicate that a coating of epon and glass should be first applied all over the shell, followed by a coating of epon and powdered aluminum over the inside of the shell and overlapping the joint on the outside by 1/2 in., and then a layer of Kanigen nickel on the top of the latter layer. This Kanigen liner can be left as is when the Inconel "X" liner is used.

A means to mechanically raise the core of the Levitron to permit low-energy tests has been devised. It consists of an elevator with lift rods extending through four bottom ports of the liner. It is designed to be load-equalizing, and uses two hydraulic rams and two hand pumps.

Unipolar Generator

Raymond E. Keyes

As the result of our studies that revealed an undesirable stator separation under the type of operation planned for the generator, Raymond Keyes (Mechanical Engineer) and Hugh Van Ness (Electrical Engineer) visited Allis-Chalmers on October 14 and 15. Allis-Chalmers agreed to modify the unit by deleting their buss clamp and installing prestressed bolts between stator buss plates, which should eliminate the displacement of the stator under load.

Design work on the switch for the generator has been halted, pending results of current tests on contact material by the Electrical Engineering Department. Present tests seem to point in the direction of increasing contact load considerably or increasing contact area by using a sliding shoe in lieu of a roller contactor.

Table Top

James F. Ryan, Jr., and John R. Benapfl

A purchase order has been issued and delivery is expected about the end of November 1959 for the fast vacuum shutter to be used with the vacuum spectograph.

The design of the 150-kv accel-decel probe is about 90% complete and about one-fourth of the parts has been built. The delay now is in obtaining the nickel-iron (Hypernick plate) for the vacuum chamber. We have been promised delivery 6 weeks after the termination of the steel strike.

A new contact cylinder of copper tungsten for the mechanical crow-bar switch has been received. It has been mounted on a new guided carrier and assembled in the driver. Work is in progress to measure the speed of closure, as the new cylinder is somewhat heavier. The switch will be installed in the Table Top circuit as soon as checking is completed.

Toy Top

John R. Benapfl

Design is progressing satisfactorily on the new three-stage compression Toy Top experiment. The proposed date of completion is February 1, 1960. The main feature of design is to provide the ultimate in flexibility; there will be no obstacles to limit coil positioning, and the universal support cradles will hold any available coil or glass of any diameter. The supporting tables can be readily lengthened or shortened, as also can the forevacuum lines to the diffusion pumps.

Low-Energy Neutral Beam Experiment

William S. Neef, Jr., and Eugene T. Bradley

Tests were conducted on several methods of electrical connection between the pancakes of an "Alice" coil section. A bolted silver-plated terminal tab was found satisfactory, and detailed drawings to be used during coil assembly were completed. Tooling for the coil terminals is nearing completion and the first pancake should be wound in late November.

The Linde Company completed a concrete pad and installed a 500,000-SCF liquid nitrogen dewar with associated pumps and motors to supply the "Alice" coils in Building 180. A new concrete pad for vacuum forepumps was completed adjacent to the south wall of Building 180.

Bakable-seal development is continuing along two lines; the first is to test various materials in conventional pinch flanges, and the second is to develop differentially pumped closures using double-seal hard gaskets and a combination hard and soft gasket. OFHC copper gaskets have continued to indicate poor reliability after a 400° bake-out. Some of the OFHC gaskets held for 24 hours after bake-out and then started to leak.

Cupro-nickel 70-30 gaskets have been tested on the evaporator tanks for "Alice" and have been baked at 450°. After the first thermocycle at 450° the cupro-nickel gaskets were tight, but after the second bake-out at 450° both gaskets showed leakage. These gaskets are 16-1/8 in. o.d. and were made from 50-mil cupro-nickel without finishing the faces of the gaskets. We are now in the process of machining a variety of gaskets from 90-10 cupro-nickel, which should give better results as it can be annealed to a considerably lower Rockwell number.

The hard-seal gasket shown in Fig. 42 utilizes our current knowledge of pinch-gasket construction to effect a double-pinch differentially pumped seal. In the same space an H-shaped seal, also differentially pumped can be tested. The combination design shown in Fig. 43 features a metal seal that is simply machined (no critical dimension) adjacent to the high vacuum with a silicon rubber water-cooled O ring backing it. Mating flanges in the combination seal are identical, and any flange can therefore be mated to any other flange. The re-entrant cuts in the flanges are to reduce the effects of thermostresses resulting from breakout.

Both designs use a number of simple C clamps to hold the flanges instead of a circle of bolts, in order to eliminate flange rotation.

In order to evaluate the results of neutral-beam-source development it was decided to build a small version of the "Alice" experiment, referred to as "Baby Alice," with 9-in. modular mirror coils in a nonbakable vacuum system. Several components of the "Alice" machine will be used, such as the liquid-nitrogen-cooled neutralizer and the titanium pumps. This machine was completely designed and 75% constructed and assembled during the past 3 months. A drawing of this experiment is shown in Fig. 44.

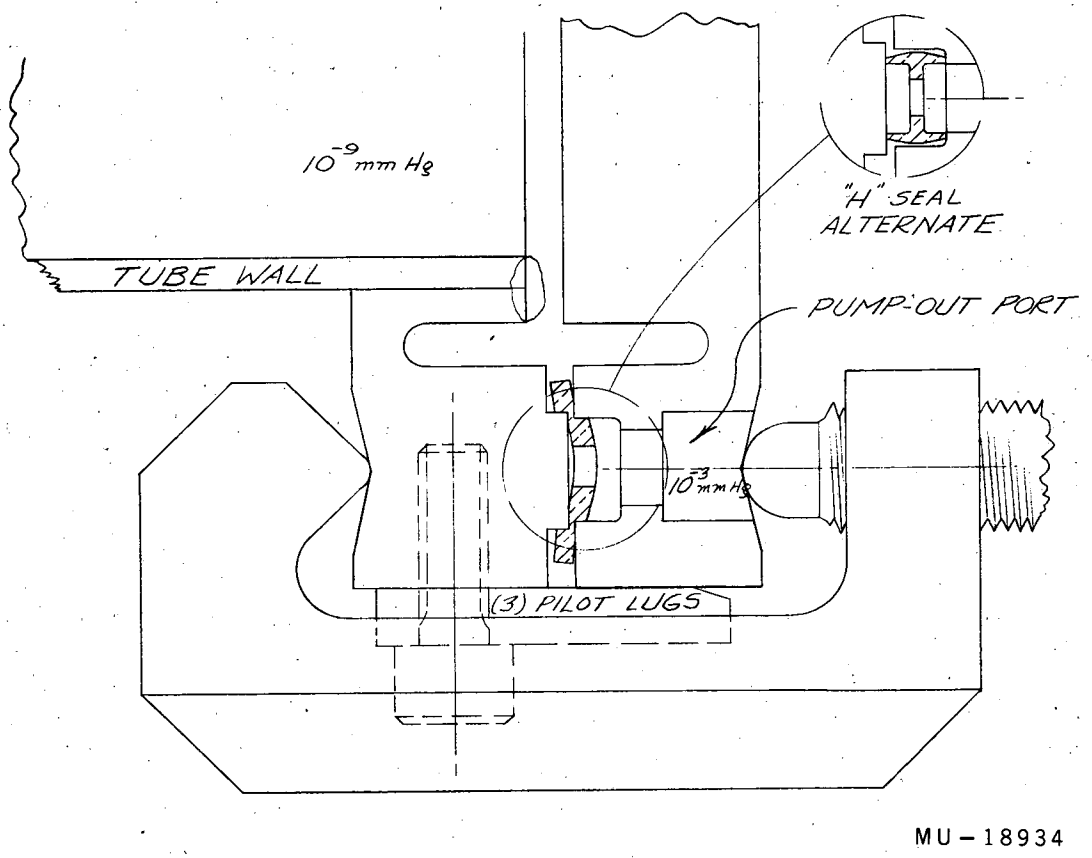

Fig. 42. Differentially pumped hard seal.

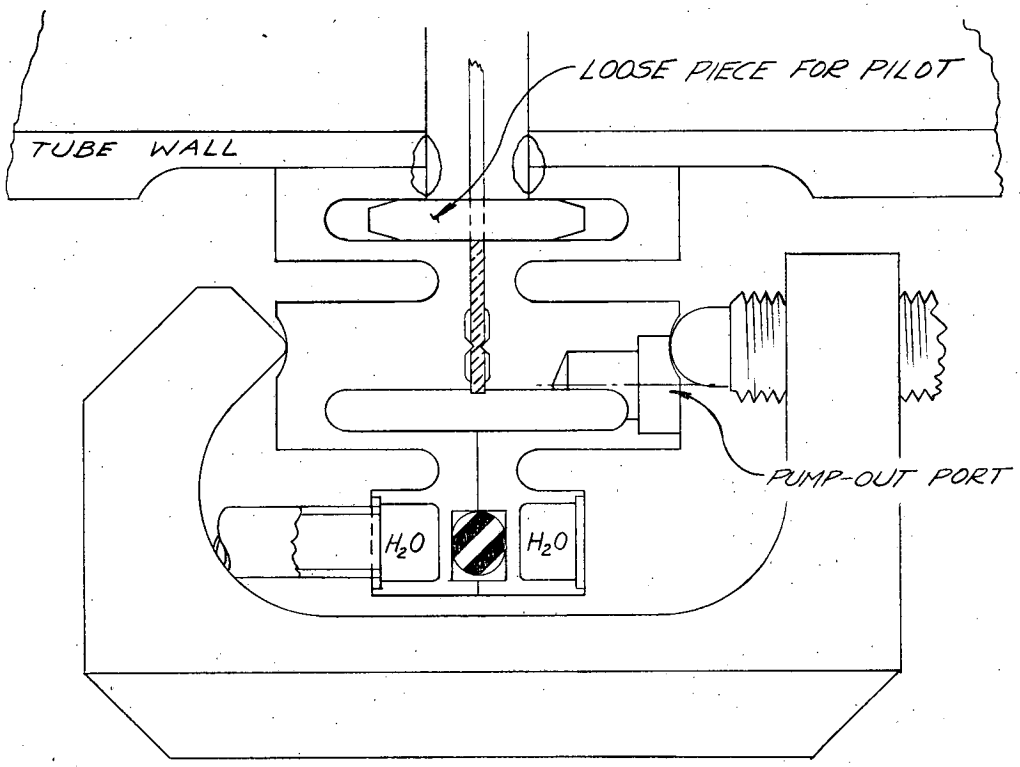

MU-18932

Fig. 43. Combination seal.

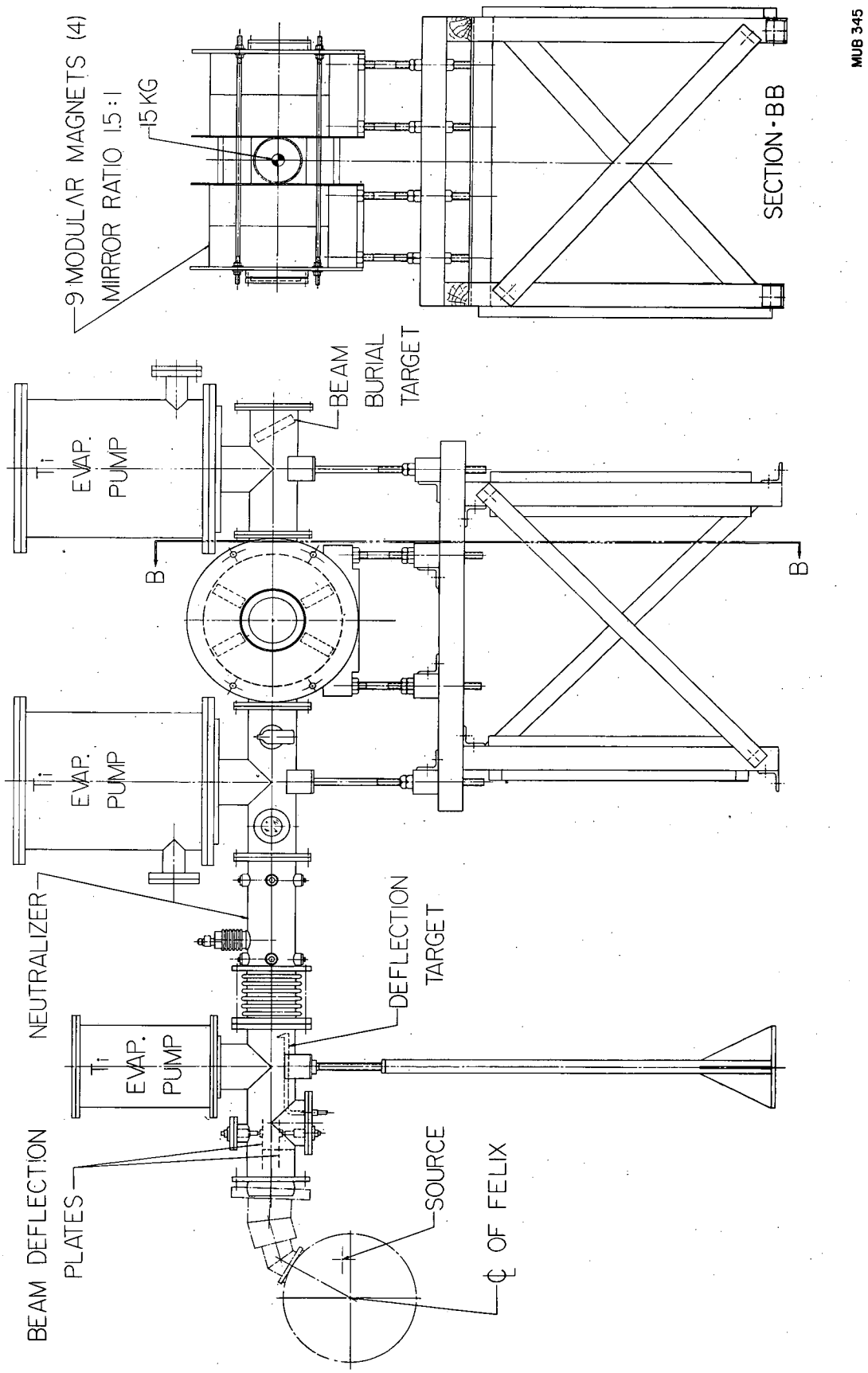

Fig. 44. Baby Alice apparatus.

One new feature designed into this machine is a system of electrostatic beam deflection. The beam will be deflected to a water-cooled target until the moment of required injection. This will eliminate the need for a high-speed water-cooled valve to control beam admission to the reaction chamber.

Magnetic shielding material to surround the beam deflector and the neutralizer is being fabricated. The material is Netic, manufactured by the Perfection Mica Company. It has twice the shielding effect of mu-metal, according to our tests.

Atomic- and Molecular-Beam Research

Charles A. Hurley

Because of the machinists' strike the fabrication of the major portion of hardware has been delayed. We now expect delivery by January 1, 1960. Work is progressing on the beam chopper, the ion source, and the jib crane.

Astron

Charles A. Hurley and James F. Ryan, Jr.

Several layouts were made for a new pulsed electron gun (200 amp, 720 kv). The one that shows the greatest possibilities (Fig. 45) has the transformer cores closely packed and immersed in oil. The oil-to-vacuum separation is made by a 12-in.-diameter ceramic column with integral accelerating plates. A 10-in. matrix cathode has been designed and request for bids have been released. Mechanical design studies have been made for the passive circuit assembly.

Layout of the accelerator (Fig. 46) and some details have been drawn for a typical modular unit of 480 kilovolts. Final decision on gradient and core material have not been reached, but detailed drawings of a typical ceramic and metal accelerating column were made so that estimates could be obtained from ceramics fabricators. No replies have been received to date.

A method has been set up to calculate optimum size of cores for various core materials and to compare over-all costs of the accelerator for various core materials and various voltage gradients.

Low-Temperature Refrigeration

Clyde E. Taylor

The new three-stage, -285°F cascade refrigerator was completed. The rotating seals on the low-pressure compressors proved unsatisfactory, even after modification to provide a higher face loading. New seals have been designed and ordered. The older #2 refrigerator continues to operate satisfactorily and has been running nearly continuously for about 7 months.

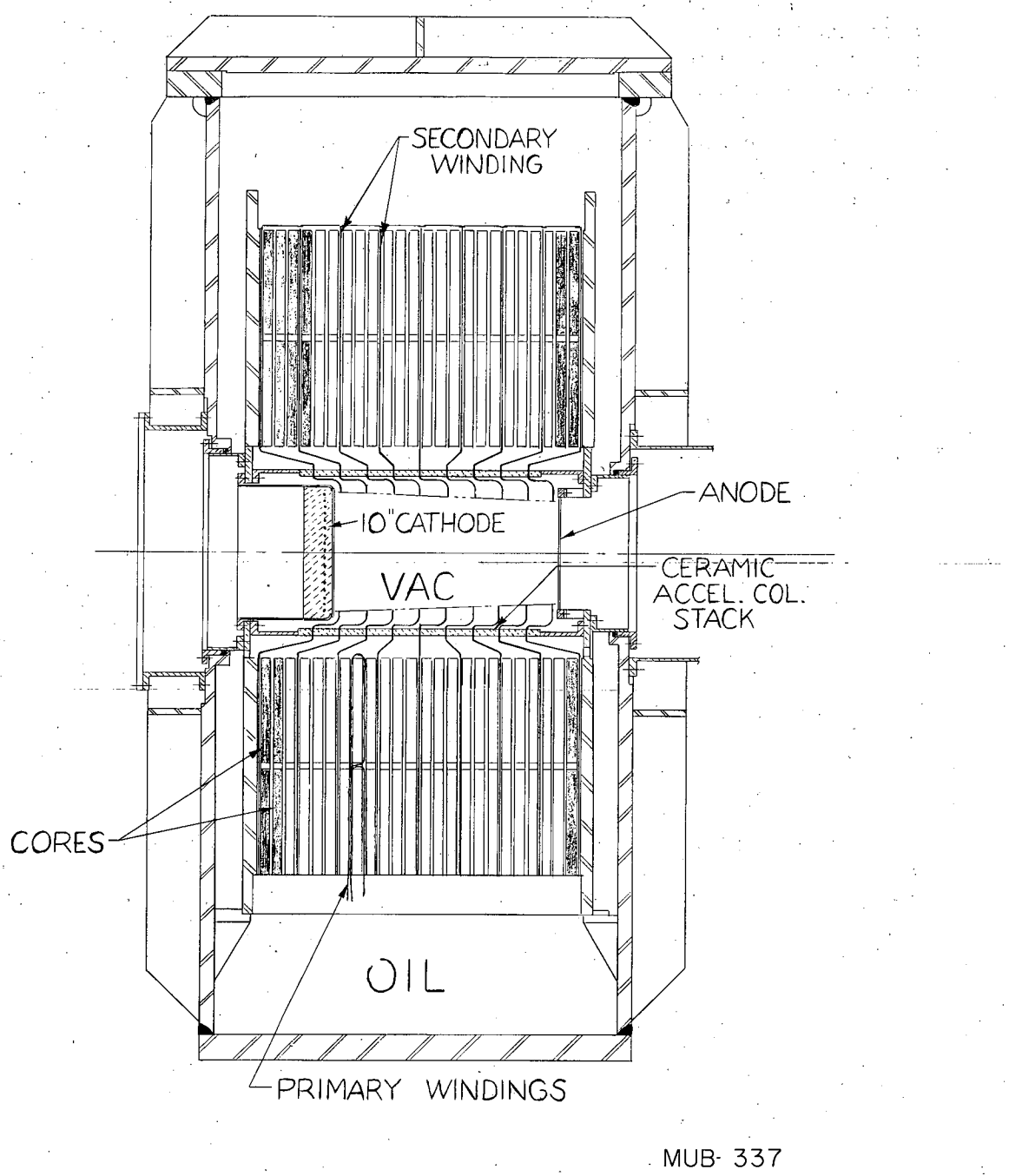

Fig. 45. Astron electron gun–preliminary.

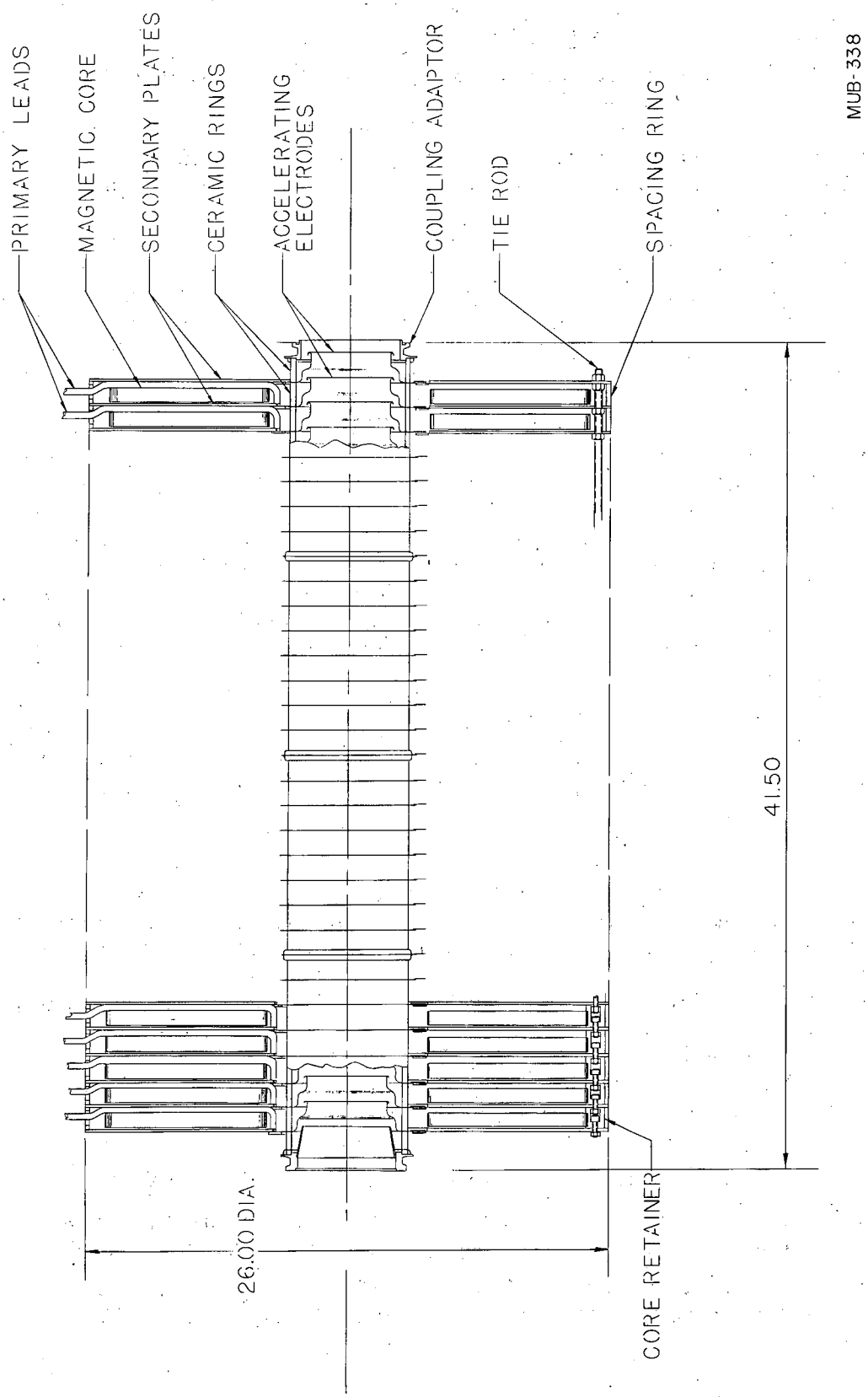

Fig. 46. Astron induction accelerator–preliminary.

Cryogenic Coils

Clyde E. Taylor, Joseph C. Behne, Robert L. Nelson,
Richard G. Mallon,* and Arturo Maimoni

A report summarizing our closest examination of conductor metals to date has been issued.[1] Sodium appears to have a clear advantage over aluminum, based on reasonable metal purities. Figure 47, from the above report, shows the relative power requirement (compared to Cu at 300°K) vs conductor temperature for various metal purities. Power saving is by a factor of 6.5 for moderate-purity sodium having a residual resistivity of 0.9×10^{-9} ohm-cm at 10°K, and by a factor of 3.6 at 20°K for the purest aluminum commercially available in useful shapes. These values are based on a 100-kG central field and a refrigerator having 35% Carnot efficiency.

A more optimistic figure for aluminum was given in a recent memorandum report based on some unpublished British data.[2] As more data become available, our prediction of aluminum resistivities will have more meaning. Meanwhile, we plan to continue to work with sodium; we will also construct an aluminum coil for testing as soon as wire of proper purity becomes available to us. We have measured residual resistivities at liquid helium temperature of a commercially available Swiss aluminum, "Super-Reffinal," from Aluminum-Industrie A G, with encouraging results:

$$\rho_{300^\circ K}/\rho_{4.2^\circ K} = 1000 \text{ to } 1500$$

after annealing. Before annealing, this ratio was only about 1/5 as great. A measurement at liquid hydrogen temperature in Berkeley gave

$$\rho_{300^\circ K}/(\rho_{20^\circ} - \rho_{4.2^\circ K}) = 2380,$$

which gives a resistivity of about 1.67 times that given by the Block-Gruneisen theory. Other data substantiate that the lattice resistivity of aluminum is considerably higher than the theoretical values.[1]

We now have on hand two 55-gallon drums of reactor-grade sodium, and have started to draw off samples for resistivity measurement. Sodium from one drum gives a residual resistivity ratio

$$\rho_{273^\circ K}/\rho_{4.2^\circ K} = 815.$$

---

*Consultant to LRL from Astra, Inc., Raleigh, North Carolina.

[1] Richard G. Mallon, Effect of Choice of Electrical Conductor on Power Requirements of Low-Temperature Magnets, UCRL-5792-T, Nov. 1959.

[2] Raymond J. Corruccini, Choice of Conductor for Cryogenic Electromagnets, N. B. S. Boulder Laboratories Memorandum Report CM-2, Oct. 1959.

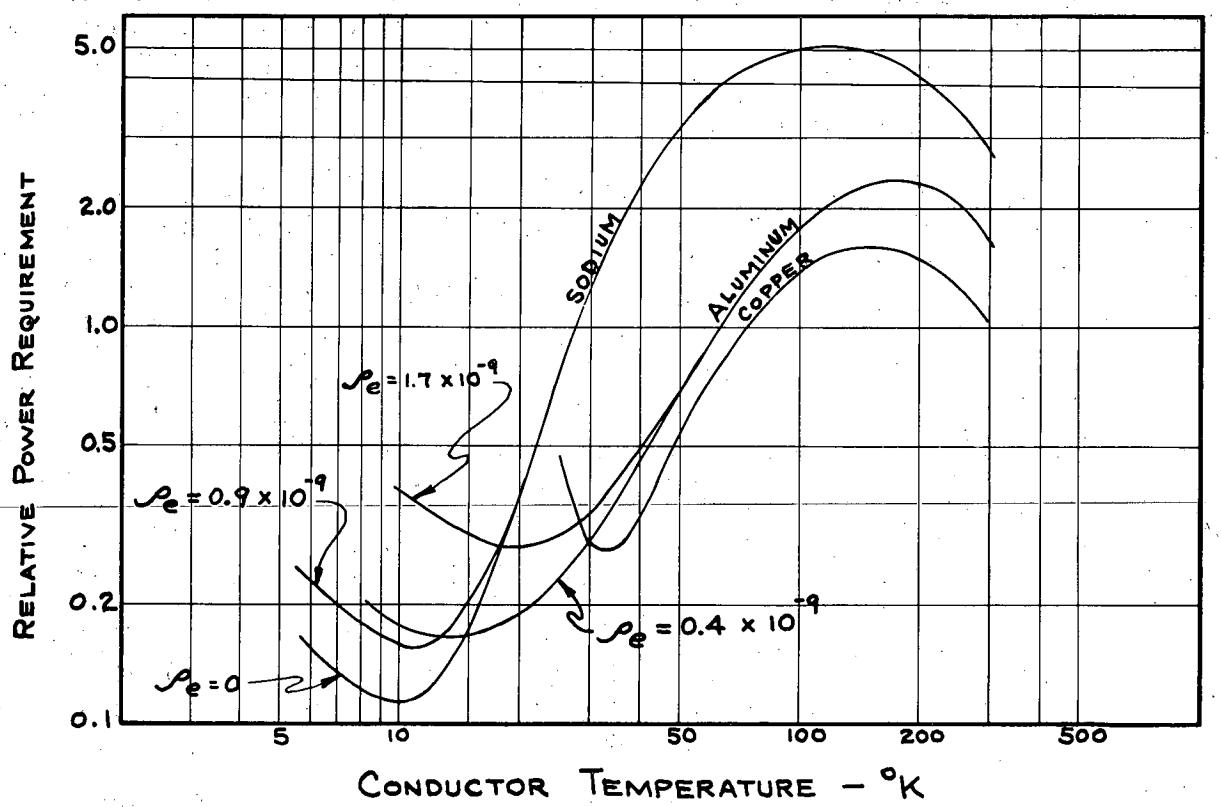

MU-18933

Fig. 47. Relative power requirements of copper, aluminum, and sodium.

The ratio required to give the factor-of-6.5 power saving, as shown in Fig. 47, is 4700. Our apparatus for nondistillation purification of sodium is assembled; construction of this apparatus was delayed by difficulties in welding on the liquid-level-indicating probes. We have found it very convenient to use a borrowed induction heater for heating sodium containers to 800°C ±, and we will use this technique instead of resistance-wire heaters in our purification apparatus.

The 8-in. test coil is being designed. A few tests of low-temperature gasket seals, of electrical resistance of contacts, and of turn-to-turn electrical insulation will be made before the design is released. All welding techniques for use on the thin square tubing have been successfully developed.

It is planned to test this coil by filling a 9-ft^3 container with helium at 150 atmos pressure, cooling this container to about 12 to 14°K by using our helium gas refrigerator (now being modified by Arthur D. Little, Inc.), and expanding the gas through the coil. Isentropic expansion of the gas in the container will cool it to the required 7°K ± or lower. The control system for this test is now being designed. This method of testing appears more convenient than using large quantities of liquid helium from some liquefaction facility outside Lawrence Radiation Laboratory.

The surplus hydrogen-liquefaction plant from the Marshall Islands has been received, and several components such as compressors and large dewars are being prepared for use in our coil test.

Bids for a high-current power supply were received. Because the cost appeared excessive, other means of powering the coil test are being studied. For instance, surplus submarine batteries, which are periodically available, will provide the required power.

Efficiency, size, cost, and practicality of a refrigeration machine to operate between about 10°K and room temperature is very much affected by variation of the many parameters in the cycle. To obtain the optimum cycle, a code allowing for many possible approaches to the problem was set up for study on the IBM 704 computer. As time permits, the results of these cycle studies will be summarized in report form. No additional work is planned on refrigeration-cycle analysis.

ELECTRICAL ENGINEERING DEVELOPMENT

Vernon L. Smith

Pyrotron

David R. Branum

Table Top II

During the past 3 months, the machine has been used by the contract physicist from Sylvania.

For this operation, there were 2,930 bank pulses at a level + 10 and - 10 kilovolts (i.e., 20 kilovolts to the load). This makes a total pulse count of 54,330 since the machine was constructed in 1955. The average bank voltage was + 10 and - 10 kv.

During the last week of November, one series string of WE5555 crowbar ignitrons developed low-impedance ignitors and became erratic in their firing. The dc resistance of the ignitors ranged from 4 to 9 ohms; normally, the ignitor resistance for this type of ignitron is 200 to 900 ohms. The low impedance is too low for reliable triggering with the pulse circuits of Table Top II. The low impedance of the ignitors of these tubes is a result of ignitron wall-material arc products, causing the mercury of the cathode to wet the ignitor and partially short it out.

The four bad Westinghouse type-5555 ignitrons were in service for more than 2 years for a total bank-pulse operation of 21,400 at an average level of ± 10 kv. There were approximately 100 operations at a level of ± 16 kv.

The faulty string was removed and replaced with four special General Electric type-5555 ignitrons. The General Electric ignitrons were purchased for a trial more than a year and a half ago, and this time was the first opportunity to use all four in the same circuit so that an average life could be obtained.

The General Electric ignitrons are being closely watched, since regular GE type-5555 ignitrons have not held up in Table Top's crowbar service for more than 1000 pulses.

Besides the effort on the machine itself, there have been a few side experiments that have used Electronics Engineering effort and time.

A small experimental pulse setup was built to study the operation of a fast-acting mechanical valve for study as a source pulser for the machine. Later on an additional pulse circuit will be added to shock-ionize the gas from the valve.

Work is continuing on the electronics for the 50-kv calibrating electron gun (JN 203-N). A low-level deflection circuit has been built and is now installed on the gun experiment. This allows the gun to be operated up to

the 5-kv level. An output stage is being built to allow the gun to be operated up to 50 kv. This will require a 3-kv deflection system.

Commercial power supplies for the biasing of the gun are on order, and a cart to contain all the electronics is now under construction.

The six special 3/4-in. photomultipliers with their transistorized amplifiers have been delivered from Electronics Engineering and are awaiting use on the machine. Two of the photomultipliers had low gain, and since the requirement was that all six have the same output with the same high voltage, the other four units were set down in gain to equal the low-output models. More RCA 3/4-in. photomultipliers are on order, and the units will be increased in gain at a later date.

Toy Top II

A new program for the machine was started in October, and it was decided by the operating crew to call this machine variation Toy Top III. The new program includes considerable Electronics Engineering effort. A total of 600,000 joules of energy will be added to the Toy Top capacitor banks, and banks No. 1 and No. 2 will be completely redesigned.

The last section of bank No. 3 will be filled with Tobe 14+-mf capacitors to give an additional section of 200,000 joules at ± 20 kv.

A four-section 400,000-joule bank will be constructed in the room below Toy Top III and will be made so that the sections can be "fired" individually or together in groups of two or four.

Bank No. 1 will be constructed as a small ± 20-kv "Green River" type of bank with a rise time into a 0.5-μh load of 8 μsec with an efficiency greater than 50%. Bank No. 1 will be approximately 34,000 joules.

Sometime in early 1960, bank No. 2 will be redesigned into a fast bank also.

Also at a later date, one section of bank No. 3 will be made separately controlled; thus there will be three separately controlled 40-kv banks: Section "A" with 400,000 joules, and sections "B", "C" with 200,000 joules each.

The two additional 300-kw dc power supplies have been installed and are now being connected to the Toy Top console control system.

The two 20-kv bank charging supplies are still under construction; completion is expected early in January 1960.

The data-reduction system is still held up owing to the malfunctioning of the nonlinear readout system. The complete system was sent back to the factory for repairs, but on return had developed new faults. It is now under repair in Pyrotron Electronics Maintenance, Bldg. 157.

Pyrotron - Miscellaneous

H. W. Van Ness

Felix Area

The "Baby Alice" experiment is being assembled in this area. About 80% of the electronic installation is complete.

Grid Source Development

A filter circuit was designed and installed in the arc high-voltage supply. The arc high-voltage current regulator is still in the design stage.

Pinch and Collapse

H. W. Van Ness

Gamma Bank Area

Construction of a 1-farad electrolytic capacitor bank is 50% complete. Design investigation for other components and circuitry for the toroidal Levitron experiment is in progress.

Plasma-Acceleration Experiment

Tests of capacitor-ignitron "module" for the fast bank are nearly complete. The ignitron tubes will be heated electrically to reduce arc-formation time to around 0.1 microsecond. Without heating, the arc-formation time is around 0.5 μsec. Material to complete the bank will be ordered within 2 weeks.

Sodium Radio-Frequency Analog Experiment

A low-frequency cw oscillator (10 to 100 kc) will be constructed to supplement the 5-kw 20-kc relaxation oscillator for further experiments.

300-kv Marx Bank Area

Because of budget limitations, plus very poor capacitor performance, this bank will not be completed. A meeting with the capacitor manufacturer, Cornell-Dubilier, was held. They admit that practices and quality control involved in manufacture of these units were very poor. We have proposed a test program which could be run at their expense, also a basic set of specifications which the capacitors would have to meet to be useful in other applications. All capacitors failed to date would be replaced. The remaining capacitors would be retained if the test of a sample lot were satisfactory. Cornell-Dubilier will advise us within a week or two whether they will agree to these terms.

Energy-Storage-System Investigation

Because of budgetary conditions, effort has been reduced on this program pending a final decision on its future course. Owing to numerous delays, the manufacturer will not deliver the machine until around December 15.

Final agreement has been reached with Allis-Chalmers concerning the method to be employed in bracing the machine to withstand the pulse forces.

High-Field Pulse Magnet Capacitor Bank

As a result of a capacitor failure which caused extensive damage, the bank was rebuilt to include fusing throughout.

Switch Development

D. B. Cummings

Mechanical Switching

The long-awaited silver-tungsten contact assembly has been installed on the fast mechanical crowbar relief switch. The unit has been timed and tested for voltage breakdown. It is being readied for return to the Table Top bank for testing these materials.

Ignitron Development

1. Tube Tests

Extensive tests on tubes with vacuum-melted molybdenum anodes still show very good results. The ignitors become wetted and difficult to fire. However, they can be fired with our standard 3-kv thyratron ignitor firing circuits if the series resistance is reduced to 1 ohm or less. Tests here show the double-pantleg design and simple radiused type to be essentially equal in crowbarred service at 20 kv. This is in contrast to results on ringing tests at LASL, where the double-pantleg tube appears better. Comparative tests between manufacturers failed because of cracked anode seals. A trail of molybdenum prepared by sintering instead of vacuum casting failed for the same reason. Cracked anode seals appear to be cured with a slightly flexible epoxy potting.

Inspection of prefiring tubes shows extensive arc tracking in the throat and eroded glass at the bottom of the anode seal. It is possible that the success of the double-pantleg design in ringing service is due to the removal of poorly outgassed metal from this region. We plan to try this principle with a simpler, much less expensive tube.

2. Ignitron Mechanisms Investigation

This work is almost completed. The variation of arc-front velocity and probe (auxiliary anode) floating potential with peak circuit current are consistent with a Malter-effect arc-spot-formation mechanism.

Microwave Diagnostic Experiments

Harlin L. Bunn

P-4 Experiment

1. Swept-Frequency Receiver

The S-band swept-frequency receiver designed for studying electron-cyclotron radiation has been relocated from the machine to the console area. An overhead waveguide, which can be removed when the crane is in use, has been installed to channel the plasma radiation to the receiver. No change has been made in the antenna used previously.

Work is in progress to inject electrons into the end of the plasma column. The receiver will be used to try to detect effects of this injection on the plasma.

2. 4-mm Interferometer

A circuit has been installed on the interferometer to shut off the klystron supply voltage when the temperature of the body of the DX151 klystron exceeds 80°C. This consists of a thermistor sensing element which is part of a bridge circuit used to drive a relay to shut off the power supply.

Toy Top Experiment

Installation of a receiver with helical antennas operating at 1100 Mc and 1660 Mc has been completed. The noise figure of the receiver was measured as 8 db. This receiver will be used to study plasma radiation when two plasma sources at opposite ends of the machine are fired simultaneously.

A harmonic receiver has been designed for studying synchrotron radiation. A common local oscillator at 23 kMc provides driving power for the first, second, and third harmonics. The second and third harmonics are achieved by driving crystal multipliers, FXR Models Q780A and M780A, with a 1N53 crystal. Measurement of the noise figure at 46 kMc yielded a figure of 28 db. Lack of a noise diode at 69 kMc prevented a corresponding measurement. It is believed that the noise figure is about the same for the third harmonic. These figures are rather high because the amount of power available at the second and third harmonics for local oscillator injection is rather small. A more elegant scheme is to use three separate backward-wave local oscillators. Supply sources have been determined for these BWO's. At present no authorization has been given to build these receivers. The cost is fairly high because the BWO's are quite expensive.

Advanced Development

1. Noise-Diode Power Supply

A pulsed power supply for pulsing noise diodes used in electron-temperature measurements has been designed. This eliminates the need for a mechanical modulating wheel for calibration purposes.

2. Telemetering Circuits

Work has continued on a circuit for monitoring high-voltage probe characteristics. A fair amount of success has been achieved, and it is hoped that the design will be complete in the near future.

3. Low-Loss Waveguides

a. TE_{01} Waveguide

A transition from rectangular to circular TE_{01} mode waveguide has been built for the K band. This is a resonant slot structure studied by Microwave Associates. The band width is about 6%. The loss from two units separated by a 10-ft length of circular pipe is less than 1 db. A new design centered at 69 kMc is being fabricated and will be tested in the next quarter. If this is successfully completed the units will be installed on the P-4 machine so that the interferometer system can be relocated at the console.

The Bell transition and the Marie' transition are being electroformed for testing.

b. H Guide

An H-guide launcher has been designed for this type of waveguide. The loss per unit is about 0.6 db for the Ka band. Measured loss per foot is about the same as for standard rectangular waveguide. Further studies are to be made for the 50- to 75-kMc band, where it is expected that the loss will be much less.

4. Gas Discharge Tube

A gas discharge tube designed for use with the Elliot Brothers 35-watt Ka band klystron has been tested. Breakdown occurred as calculations predicted. Coleman's group at the University of Illinois has started this investigation also, so that further work here will not be continued. Their previous work has been confined to lower frequencies and pulsed sources.

5. Antennas

One of the fundamental limitations on the use of microwaves in determination of electron density is that in very dense plasmas with a column size approaching the cross section of the horn-antenna radiation beam, the energy scatters around the column instead of going through it. This leads

to erroneous results. Studies are to be initiated on pencil-beam antennas for use in correcting this limitation.

6. Pulsed Interferometer

The interferometers used thus far have been of the cw type. Studies are to be conducted on the possibility of using pulsed tubes, with some means of phase control for multitube installation. The reason for this study is that very-high-frequency pulsed tubes can be designed and built with fairly high power levels, while cw tubes are much more difficult to build and consequently are much more expensive.

Astron

Kris Aaland

Induction Accelerator

A visit to six different manufacturers of magnetic core revealed the following:

1. In general, most companies did not have sufficient test facilities to develop pulse data.

2. The experience of core manufacturers has been limited to applications involving less than 2 volts per lamination. Excessive voltage gradients do not arise in normal transformer design.

3. Tolerances of properties such as permeability and saturation flux density are $\left.\begin{matrix}+0\\-30\end{matrix}\right\}$ %.

4. It may be possible to eliminate the final annealing stage in large toroids using 50% nickel-steel. This is because smaller stresses occur when large-diameter cores are made.

5. Economical brick-size units may be machined to sufficient accuracy (1 mil) and delivered within 10 weeks in great quantities. Ferrite can be obtained in a 50-cm (o. d.) single piece at higher cost per unit volume and with an 8-month delivery time.

6. Several small-magnetic-core samples were obtained.

Testing

In view of the results of our visit to the manufacturers of magnetic core, a pulse tester was designed. B-H curves for a 0.30-μsec pulse were taken and are shown in Fig. 48.

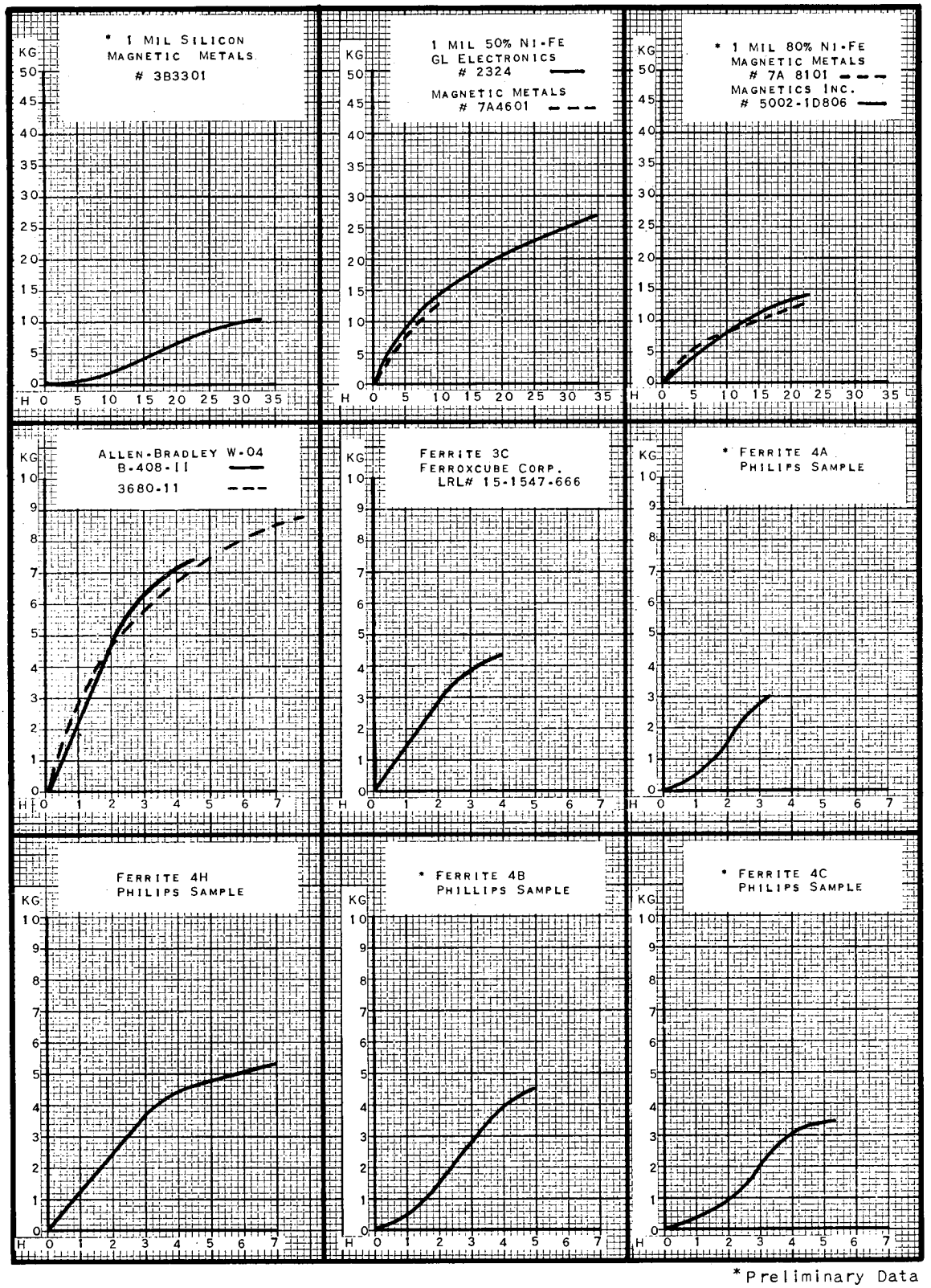

*Preliminary Data

MUB-341

Fig. 48. Delta B-H curves for 0.3-μsec pulse.

Discussion of Testing

The voltage pulse has a flat top of 0.30-μsec duration. All the measured points have optimum dynamic bias.

The data on 50% NiFe and on ferrite types Allen-Bradley W-04, Ferroxcube 3C, and Philips 4H are accurate. Inrush current is presented in Fig. 49 and is low for 50% and 80% nickel-steel and for W-04, 3-C, and 4-H types of ferrite.

Of the high-flux-density materials, 50% nickel-steel seems preferable. This material has a high pulse permeability and the cost is about 40% more than grain-oriented silicon steel. Allen-Bradley type W-04 has the highest pulse permeability. The total flux change is about 9000 gauss, or almost the same as for 50% NiFe if the stacking factor is considered.

Switching

The induction accelerator will require that large changes in flux be established in the magnetic material. A one-turn primary is planned. This means a high current pulse if the primary voltage is to be reasonable: 16 kv across the primary of a 1-mil grain-oriented silicon steel core required about 1200 amp to develop a 16-kv 0.25-μsec flat-top secondary voltage pulse. Therefore, a study of inexpensive high-voltage high-current radar-modulator-type switches is being made. Results to date are as follows:

1. Thyratrons

Type 1257, glass-enveloped, 33 kv, 2000 amp rating. Test results in a coaxial circuit with a 12.5-ohm pulse-forming network and a 12.5-ohm load show a rise time of 20 mμsec from 10% to 90% current. Peak current was 1000 amp.

A ceramic-type GL-7093 (lower inductance) has been used successfully in core testing.

A 5C22 is being tested at 1600 amp (five times rating) in a 16-kv 10-ohm circuit, and several tubes have performed successfully. No failures have been recorded as yet, and one tube has run more than 165 hours. Repetition rate is 20 pps, rise time is 50 mμsec, and pulse duration is 0.25 μsec.

Several thyratron manufacturers are of the opinion that their tubes operate more than 1000 hours in applications involving:

(a) low repetition rates (60 pps and less),

(b) short pulse duration (0.5 μsec an less),

(c) high currents (5 to 10 times rating).

The suggested silicon steel core requires a current rise equivalent to a voltage rise of about 0.05 μsec.

NOTE: 1 Horizontal Division = 0.1 u Second

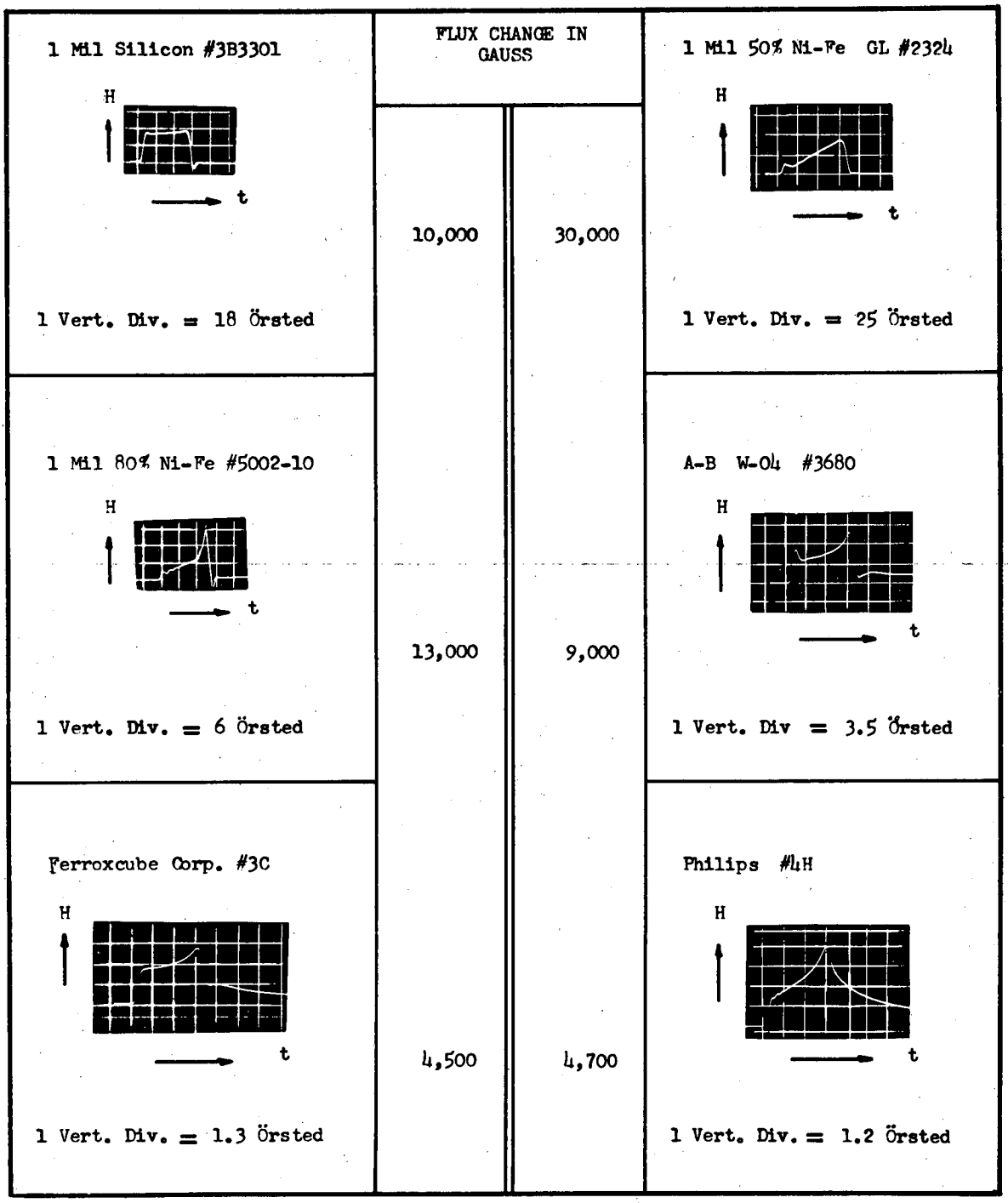

MUB-350

Fig. 49. Pulse excitation current wave shapes.

This limit may require the use of ceramic tubes, which are more expensive (a factor of about 2 to 1), in order to take advantage of their lower inductance. The cost of switching has a marked effect on the size of magnetic core required if an optimum cost condition is realized. A lower cost of switching allows a reduction in core area required (more current, less magnetic material).

2. Hard Tubes

Some Central Electronics type X-45, claimed to handle 30,000 v and 200 amp, are ordered for evaluation.

From recent experiences, a hard-tube switch with proper feedback seems very desirable.

3. Modulator

A magnetic modulator is also being considered.

Miscellaneous

1. Coil A Pulser

A 200-amp transistor relieving switch has been added. Current may now be sustained to dc.

The coil oscillates undesirably at 400 and 30 Mc. Also, the thyratrons are triggered by stray x-rays.

We are designing a hard-tube closed-loop switch to take the place of the thyratron and the ignitron.

2. Dual Delay Unit

This unit was completed with a range of 2 μsec to 50 sec. (This is shown in Dwg. No. LE-5504, on file at Livermore.)

3. Support to Physicists

A programmed distrubance was introduced into a model 200-gauss field for checking Hall devices.

Atomic- and Molecular-Beam Cross-Section Measurements

David R. Branum

The cross-section experiment has been moved into the new Building 180 and work is continuing on installing the vacuum power-control system and the general experimental control systems.

A chopper wheel and drive has been designed by Mechanical Engineering and a small motor is now under test to see if it will function in vacuum (at 10^{-5} mm Hg). A light detector for the chopper-wheel speed monitoring is now under development.

The ion gun that is being developed for the cross-section experiment has been moved to Bldg. 180 and its control-power vacuum system is now being installed. An rf oscillator and its power supply are in the Electronics Fabrication Shops.

TALKS AND PUBLICATIONS

Cryogenics Engineering Conference, University of California, Berkeley California, September 2-4, 1959.

R. F. Post and C. E. Taylor, Air-Core Cryogenic Magnet Coils for Fusion Research and High-Energy Nuclear Physics Applications (UCRL-5630-T, Nov. 1959).

C. E. Taylor and R. F. Post, the Design of Large Cryogenic Magnet Coils (UCRL-5631-T, Nov. 1959).

Second RCA Plasma Physics Symposium, David Sarnoff Research Center, Princeton, N. J., September 21-22, 1959.

Oscar A. Anderson, Status of Sherwood Program at Berkeley (invited paper).

Magnetic Field Design Symposium, Princeton, N. J., October 1-3, 1959.

W. S. Neef, Jr., Magnet Construction Techniques for a Liquid-Nitrogen-Cooled Mirror Machine (UCID-4060, Sept. 1959).

American Institute of Electrical Engineers Fall General Meeting, Chicago, Illinois, October 11-16, 1959.

H. W. Van Ness, Megajoule Energy Sources for 10^{10}-Watt Pulses (UCRL-5586, July 1959).

National Electronics Conference, Chicago, Illinois, October 12-16, 1959.

Ferd Voelker, The Electrical System for the Astron Injector (UCRL-8913, Sept. 1959).

12th Annual Gaseous Electronics Conference, Washington, D. C. October 14-16, 1959.

W. R. Baker, A. Bratenahl, A. W. DeSilva, and W. B. Kunkel, Viscous Effects in Highly Ionized Rotating Plasmas (UCRL-8861 Abstract, Aug. 1959).

T. K. Allen, G. A. Paulikas, and R. V. Pyle, Diffusion of Plasma Across a Magnetic Field (UCRL-8886 Abstract, Aug. 1959).

Astronomy Department, University of California, Berkeley, California November 4, 1959.

W. A. S. Lamb, Low-Energy Nuclear Reactions of Astrophysical Interest (invited paper).

Research Progress Meeting, Lawrence Radiation Lab., Berkeley, Calif., November 12, 1959.

Norman Milleron, Ultrahigh-Vacuum Research.

Information Division
sa

This report was prepared as an account of Government sponsored work. Neither the United States, nor the Commission, nor any person acting on behalf of the Commission:

A. Makes any warranty or representation, expressed or implied, with respect to the accuracy, completeness, or usefulness of the information contained in this report, or that the use of any information, apparatus, method, or process disclosed in this report may not infringe privately owned rights; or

B. Assumes any liabilities with respect to the use of, or for damages resulting from the use of any information, apparatus, method, or process disclosed in this report.

As used in the above, "person acting on behalf of the Commission" includes any employee or contractor of the Commission, or employee of such contractor, to the extent that such employee or contractor of the Commission, or employee of such contractor prepares, disseminates, or provides access to, any information pursuant to his employment or contract with the Commission, or his employment with such contractor.